Universidade de Aveiro Departamento de Química
Ano 2021

Inês de Jesus Fernandes

Bioencapsulamento de células estaminais e endoteliais para criação de modelo *in vitro* de ossificação endocondral

Bioencapsulation of stem and endothelial cells towards an *in vitro* model for endochondral ossification

Universidade de Aveiro Departamento de Química
Ano 2021

Inês de Jesus Fernandes

Bioencapsulamento de células estaminais e endoteliais para criação de modelo *in vitro* de ossificação endocondral

Bioencapsulation of stem and endothelial cells towards an *in vitro* model for endochondral ossification

Dissertação apresentada à Universidade de Aveiro para cumprimento dos requisitos necessários à obtenção do grau de Mestre em Biotecnologia, realizada sob a orientação científica da Doutora Maria Clara Rosa da Silva Correia, investigadora Pós-Doutorada do Departamento de Química da Universidade de Aveiro e do Professor Doutor João Filipe Colardelle da Luz Mano, Professor Catedrático do Departamento de Química da Universidade de Aveiro

.

Financial support from the Portuguese Foundation for Science and Technology (FCT) through the projects “CIRCUS” (PTDC/BTM-MAT/31064/2017), and “CICECO-Aveiro Institute of Materials” (UIDB/50011/2020 & UIDP/50011/2020) financed by national funds through the FCT/MEC and, when appropriate, co-financed by FEDER under the PT2020 Partnership Agreement. The authors also acknowledge funding from the European Research Council (ERC) through the project “ATLAS” (ERC-2014-ADG-669858), an Advanced Grant awarded to Professor João F. Mano. This work was also supported by the *“Programa Operacional Regional do Centro – Centro 2020”,* in the component FEDER, and by national funds (OE) through FCT/MCTES, in the scope of the project SUPRASORT (PTDC/QUIOUT/30658/2017, CENTRO-01-0145-FEDER-030658), as well as by the Marine Biotechnology ERA-NET project BLUETEETH (ERA-MBT/0002/2015) funded by FCT under EU FP7 (Grant Agreement number: 604814).

À minha família.

o júri

presidente	Doutora Ana Maria Rebelo Barreto Xavier Professora Auxiliar do Departamento de Química da Universidade de Aveiro
vogal-arguente principal	Doutor Hugo Agostinho Machado Fernandes Investigador Principal Convidado da Faculdade de Medicina da Universidade de Coimbra
vogal-orientador	Doutora Maria Clara Rosa da Silva Correia Investigadora Pós-doutorada do Departamento de Química da Universidade de Aveiro

agradecimentos

Muito obrigada à minha orientadora, Clara. Por todos os conselhos e pela inspiração dentro e fora do contexto académico. Um exemplo a seguir. Muito obrigada ao professor João Mano por ter trazido este ramo de investigação para Aveiro e por me ter dado a oportunidade de trabalhar em Engenharia de tecidos, a desenvolver este trabalho que tanto me ensinou.
Muito obrigada à Sara que sempre me deu alento e também muita orientação. Estou muito feliz por ter tido a tua ajuda neste grande desafio. Obrigada por me animares sempre!
Obrigada à minha família. Pelo amor, pelo apoio! Por terem criado os alicerces do que sou hoje. Pelos ensinamentos que a universidade não conseguiria dar. Obrigada mãe, pai e maninha! Mãe obrigada por estares sempre aqui e por me ensinares o que é realmente importante.
Obrigada ao Miguel, meu namorado, meu companheiro. Estou muito feliz por tudo o que aprendemos juntos até agora. Obrigada pelo carinho, por me entenderes e me acalmares.
Obrigada a quem esteve recorrentemente presente nos momentos bons e menos bons do laboratório. Obrigada à minha Aninha, que tantas vezes me ajudou e me fez relembrar que as pessoas são realmente uma das coisas mais importantes que se leva desta experiência. És linda! Obrigada à Elisa, a minha comparsa do final de turno, e ao Diogo, que sempre fez por manter o pessoal unido!
Obrigada à minha Guida, que tem estado nos bons momentos e nos menos bons da minha vida já faz alguns anos. Que venham mais!
Obrigada Gi e Ricardo, de quem sinto tantas saudades e que me dão sempre as melhores energias!
Obrigada ao Saúl, Olinda, e Lisete pelo bem que me fazem ainda hoje!

palavras-chave

Bioencapsulamento, células endoteliais, células estaminais mesenquimais, co-cultura 3D, cordão umbilical, cultura dinâmica, engenharia de tecidos, layer-by-layer, ossificação endocondral, regeneração óssea, vascularização *in vitro*

resumo

No passado, a maioria das estratégias de engenharia de tecidos ósseos baseavam-se na ossificação intramembranar (IMO). O tecido ósseo era obtido *in vitro*, no entanto, depois da implantação a falta de vascularização provocava morte celular no interior do tecido. Na última década, as estratégias baseadas na ossificação endocondral (ECO) têm sido cada vez mais exploradas. A secreção de fatores osteogénicos e angiogénicos pelas células presentes nos *templates* de cartilagem hipertrófica permitem a regeneração do tecido ósseo como ainda ajudam na vascularização do mesmo. No capítulo *I*, as estratégias mais recentes de ECO, utilizadas na engenharia de tecido ósseo, são comparadas e debatidas. Por sua vez, no capítulo *II* são descritos os métodos utilizados para criar uma estratégia de ECO *in vitro*. No capítulo *III*, são apresentados e analisados os resultados da caracterização dos microtecidos ósseos obtidos. O modelo criado de ECO *in vitro* consiste na co-cultura de *microtemplates* 3D cartilaginosos com células estaminais mesenquimais do cordão umbilical (UCMSCs) e células endoteliais isoladas da veia do cordão umbilical (HUVECs). Hipoteticamente, este microambiente privilegiado irá simular as condições do processo de ECO, gerando microtecidos ósseos vascularizados. Para o efeito, *microtemplates* 3D constituídos apenas por UCMSCs foram criados, cultivados por 21 dias e depois co-cultivados com UCMSCs e HUVECs em microcápsulas liquefeitas e com membrana em multicamada, em condições dinâmicas, por mais 21 dias. Foram testadas microcápsulas com *microtemplates* 3D induzidos à condrogénese e cultivados com (ECO) e sem (controlo ECO) fatores de diferenciação osteogénica. Foram também testadas microcápsulas com *microtemplates* 3D não-induzidos, cultivados com (IMO) e sem (controlo negativo) fatores de diferenciação osteogénica. Os resultados mostraram que ambos os *microtemplates* 3D e microcápsulas mantiveram a sua viabilidade celular durante os respetivos 21 dias. A natureza cartilaginosa dos *microtemplates* 3D cultivados em meio condrogénico foi confirmada. Após 21 dias de encapsulamento, as microcápsulas ECO apresentaram evidências de produção de matriz extracelular óssea e uma maior mineralização da matriz, sendo esta a única condição com o rácio cálcio/fósforo (Ca/P, 1.71) perto da hidroxiapatite (HA) nativa (1.67). Para além disso, ambas as condições ECO e controlo ECO induziram um acentuado recrutamento de células endoteliais. Estes resultados evidenciam a relevância do uso de *microtemplates* 3D induzidos à condrogénese na criação e vascularização de tecido ósseo, realçando assim a vantagem da ECO sobre a IMO. Em suma, esta estratégia de ECO e bioencapsulamento mostrou-se promissora na regeneração óssea. Por fim, no capítulo *IV* são discutidas as principais conclusões do trabalho e o potencial das estratégias de ECO no futuro da engenharia de tecidos e medicina regenerativa.

keywords

3D co-culture, bioencapsulation, bone regeneration, endochondral ossification, endothelial cells, dynamic culture, *in vitro* vascularization, layer-by-layer, mesenchymal stem cells, tissue engineering, umbilical cord

abstract

In the past, most bone tissue engineering (TE) strategies were focused on the recapitulation of intramembranous ossification (IMO) process. Bone-like tissues were successfully obtained *in vitro*, however, after implantation the created tissues lack of a functional vascular supply, resulting in necrotic cores. During the last decade, approaches based in endochondral ossification (ECO) have been increasingly explored. The secretion of osteogenic and angiogenic factors by the cells present in the hypertrophic cartilage templates allows bone tissue repair but also helps tissue vascularization. In chapter *I*, the most recent ECO approaches used in bone TE are highlighted and discussed. Chapter *II* describes the methods used to develop an in vitro ECO approach. In chapter *III*, the results obtained related with the characterization of the obtained bone-like microtissues are presented and discussed. The developed in vitro ECO model relies in the co-culture of 3D micro-cartilaginous templates with umbilical cord-derived mesenchymal stem/stromal cells (UCMSCs) and human umbilical vein endothelial cells (HUVECs). Our hypothesis is that such engineered and privileged microenvironment would mimic the ECO process, leading to the *in vitro* production of vascularized bone-like microtissues. For that, MSCs-only 3D microtemplates were produced at high-rates and cultured *in vitro* for 21 days. Then, such microtemplates were co-cultured with UCMSCs and HUVECs within liquefied and multilayered microcapsules, in dynamic conditions, for another 21 days. Microcapsules with chondrogenically-primed 3D microtemplates were cultured with (ECO) and without (ECO control) osteogenic differentiation factors. Also, microcapsules with non-primed 3D microtemplates were cultured with (IMO) and without (negative control) osteogenic differentiation factors. Results show that both 3D microtemplates and microcapsules were able to maintain cell viability up to 21 days. The cartilaginous nature of the 3D templates cultured in chondrogenic medium was confirmed. After 21 days of encapsulation, the ECO microcapsules presented evidence of bone extracellular matrix production and higher matrix mineralization, being the only condition to present a calcium/phosphorous (Ca/P) ratio (1.71) close to the native hydroxyapatite ratio (1.67). Furthermore, both ECO and ECO control conditions successfully induced endothelial cell recruitment. These data show the relevance of using chondrogenically primed 3D microtemplates in bone repair, highlighting the advantage of ECO over IMO approach. In conclusion, this ECO bioencapsulation approach revealed to be a promising bone regeneration strategy. Ultimately, chapter *IV* discusses the main conclusions and future perspectives related to the potential of ECO approaches in tissue engineering and regenerative medicine.

Contents

List of figures

List of Tables

List of abbreviations

AA – Ascorbic acid

ALG – Alginate

APC - Allophycocyanin

ASCs – Adipose stem/stromal cells

ATB – Antibiotic - antimycotic

BMMSCs – Bone marrow mesenchymal stem/stromal cells

BMP – Bone morphogenic protein

BSA – Bovine serum albumin

CHT – Chitosan

Col I – Collagen type I

Col II – Collagen type II

Col X – Collagen type X

ECGS – Endothelial cell growth supplement

ESCs – Endothelial stem cells

ECM – Extracellular matrix

ECO – Endochondral ossification

EDS – Energy-dispersive X-ray spectroscopy

EPCs – Endothelial progenitor cells

FBS – Fetal bovine serum

FITC - Fluorescein isothiocyanate

GAGs – Glycosaminoglycans

H&E - hematoxylin-eosin

HA – Hydroxyapatite

HUVECs – Human umbilical vein endothelial cells

HyA – Hyaluronic acid

IGF – Insulin-like growth factor

IHH - Indian hedgehog

IL – Interleukin

IMO – Intramembranous ossification

ITS – Insulin-transferrin-selenium supplement

LbL – Layer-by-layer

MMP – Matrix metalloproteinase

MSCs – Mesenchymal stem/stromal cells

OCN – Osteocalcin

OPN – Osteopontin

OSX – Osterix

PLL – Poly(L-lysine)

PTH - Parathyroid hormone

SEM – Scanning electron microscopy

TE - Tissue engineering

TERM – Tissue engineering and regenerative medicine

TGF- β3 – Transforming growth factor-β3

TNF – Tumor necrosis factor

UCMSCs – umbilical cord mesenchymal stem/stromal cells

VEGF – Vascular endothelial growth factor

β-TCP – β-Tricalcium phosphate

I. Tissue engineering strategies based in Endochondral Ossification for bone regeneration

Abstract

Bone tissue presents an incredible intrinsic self-repair capability. However, large bone defects may result in cessation of the regenerative process. Aiming to solve challenges related to large bone non-unions and defects, the primordial bone tissue engineering (TE) approaches intended to recapitulate the intramembranous ossification (IMO) process. IMO consists in a natural bone production mechanism where mesenchymal stem/stromal cells (MSCs) are directly stimulated to differentiate into osteoblasts. However, after implanted these tissues lacked a functional vascular supply, resulting in necrotic cores. Recently, endochondral ossification (ECO) recapitulation is being increasingly explored in bone TE. ECO recapitulates the development and repair process of most bones. Such process is characterized by the condensation of MSCs, following their differentiation to form cartilaginous templates. Ultimately, the hypertrophic differentiation of such templates results in the release of osteogenic and pro-angiogenic factors. Beyond the transformation of the cartilaginous template into newly deposited bone tissues, the release of key biomolecules consequently induces tissue vascularization. This promising approach has been explored with a plethora of cell types, culture conditions and biomaterials. This review highlights and discusses the most recent and successful strategies for the application of ECO in bone TE to up-scale tissue engineered hypertrophic cartilaginous grafts suitable for promoting bone regeneration through ECO.

1. Introduction

Bone Tissue Engineering and Regenerative Medicine (TERM) strategies aim to solve challenges related to large bone non-unions and defects, that may be caused by trauma, congenital anomalies, infection, or surgical resection. Although bone tissue presents an incredible intrinsic self-repair capability, large bone defects may result in the cessation of the regenerative process.[1,2] Moreover, health conditions, such as osteoporosis, diabetes, and genetic factors, increase the chances of suffering a fracture and/or delayed repair.[1,3,4] Bone grafting has been used over the last years and remain the golden standard to repair large bone defects.[2,5,6] Although these surgical procedures are generally successful, 10% of the bone grafts do not fully recover, which results in bone non-unions. Furthermore, these techniques are invasive and painful, and may lead to disease transmission, infection, and compatibility issues.[2,5,7]

During the last decades, less invasive surgery techniques have been emerging. For instance, the kyphoplasty is used to repair spine compression fractures through a minimally invasive half-inch incision, followed by poly(methyl methacrylate) injection, to create an internal cast in the fractured cavity.[8,9] Likewise, the use of robots to support or perform a surgery, such as Mako®, allows the total hip replacement with more precision and less blood losses.[10] However, these minimally invasive surgeries are unsuccessful to treat most large bone defects. Therefore, bone TERM strategies are being developed to surpass these drawbacks, including to replace inert prothesis applications, and to improve bone grafting.

The scientific community has been focused on the recapitulation of the ontological processes that occur during bone formation/healing in order to develop close-to-native bone TE strategies. In the bone native environment, bone is formed by two distinct mechanisms, namely by endochondral or intramembranous ossification. Briefly, endochondral ossification (ECO) is characterized by the chondrogenic differentiation of recruited mesenchymal stem/stromal cells (MSCs) forming an initial cartilaginous template, followed by hypertrophic differentiation that will result in the release of pro-angiogenic factors. The release of such biomolecules consequently leads to the vascularization and remodeling of the previously formed cartilaginous template, giving rise to newly deposited bone tissues. In the case of intramembranous ossification (IMO), MSCs are directly stimulated to differentiate into bone cells, namely osteoblasts. The majority of the bone TE strategies have been focused on the recapitulation of the IMO process. However, the long bones of the body are developed by the ECO process. A major hurdle that has been hampering the translational of IMO-based TE strategies into the clinics is the lack of a functional vascular supply of the created tissues, resulting in necrotic cores after implantation.[2,11] Recently, ECO recapitulation is being increasingly explored as an alternative to crossover those limitations in bone TE. ECO seems to bring advantages when it

comes to vascularization because, at the same time hypertrophic chondrocytes are secreting osteogenic factors to transform the cartilage template into bone tissue, they are also secreting angiogenic factors which induce tissue vascularization. In the case of the majority of IMO approaches, the bioengineered tissues must be pre-vascularized *in vitro*, otherwise, after implantation, the blood vessels of the host will not be able to perfuse the calcified matrix.[2]

This review aims to highlights the most recent and successful strategies for the application of ECO in bone TE, while describing which type of cells, culture conditions, and biomaterials can be leveraged to up-scale tissue engineered hypertrophic cartilaginous grafts suitable for promoting bone regeneration through ECO. Ultimately, future scientific trends in biomaterial science which may accelerate the ECO approach towards implementation in a clinical setting will be discussed.

2. Endochondral Ossification

ECO is the biological process responsible for the creation of every bone below the skull, except the clavicle, in human beings.[2] This process begins in the second month of gestation and goes to adulthood, however, the majority of the process occurs until birth. Furthermore, ECO is responsible for the regeneration of many of these bones, which can happen at any moment but with age, such regenerative process loses efficiency. In Figure 1 is represented a scheme of the main phases of the ECO repair. Whether bone tissue is being created or rebuilt, firstly MSCs need to migrate and condensate *in situ* due to the expression of the transcription factor SOX9. At this stage, MSCs start the differentiation to become chondrocytes, and consequently lay down extracellular matrix (ECM) rich in collagen type II (Col II), aggrecan and sulphated glycosaminoglycans (GAGs), giving rise to a hyaline-like cartilaginous template.[2,12] Chondrocytes inside this template enter in a hypertrophic state, secreting key biomolecules, including collagen type X (Col X), vascular endothelial growth factor (VEGF), alkaline phosphatase, matrix metalloproteinase (MMP)-13, and bone morphogenic protein (BMP)-6.[2,11] The release of these molecules causes a cascade of events, namely an increase in the volume of hypertrophic chondrocytes, the calcification of the template, and the modification in the composition of the newly deposited ECM from Col II to Col X. The secretion of MMP-13 helps in the degradation of cartilage-Col II, allowing hypertrophic chondrocytes to increase their volume, while facilitating the invasion of the diaphysis (bone central part) by blood vessels of the periosteal bud. Being established a vascular network, osteoprogenitor cells, such as osteoclasts and osteoblasts, are able to migrate to create the primary ossification center (POC). More recently, it has been found evidence that osteoblasts at POC are not just brought by the periosteal bud but also they are a result of a chondrocyte-to-osteoblast transformation.[13] Here, bone deposition starts with the osteoclasts helping at the degradation of the hyaline cartilage, which act as canals guiding blood

vessels invasion, and osteoblasts producing bone tissue. At the same time, the medullary cavity starts its formation at diaphysis and the secondary ossification center (SOC) at epiphyses (bone end parts). Even after birth, bone continues to grow due to the presence of cartilage tissue that exists at the epiphysial growth plates. When bone reaches its full length, these plates become bone, and the cartilage tissue will only remain at the connection regions with other bones.

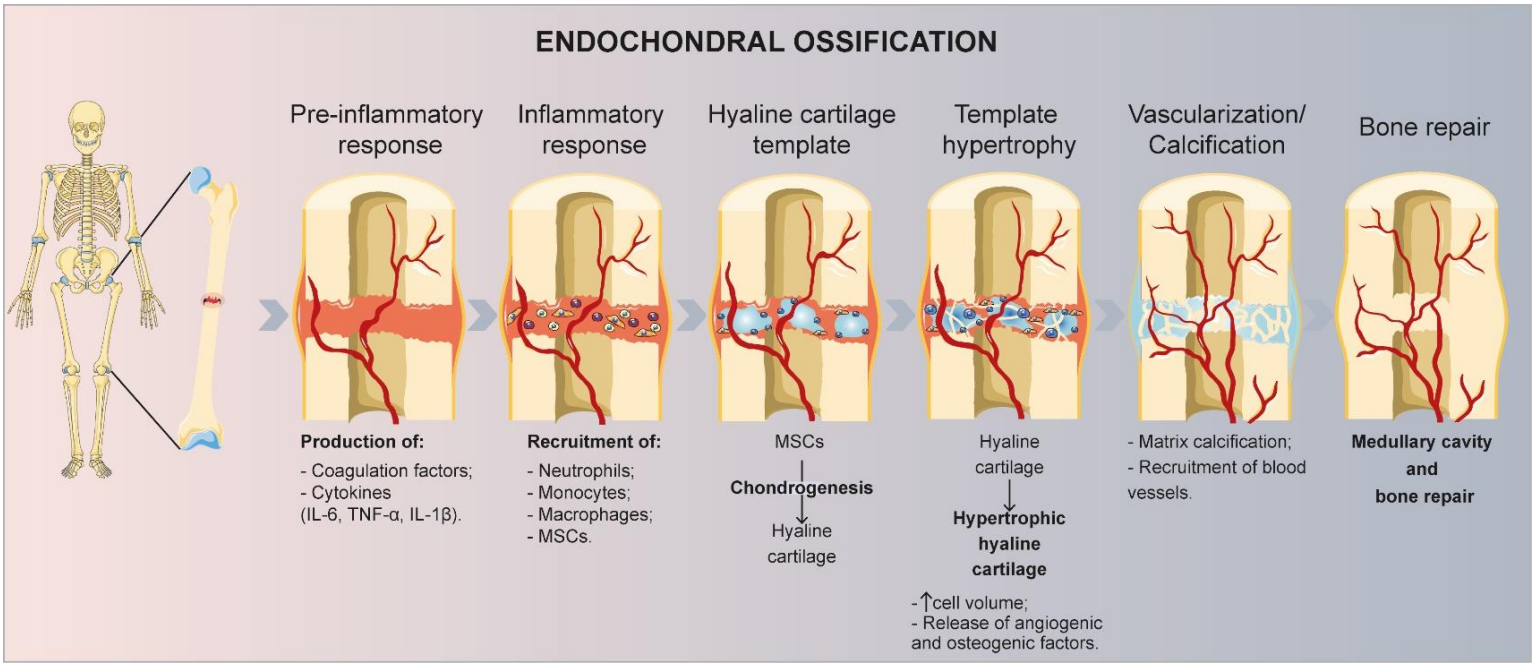

Figure 1. Schematic representation of the endochondral ossification repair process.

2.1 Regulation mechanisms of Endochondral Ossification

2.1.1 Immune Response

The regeneration of a large bone defect always starts with an inflammatory process as a response from the immune system. Briefly, the damage of the vascular tissues causes a demand for coagulation factors, such as factor *XIII* and tissue factor, which leads to the formation of a fibrin clot.[14] Combined with the secretion of inflammatory cytokines, such as tumor necrosis factor (TNF)-α, interleukin (IL)-6, and IL-1β, angiogenesis is induced, giving rise to the innate immune response.[15–17] Neutrophils, monocytes, and macrophages are the first immune cells acting on the injury place, releasing cytokines and growth factors that recruit adaptive immune cells, namely T and B lymphocytes, which initiate the natural healing process.[18,19] Neutrophils contribute to the reconstruction of the tissue and recruit myeloid and MSCs to the injury site. At the same time, the recruited monocytes adhere at the injured site and differentiate into macrophages, and together with resident tissue macrophages of bone, termed as osteal macrophages or osteomacs, contribute to the

removal of dead cells, while also aiding in bone healing.[2,20] In particular, osteomacs have been shown to support osteoblast maturation, maintenance and function.[21,22] In a simplistic perspective of the native environment, macrophages can express two polarization states during the healing process, namely the pro-inflammatory "M1" phenotype and the anti-inflammatory/pro-healing "M2" phenotype. Bone-specific growth factors, such as TGF-β and BMPs, are produced during the inflammatory response in order to attract MSCs.[2,20] "M2" macrophages are important for the attraction of MSCs, tissue repair, including the recruitment of blood vessels, and for ending the inflammatory process through the release of IL-10, IL-1ra, TGF-β1, and VEGF-A factors.[20,23] The condensation of the recruited MSCs starts the ECO process. Simultaneously, MSCs produce cytokines that help to finish the inflammatory response in that region.[20] MSCs have been described as capable of modulating other cell behaviors, including immune cells, due to its paracrine signaling through Notch and prostaglandin E2 (PGE2) pathways. This immunosuppressive function of MSCs that mediates inflammatory responses in the surroundings leads to the improvement of the microenvironment conditions that promote bone healing. For that reason, the crosstalk between macrophages and MSCs, particularly how immune cells control the differentiation and activity of bone cells, is currently a major question in the osteoimmunology field.[20,23] ECM constituents also have a modulatory effect on the immune system.[11,20,24] Collagen type I, one of the main constituents of the ECM of bone, is capable of interacting with macrophages when it is denatured through its scavengers receptors, thus identifying a bone defect and, consequently, the induction of the production of pro-inflammatory cytokines by macrophages. Another main ECM constituent of bone is the hyaluronic acid (HyA), a GAG, which can have distinct effects on the immune system based on its molecular weight. Low molecular weight HA is present in damaged ECM due to fragmentation in response to glycosidase activity upregulated by environmental cues such as pH and oxygen species. Therefore, HA with low molecular weight induces macrophages to express the pro-inflammatory M1 phenotype. On the contrary, healthy ECM contains high molecular weight HA, thus inhibiting the production of pro-inflammatory mediators by inducing the expression of IL-10 by macrophages.[20,25] In the particular scenario following the implantation of a biomaterial aiming towards bone regeneration, also a similar immune response will occur. The main ECM components, such as collagen, fibrin, hydroxyapatite, and hyaluronic acid, have been widely used for the development of scaffolds, individually or jointly. Nonetheless, these scaffolds cannot provide an equal complex set of physical and biochemical cues as those provided by the natural ECM. Therefore, the study of the interaction of the different cells that act as central players during bone remodeling/regeneration, including MSCs and osteoprogenitor cells, with immune cells, or the effect of ECM constitution on the immune system, is essential to breadth and depth our understanding and thus propose effective bone regeneration approaches.[20] The biological performance can be enhanced

by adding several biofactors known to improve osteogenesis and angiogenesis, as well as inhibitors of the inflammatory phase.[20] Thus, the scientific community is focused in the discovery of which biomolecules positively influence the ECO process. Pro-inflammatory molecules, such as IL-1β, may beneficiate ECO after injury because it is described as highly relevant to control the inflammation process.[26] However, it seems that an anti-inflammatory environment with "M2" macrophages is more compatible with MSCs activity.[20] This orientation of the macrophage phenotype *in vivo* represents a challenge because of the multitude of signals existent that will lead to the expression of undesired functions.

2.1.2 Hypertrophy

The regulation of hypertrophy is performed through local and systemic factors. After the condensation of MSCs, *SOX9* is expressed to promote the differentiation into chondrocytes. When *SOX9* is not expressed, the cartilaginous template cannot be formed, as showed in knockout mice.[27] That can also result in the absence of Col X, indicating that the production of SOX9 is important for the existence of a hypertrophic stage.[28] Furthermore, it seems to be involved in the production of cartilage matrix proteins by the endoplasmic reticulum by controlling the expression of a basic leucine zipper transcription factor. During cartilage development, *SOX9* is activated by cyclic-AMP-dependent protein kinase A (PKA), which is activated by parathyroid hormone-related peptide (PTHrP).[27]

Considering the ability of chondrocytes to proliferate, they can be classified in proliferative chondrocytes or non-proliferative chondrocytes. Non-proliferative chondrocytes are in a pre-hypertrophic state secreting the Indian hedgehog (IHH) factor. IHH promotes hypertrophy, as well as the proliferation of chondrocytes. Simultaneously, such microenvironment promotes the recruitment of MSCs and their differentiation into osteoblasts, as well as the production of the PTHrP in the perichondrium. PTHrP avoids that such proliferative chondrocytes turn into pre-hypertrophic chondrocytes. The regulation of these two pathways is made by negative feedback, which regulates the growth of the proliferative region and make the connection between cortical and longitudinal bone formation.[29] Scotti *et al.* highlighted the importance of the IHH pathway in the maturation of the cartilaginous template of ECO. For that, a cyclopamine derivative was used to perform a functional inhibition of the IHH pathway. Results showed that the expression of genes involved in the IHH and parathyroid hormone signaling, as well as chondrogenic/hypertrophic and osteogenic genes were significantly reduced.[30] Of note, IHH is only involved in osteoblastogenesis during ECO, and not during IMO, and thus it is hypothesized that it may have influence in the chondrocyte-to-osteoblast transformation.[13] In the perichondrium, fibroblast growth factor-18 (FGF-18), as well as

insulin-like growth factor 1 (IGF-1) are produced to inhibit the proliferation of proliferative chondrocytes.[29] RUNX2 is also an important transcription factor expressed by hypertrophic chondrocytes for bone development and osteoblastogenesis. Different studies evidenced that the lack of *RUNX2* inhibits chondrocytes to undergo hypertrophy. Other important molecule is the core binding factor-β (CBF-β), a co-activator of RUNX2, CCAAT/enhancer-binding protein-β (*C/EBP-β*) and activating transcription factor 4 (ATF4), which are key mediators of hypertrophy in chondrocytes. RUNX2 also contributes to Osterix (*OSX*) expression, an essential transcription factor required for osteoblastogenesis during both ECO and IMO. Particularly, in ECO, *OSX* subsequently stimulates the expression of MMP-13, which is responsible for the calcification and degradation of cartilage templates.[27] Proliferative and hypertrophic chondrocytes, as well as perichondrium cells, secrete TGF-β and BMP factors, which are key mediators during ECO, namely in the regulation of proliferation and differentiation of MSCs-derived chondrocytes.[31]

The canonical form of the Wnt signaling pathway is also a key player in the mediation of the hypertrophic state of chondrocytes. Wnt canonical pathway controls the activation of β-catenin, which binds to lymphoid enhancer factor (LEF) and T cell factor (TCF) proteins. The resultant complex can promote the expression of *RUNX2*, which induces hypertrophy. This phenomenon only occurs when the Wnt canonical pathway is activated, otherwise, β-catenin is degraded. In that scenario, chondrocytes will not be able to undergo hypertrophy, and consequently, a hyaline-like cartilaginous template is rather obtained expressing high levels of Col II and aggrecan.[13,32] Moreover, the Wnt pathway seems to be involved in the regulation of chondrocyte-to-osteoblast transformation, since when β-catenin gene was deleted from hypertrophic chondrocytes, bone formation substantially decreased.[33] Inhibition or enhancement of this signaling pathway have showed to control cartilage and bone formation in an on/off fashion.[34,35] Furthermore, the activation of Wnt pathway during the chondrocyte-to-osteoblast transformation enhances bone formation.[34]

The Notch pathway is another important signaling pathway in the ECO process, and particularly relevant during hypertrophic maturation.[13,36] The Notch pathway is triggered by cell-to-cell contact. When a ligand binds to the Notch receptor leads to its proteolytic cleavage and the translocation of the Notch intracellular domain to the nucleus, which initiates the signal cascade by the transcription of HEY1 and HES genes.[13] When the Notch pathway is inhibited during the final stages of ECO, the bone healing process is jeopardized, originating shorter limbs composed by high populations of hypertrophic chondrocytes.[37] Notch is also important for the preservation of osteochondro-progenitors multipotency.[36]

3. Endochondral Ossification in Tissue Engineering

3.1 Cell sources

MSCs are the most used source of cells for bone engineering, due to their fast proliferation, multipotency, self-renewal capacity and ability to secrete a wide range of cytokines and growth factors.[11,38] Such secreted bioactive molecules have anti-inflammatory and immunosuppressive effects, which allow MSCs to play an immunomodulatory role, thus regulating inflammation and tissue regeneration.[38–40] This feature is innate in MSCs because they are naturally released after an injury, making them exposed to several signals associated with tissue damage and bone repair. Consequently, MSCs are more likely to respond to those signals. The production of such cytokines represents another advantage of using MSCs because it decreases the need for supplemental growth factors in cell culture medium.[11,39] Also, these cells have shown to possess an immune privilege because they seem to not trigger an immune response.[38,39,41,42] In fact, these cells have extremely important roles in the ECO process. They can easily differentiate into chondrocytes and osteoblasts, they enhance cell proliferation and differentiation, and still turn the microenvironment permissive to chondrocytes hypertrophy.[20] MSCs are present in several tissues, including bone marrow, adipose tissue, synovial membrane, periosteal, and umbilical cord.[11,43] The selection process must consider the specificities of each tissue and the advantages/disadvantages of each isolation procedure. Bone marrow mesenchymal stem cells (BMMSCs) have been the most used source of cells in bone TE strategies, and specifically those recapitulating the ECO process, due to a number of appealing factors, namely their ability to differentiate into chondrogenic[44] and osteogenic[45] lineage, extensive characterization *in vitro,* and well-established isolation protocols.[11,46] During the healing process, BMMSCs are recruited to the injury site, which might indicate that these cells are highly sensible to the bioactive molecules released during healing. In fact, these cells show appetence to respond to several molecules released after bone damage and during inflammation and bone repair.[11] Furthermore, they were successfully applied in different ECO approaches, showing the ability to differentiate into chondrocytes and to achieve a hypertrophic phenotype *in vitro,* and ultimately contributing to the development of bone-like tissues *in vivo* .[46–49] Bone marrow was described as a wealthy source of MSCs.[50] However, the highly invasive collection procedure, and the decline of BMMSCs in number and differentiation capacity with increasing donor age and *in vitro* passage are major disadvantages.[51] BMMSCs grafts have shown the capacity to regenerate bone defects in several animal models. Ceramic scaffolds seeded with BMMSCs have been successfully tested in clinical trials in order to repair large bone defects. Hydroxyapatite ceramic scaffolds seeded with BMMSCs were created to be compatible with the bone defect that was being studied. Impressive results were obtained *in vivo,* since past 7 years the implants showed good integration without any

fracture.[52] On the other hand, adipose-derived mesenchymal stem/stromal cells (ASCs) are becoming highly attractive in TE, mainly due to their ease of collection from liposuctions, and high abundance. Additionally, the use of ASCs adds value to a tissue that normally is discarded.[51,53] Studies using osteogenically-induced autologous ASCs seeded in a scaffold composed by polylactic acid and coated with fibronectin[54] or in a coral graft[55] showed bone healing in rabbit and canine models, respectively. Interesting results were shown *in vivo* using ASCs seeded in scaffolds composed by β-tricalcium phosphate and immobilized BMP-2. Such microvascular construct was aimed to be used for a maxillary reconstruction, and showed bone healing and tissue integration upon implantation.[56] ASCs combined with fibrin glue, and cancellous bone grafts were used to treat severe calvarial defects. [57] Results showed deposition of new bone and almost complete calvarial continuity. More recently, fractionated human adipose tissue was obtained by washing and shuffling liposuction samples through syringes until small tissue particles were obtained. Those particles were cultured in proliferation medium, instead of isolated ASCs, and combined with a dispersion of ceramic granules. Afterwards ASCs differentiated within the composites into hypertrophic chondrocytes. The composites were implanted in nude mice and resulted in reproducible bone and bone marrow-like tissue.[58] Umbilical cord stem cells (UCMSCs) have also been used due to their promising characteristics. The umbilical cord is a perinatal tissue rich in MSCs. These cells are in a development level between adult MSCs and embryonic stem cells (ESCs). These MSCs are isolated from an otherwise discarded tissue and public and private companies have been storing them in cryobanks.[53,59,60] In the past, the umbilical cord was considered a poor source of MSCs. However, the isolation protocols have been significantly improved, and nowadays the umbilical cord is considered a promising source, allowing to obtain UCMSCs with high efficiency.[50,59] UCMSCs immune properties have been tested and it was found that they also have immunosuppressive properties and low immunogenicity, indicating that may be possible to use them in allogeneic transplants.[61–64] Additionally, UCMSCs were considered to have an increased immunomodulation ability compared to BMMSCs and ASCs.[62] UCMSCs combined with collagen microbeads were used to create bone constructs, and then implanted to evaluate their potential to create bone. Interestingly, prior to implantation, UCMSCS were expanded in culture medium supplemented with human platelet lysate, instead of fetal bovine serum (FBS). UCMSCs maintained their proangiogenic potential and the ability to differentiate into the osteogenic lineage. Importantly, the constructs prompted bone and vascular formation when implanted in mice. Furthermore, BMMSCs and ASCs were also used and compared to UCMSCs. UCMSCs seemed to easily differentiate into chondrocytes, while also showing an enhanced proangiogenic activity and low levels of inflammatory responses.[60] MSCs isolated from bone marrow, adipose tissue and umbilical cord were compared regarding their morphology, easiness of isolation, colony frequency, expansion potential, the ability in

differentiating into multiple types of cells and immune phenotype. No significative differences could be found in their morphology and phenotype (fibroblastoid morphology, a multipotential differentiation ability, and the classic protein markers). However, the isolation yield of UCMSCs was the lowest (63%). In contrast, UCMSCs showed the highest proliferation potential. Additionally, while ASCs and BMMSCs successfully differentiated into the classical triple lineage, namely chondrogenic, osteogenic, and adipogenic, UCMSCs could not undergo adipogenic differentiation.[51] MSCs are also found in other tissues, like the dental pulp, but this source remains less explored. Dental pulp it is another interesting source of MSCs and that would otherwise be discarded during dentist interventions. Dental pulp-derived MSCs (DPMSCs) show good angiogenic and osteogenic potential [65–69] and were already used in an *in vivo* ECO experiment. In that experiment, DPMSCs were seeded in collagen scaffolds, and subsequently implanted in calvaria critical defects. The cells were not induced to undergo chondrogenic differentiation before implantation. During a follow-up of three months, it was possible to observe DPMSCs subsequently undergoing chondrogenic differentiation, chondrogenic hypertrophy, and finally to form new bone tissue.[68]

During the initial acute immune response, macrophages are recruited to the injury site and remain *in situ* until the end of the regeneration process. Macrophages are one of the first cell types to arrive at the injury place, cleaning cell debris and protecting the tissue from pathogens. Furthermore, they produce growth factors that will recruit other type of cells to start the natural bone regeneration. Macrophages are also key elements in this process because they have the ability to change their phenotype depending on the stimuli from the surrounding environment. During the early stages of bone repair, macrophages tend to assume the M1 pro-inflammatory phenotype. Following the normal regenerative process, macrophages start to switch to the "M2" anti-inflammatory phenotype. Only an efficient and precise timely switch from the "M1" to the "M2" macrophage phenotype results in an appropriate production of molecular cues crucial to support bone regeneration. To mimic the natural microenvironment of bone tissue, macrophages are frequently used in ECO studies. Schlundt *et al.* observed the effect of macrophages in early and late stages of bone regeneration, namely during inflammation and ossification, respectively. The reduction of macrophages using clodronate liposomes *in vivo* resulted in no significant effects on the early stages of bone healing. However, the reduced number of macrophages affected the ECO, specifically the maturation of the chondrogenic stages towards woven bone formation. Furthermore, it was concluded that "M2" macrophages were essential in the ECO stage. The stimulation of macrophages into a pro-healing "M2" phenotype, in a collagen scaffold with IL-4 and IL-13, improved bone formation *in vivo*, with significantly higher callus and bone volumes, when compared with a control collagen scaffold only with PBS treatment.[70]

Another option is the use of mature and differentiated progenitor cells, such as chondrocytes and chondroprogenitors, for endochondral bone repair**.** Porcine articular chondrocytes were successfully

used to recreate the ECO process *in vitro*, using polycaprolactone scaffolds loaded with BMP-2. Upon implantation bone formation also occurred, but only in the periphery of the scaffold.[71] Chick embryo chondrocytes were successfully used to produce bone following *in vivo* implantation.[71] Despite being reported that chondroprogenitors cells in a transient hypertrophic phenotype are able to induce ECO,[72] probably they will not be approved for therapeutic use because they will be limited by their mature phenotype, thus limiting their proliferative ability, as well as by the inherent risk of arthritic development. However, they may be used as model systems for research purposes.[73,74] The endothelial progenitor cells (EPCs) can be also useful for ECO strategies. EPCs are found in the bone marrow and peripheral blood, and can be used to enhance vascularization during ECO, due to its pro-angiogenic ability. EPCs have already been used to create an *in vitro* vascular network by inducing their differentiation to obtain endothelial and smooth muscle cells. I*n vivo,* EPCs were shown to be able to identify damaged areas and consequently mobilize themselves. It is possible to obtain two distinct populations of EPCs depending on its isolation protocol, namely early and late EPCs. Usually, late EPCs are the most used in TE strategies, and they are formed after 14-21 days of culture.[75] EPCs can be easily retrieved during surgery for fracture repair, and have the potential to undergo chondrogenesis, hypertrophy, and calcification *in vitro*.[76] More recently, peripheral blood $CD34^+$ cells were used intravenously in nude F344/N Jcl rnu/rnu rats and showed to enhance bone regeneration by ECO.[77]

Although several studies use only one type of cells to recreate the ECO process, co-culture systems have been applied to better mimic what happens in the native environment following a bone injury, where several types of cells are recruited and interact together to proceed with bone repair. Their crosstalks are crucial for a successful bone regeneration occur. For example, MSCs directly influence macrophage polarization and regulate part of the immune response. On the other hand, the proteins secreted by immune cells regulate the behavior of MSCs and the progress of ECO.[20,39] Co-culture systems are being adopted, for example, to overcome vascularization problems. As previously explained, MSCs play a key role in cell inter-communication during ECO, including in bone vascularization because of the angiogenic factors that they produce, which induce the differentiation of EPCs and, consequently, the production of osteogenic growth factors by EPCs that lead to MSCs differentiation. Co-culture of BMMSCs and EPCs presented improvements in bone formation and more pronounced neovascularization compared to mono cultures.[39] In an attempt to enhance bone formation, Correia *et al.* co-cultured hASCs and human adipose-derived microvascular endothelial cells (hAMECs) in semi-permeable and liquified capsules, with or without osteogenic supplementation. Results showed that osteogenesis was enhanced when compared to mono cultures of hASCs, even in the absence of supplemental osteogenic differentiation factors.[78] Using the same system, Correia *et al.* tested the *in vivo* implantation of this system with or without *in vitro* pre-

differentiation of hASCs. Interestingly, the co-culture system without any pre-differentiation obtained similar levels of mineralization *in vivo* than the pre-differentiated ones.[79] Such results evidence that the cues secreted by EPCs cells successfully induced the osteogenic differentiation of ASCs, thus highlighting how important is the cell-cell direct contact and signaling.

3.2 *In vitro* culture conditions

In the literature, there is no consensus on the conditions, the medium composition, and days of culture necessary to recapitulate *in vitro* the ECO process. The cell type chosen for the ECO approach is an important topic that dictates the culture conditions, as well as the regulation mechanisms of the immune response and hypertrophy.

Bone tissue has a good self-regenerative capacity; however, in 10% of the cases it does not have success and when the injury causes large vascular damages this percentage increases to 46% of non-successful cases. Thus, vascularization is critical for bone regeneration.[80] VEGF is a key factor in angiogenesis which directly influences ECO. During ECO, hypertrophic chondrocytes produce VEGF to recruit the host blood vessels that consequently invade the diaphysis by periosteal bud. The inhibition of VEGF expression results in lower neovascularization and modifies the behavior of hypertrophic chondrocytes, harming the bone repair process.[39] This growth factor is extremely crucial to enhance endochondral bone regeneration and vascularization.[39,78,80] Furthermore, the presence of VEGF seems to be important for the recruitment of MSCs to the injured site. VEGF is present in the platelet-rich plasma, which besides VEGF, it possesses several other growth factors, including platelet-derived growth factor (PDGF), TGF-β and insulin-like growth factor (IGF). Strategies using platelet-rich plasma can simultaneously improve angiogenesis and bone formation, while showing improved results compared with VEGF.[81] All the described constituents of platelet-rich plasma seem to have a beneficial effect on bone regeneration. PDGF has been shown to improve vascularization during bone regeneration, to induce the proliferation of osteoblasts, and to increase the production of VEGF by endothelial cells.[82] When recombinant human PDGF was administered in Sprague-Dawley rats, higher bone density and strength could be observed resulting in a bone regeneration improvement.[83] The TGF-β superfamily is polyvalent, inducing chondrogenesis, proliferation and matrix deposition in MSCs, and possibly hypertrophy, thus acting in all the important stages of the endochondral bone formation.[11,22] Supplementation of the culture media with TGF-β2 and TGF-β3 seems to promote chondrogenesis, hypertrophy, and vascularization in MSCs. This was proved by the genetic expression of *VEGF* and *MMP13*. On the other hand, it is described that TGF-β3 together with β-glycerophosphate (β-GP) induces a higher level of mineralization than the combination of TGF-β1 and β-GP.[84] TGF-β along with thyroid hormones in the culture media for

14 days accelerate MSCs-derived chondrocytes entering in the hypertrophic state.[85] Furthermore, BMPs have an active role in bone homeostasis. In particular, supplementation with BMP-6 increased the expression of Col X, one of the main ECO markers of hypertrophic chondrocytes.[86] IGF influence endothelial cell recruitment and tubular formation. However, its effect on the vascularization during bone repair is unknown.[87] The IGF role as intermediate on the parathyroid pathway, which promotes bone healing, evidences that it may be involved in bone regeneration. The inhibition of IGF production triggered the production of bone with lower density and shorter hypertrophic zones, proving that it is related to bone development.[88] In addition to the use of the previous biomolecules, several ECO approaches use ascorbic acid, β-GP and dexamethasone as supplements to achieve hypertrophy of MSCs-derived chondrocytes, as showed in tables 1 and 2. These three components are well-known osteogenic differentiation factors used in IMO approaches. Dexamethasone induces and regulates *RUNX2* expression in hypertrophic chondrocytes. Ascorbic acid enhances Col I production by MSCs. β-GP provides phosphate for the mineralization stage, inducing the production of hydroxyapatite, and its inorganic phosphate also regulates osteogenic pathways.[89] In summary, hypertrophic media is composed by the three classical components of the osteogenic media that is applied in IMO to directly differentiate MSCs into osteoblasts, but in ECO it is applied to chondrocytes undergoing hypertrophy. Of note, previously to the hypertrophic stimulus, it is required that MSCs differentiate into chondrocytes in order to create the cartilaginous template. For that, MSCs are required to be in a 3D environment, which can be achieved either by creating cell aggregates or by seeding MSCs in 3D bioengineered matrices. Afterwards, MSCs are stimulated to differentiate into chondrocytes by *in vitro* culture for 2-4 weeks in chondrogenic medium. The different *in vitro* and *in vivo* ECO models and the respective culture conditions described in the literature are summarized in Tables 1 and 2, respectively. As showed, there are no consensus in the literature considering the time required for the chondrogenic or hypertrophic *in vitro* stimuli, and the supplemental factors added to each culture media.

3.3 Tissue Engineering Strategies

Building an ECO strategy is a complex process with many variants. There is a need to select the type of cells, the proper supplementation, the construct structure, and composition, as well as if the study will be performed *in vitro* and/or *in vivo*. Furthermore, the approach can consist in the utilization of materials and cells together, scaffold-based approaches, or individually, entitled as cell-free and scaffold-free approaches. ECO strategies were usually classified according to the *in vitro* or *in vivo* experimental study. However, increasing ECO experimental work has been made in the last decade and a composition-based classification became more appropriated. Regardless the differences between the three strategies, scaffold-based, cell-free and scaffold-free approaches all must provide

biochemical, mechanical or structural cues to the surrounding cells in order to induce tissue repair by ECO.[90] Besides, the design of TE strategies should consider important features for a proper bone tissue regeneration, including biocompatibility, biodegradability, osteoinductivity, osteoconductivity, as well as appropriate surface properties.[53] In Figure 2, are identified the cell types and biomaterials more used in each strategy.

3.3.1 Scaffold-based approaches

The most common strategy in TE relies in the combination of materials and cells to repair damaged tissue, called the scaffold-based approaches. Cells in a natural healing process have the structural support of ECM, which is essential because most cells are anchorage dependent. In TE approaches, the creation of a 3D environment that gets closer to the native environment is important to control cell behavior. The ECM produced by cells can be insufficient, so usually scaffolds are used to support cell attachment, proliferation, and differentiation. Additionally, when implanted, scaffolds fill the tissue defect, and support the tissue surrounding.[91,92] The scaffolds should allow the exchange of gases, nutrients, and growth factors to increase the cell survival rate.[52] Additionally, the ability of the implanted biomaterial to recruit and allow the invasion of the host cells and vessels is of utmost importance. The factors secreted by hypertrophic chondrocytes are what distinguish ECO from IMO repair. These factors induce blood vessels invasion, the arrival of more cells and factors and the differentiation of MSCs into osteocytes. Therefore, it is important that the architecture of the scaffold, namely the porosity and the interconnection of the pore network, is designed to allow the penetration by blood vessels of the host, following implantation. The pore size should be between 100-400 μm.[93,94]

Collagen is one of the most used polymers in ECO, since cartilaginous and osteogenic matrixes are rich in Col I. Col I mesh, Ultrafoam™, was already used in ECO approaches with ASCs and shown to obtain bone-like tissue successfully.[58] NuOss™, CopiOs™, Bio-Oss®, Collagraft™_and Vitoss® are all commercial collagen scaffolds tested for bone repair by ECO. These scaffolds contain calcium phosphate particles with natural hydroxyapatite (NuOss™, Bio-Oss®), 65% synthetic hydroxyapatite and 35% β-tricalcium phosphate (β-TCP, Collagraft™), only β-TCP (Vitoss®) or dibasic calcium phosphate (CopiOs™).[95] The presence of cells enhances the tissue repair, by their differentiation and integration within the defect, and by recruiting other cells to the defect site. Thus, BMMSCs aggregates were cultured with ascorbic acid (AA) and treated with trypsin-ethylenediaminetetraacetic acid (EDTA) to obtain a dense ECM. These aggregates were subsequently *in vitro* cultured for 4 weeks in chondrogenic medium, and ultimately implanted for 4 weeks days in mice. The aggregates that followed an ECO protocol showed enhanced bone formation

compared with the IMO control. The micro-computed tomography results revealed higher bone mineral density, total bone volume, and the ratio of bone volume to total volume in ECO constructs. These constructs also have a higher Young's modulus, as well as stronger staining of ALP and OCN markers. Furthermore, higher levels of CD31 were observed, which indicate that the host blood vessels invaded the construct, as it is expected in an ECO approach. The osteogenic markers RUNX2, BSP, VEGF were also upregulated. The co-localization of a nuclei antibody and OCN antibody implies that MSCs are responsible for bone formation in the constructs.[46] Another approach using BMMSCs seeded in a Col I scaffold were sequentially cultured in chondrogenic and then in hypertrophic media. The constructs were then implanted in nude mice for 12 weeks. Interestingly, such strategy was able to mimic the typical processes associated to bone development, mature vasculature formation, response to inflammatory signals, and large bone marrow spaces capable of hosting hematopoietic stem cells.[26]

Embryonic stem cells seeded in biphasic calcium phosphate ceramic particles were differentiated into chondrocytes and implanted in nude mice. Over the 21 days, it was possible to observe a gradual change of cartilage turning into bone. Bone was the predominant tissue and seemed to have a similar structure to bone marrow in part of its lacunae. Researchers observed that isolated chondrocytes do not produce the same results as MSCs-derived chondrocytes, because no signs of ECO were found.[96]

A gelatin methacryloyl (GelMA) hydrogel containing BMMSCs and microchannels was created by 3D printing using a sacrificial pluronic ink, aiming to improve vascularization in ECO approaches. These scaffolds were cultured in chondrogenic medium for 4 weeks. During the first 2 weeks, scaffolds were exposed to 5% partial pressure of oxygen, and then to 20% partial pressure of oxygen. Finally, the scaffolds were implanted in critical size defects of immune-competent Fischer rats. Results show that partial pressure of oxygen were important to improve the bone healing process compared to untreated scaffolds. Higher bone deposition could be observed in the control scaffolds without microchannels, although, the scaffolds with microchannels showed an improved interaction with the host cells, enhanced vascularization, and hydrogel degradation.[97]

BMMSCs were cultured in two different scaffolds, namely collagen–hyaluronic acid (CHyA) and collagen–hydroxyapatite (CHA). Constructs were sequentially cultured in chondrogenic and hypertrophic media, and then were implanted in bone defects of immune-competent Fischer F344 rats. Both ECO constructs enhanced *in vivo* vascularization, probably related with the secretion of pro-angiogenic factors. CHyA construct presented the highest cartilage formation *in vitro* and the highest bone formation *in vivo* compared with CHA.[47]

Oxygen can also be a hypertrophic differentiation cue. BMMSCs aggregates were stimulated in chondrogenic medium for 35 days using two different oxygen tensions, namely 2.5% O_2 (hypoxia) or 21% O_2 (normoxia).[98] Results revealed that normoxia enhanced hypertrophy *in vitro*, while

hypoxia resulted in hyaline cartilage formation and expression of hypertrophy inhibitors. The BMMSCs aggregates were encapsulated in sodium alginate hydrogels and then implanted in mice for 5 weeks. After implantation, aggregates were analyzed by histology regarding cartilage formation (alcian blue), calcification (alizarin red), vascular invasion (Masson's trichrome) and bone formation (methylene blue and basic fuchsin). Hydrogels with hypoxic treatment maintained an avascular cartilage-like ECM, while those subjected to normoxia were highly invaded by the host vessels. Low oxygen tensions inhibit hypertrophic phenotype.[32] Also, a rapid bottom-up approach was developed, named as cell-accumulating technique, to create 3D multilayered tissues with endothelial tubes network. This technique consists in a single-cell coating with fibronectin-gelatin nanofilms, which interact with the $\alpha_5\beta_1$ integrin receptors of cell membrane and allows a simultaneous adhesion of all the involved cells upon seeding. Using this cell-accumulation technique, a sandwich culture of fibroblasts-HUVECs-fibroblasts (4:1:4 layers) was performed for seven days, creating a widespread capillary network.[99] Thus, the 3D MSCs constructs (with 3 or 50 culture days, *in vitro*) were placed directly on this created capillary networks and cultured for seven days. During ECO, the invasion by the blood vessels is initially inhibited by the expression of chondromodulin-I, but overtime its concentration decreases and blood vessels begin to penetrate the tissue. The chondromodulin-I expression was evaluated in the constructs and the samples with mature constructs (50 culture days) had less expression than the immature ones (3 culture days), as expected. Furthermore, in the samples cultured with immature constructs the vascular network disappeared, whereas the mature ones maintained the vascular pattern.[100] Other approach consisted in the utilization of a hyaluronan-fibrin polymer, to mimic the ECM, combined with poly (85% lactide-co-15% glycolide) acid, a biodegradable polymer, to attempt ECO *in vitro* and *in vivo*. BMMSCs were seeded in the synthetic ECM and chondrogenically primed to obtain a hypertrophic cartilaginous template. Then, new BMMSCs were encapsulated in the synthetic ECM, cultured in osteogenic medium for 1 week and implanted in critical size calvarial defects of NSG/Col3.6tpz mice. *In vitro* evaluation was assessed by dimethyl methylene Blue assay, ColII and ColX immunofluorescence and DNA and ALP quantification. *In vivo* results were evaluated essentially by histology and X-ray Imaging. The hypertrophic cartilaginous template was successfully obtained and after implanted, the new deposited matrix revealed to recruit host cells and enhance bone regeneration.[101]

ECO approaches that use scaffolds usually intend to accelerate the differentiation process of MSCs. Therefore, the materials may present biochemical and mechanical cues that will guide cell differentiation, as well as controlled-delivery systems of nutrients, which also can turn these approaches more self-sufficient. UCMSCs were seeded in Orthoss® granules, which are natural bone grafts from bovine origin and present similar porosity to human spongeous bone. These constructs were cultured for 3 weeks in chondrogenic media, and subsequently in hypertrophic media for 2

weeks. As control, samples were cultured in osteogenic or basal media for 5 weeks. After 3 weeks, ECO samples presented cartilaginous matrix deposition and a slight upregulation in the expression of SOX-9, while the hematoxylin-eosin (H&E) staining evaluation of the osteogenic control did not show osteogenic differentiation. However, CFBA-1 was highly expressed in both ECO samples and osteogenic control. CFBA-1 is a transcription factor that is active in osteoblasts and trigger the osteocalcin (OCN) expression, which is an important osteogenic marker. Expression of this factor also represents cells ability to undergo hypertrophy. After 5 weeks, ECO samples presented a more evident safranin staining, a low expression of SOX-9, whereas the CFBA-1 expression was maintained upregulated. In osteogenic control was observed the production of bone matrix and CFBA-1 expression higher than ECO samples. Thus, it proves that UCMSCs are also able to undergo ECO in the same conditions defined for BMMSCs. Despite of the evidences of ECO, more osteogenic markers should have been tested for a deeper osteogenic evaluation.[59] The most promising scaffold-based strategies are summarized in Table 1.

3.3.2 Scaffold-free approaches

The scaffold-free approaches include all the strategies that do not need cells adherence to a biomaterial.[102] This strategy is used when cells are able to produce enough ECM to support themselves. Usually, cells are used as cell aggregates, tissue strands or cells sheets. Also, these building blocks should be able to unite and form larger structures.[103]

ASCs aggregates were cultured sequentially in chondrogenic and hypertrophic media, for different periods. After subcutaneous implantation in CD1 nu/nu nude mice, for 8 weeks, a successful ECO could be noticed, including bone-like ECM formation, a proper integration with the host vasculature, and [104] the presence of bone marrow components.[105] BMMSCs cultured in proliferation medium with AA for 10 days and then exposed to 0,25% trypsin-EDTA solution for 5-7 minutes, achieved the deposition of a denser and well-structured ECM, by promoting the deposition of insoluble collagen and the ECM contraction, respectively. The cell aggregates, created by this protocol, were sequentially cultured in chondrogenic medium and in osteogenic medium, for 4 weeks each, to reproduce the ECO process. Samples were also cultured for 8 weeks in osteogenic medium, representing the IMO approach (control). Chondrogenic (SOX9, COL II), hypertrophic (IHH) and osteogenic (osterix [OSX], OCN, osteopontin [OPN]) markers were evaluated during the following 56 days. ECO constructs showed the highest expressions of chondrogenic, hypertrophic, and osteogenic markers during all the experiment. In particular, the peak of the genetic expressions occurred at day 14 for the hypertrophic marker, at day 28 for the chondrogenic markers, and at day

56 for the osteogenic markers. As expected, the expression of the osteogenic markers increased when the osteogenic medium was used. During the 56 days of the experiment, ALP activity was always increasing. Interestingly, ECO constructs showed higher Young's modulus compared to IMO. It was also possible to understand that in the beginning of the *in vitro* ECO process, the MSCs condensation was mediated by N-cadherin as observed previously *in vivo*.[46] When compared to IMO, the major drawback of an ECO approach it is the time-consuming character. ECO models require an intermediate step, namely several weeks of *in vitro* manipulation to obtain the cartilaginous template that is able to induce hypertrophy of MSCs-derived chondrocytes. In an attempt to shorten the culture time of the ECO process, pulsed electromagnetic field (PEMF) stimuli has been used.[106] Firstly, rat BMMSCs were cultured in a 3D pellet culture system using chondrogenic medium and were divided into three groups. Such groups were exposed to different intensities of PEMF (1, 2, or 5 mT) for 4 weeks. The hypothesis is that PEMF induces MSCs-derived chondrocytes to undergo hypertrophy in the absence of supplemental factors added to the culture medium. Chondrogenic (GAG, COL II, *SOX9*, TGF-β3) and hypertrophic (COL X) markers were evaluated during the experiment. The three different PEMF intensities did not affect cell proliferation but seemed to decrease the maintenance of the cartilaginous template and accelerate the ECM degradation. Importantly, 1 mT PEMF samples showed the highest expression of COL X, the hallmark of hypertrophic cartilage, compared with the other groups and the control (chondrogenic supplementation and no PEMF stimuli). Thus, another group was tested by culturing the pellets 3 weeks in chondrogenic medium and 1 week in hypertrophic medium, under a 1 mT PEMF stimulus. A control group was created following the same conditions but without any PEMF stimuli. The evaluation of chondrogenesis resulted in similar results to those previously mentioned. However, COL X was more expressed in the control group than in the experimental group, indicating that PEMF may have caused the differentiation of hypertrophic chondrocytes into osteoblasts. Regarding osteogenic evaluation, 1 mT PEMF condition resulted in high expression of the BSP, COL I, and OSX markers in both experimental groups, with and without hypertrophic cues. These results showed that the last step of ECO, the formation of a bone-like tissue, was promoted, even without any hypertrophic cues. Nevertheless, it would have been important to test the behavior of endothelial cells in these conditions since ECO approaches are characterized by the release of endothelial factors, and because bone is a vascularized tissue and so it is necessary to guarantee an efficient vascularization of the construct to proclaim a valid ECO approach.[106] Another approach to minimize the *in vitro* time necessary to induce ECO consisted of developing a controlled drug delivery system, which also aimed to avoid the necessity of recurrent supplementation by culture media exchanges. For that, BMMSCs aggregates were cultured in chondrogenic media supplemented with TGF-β1, and subsequently in osteogenic media supplemented with BMP-2, for different periods to test the proper moment to exchange the culture

media. GAGs and calcium content evaluation showed that 2 weeks of chondrogenic supplementation followed by 3 weeks of osteogenic supplementation are the conditions that obtained improved chondrogenic and osteogenic differentiation levels. Then, TGF-β1 and BMP-2 were loaded in gelatin (GM) or mineral-coated hydroxyapatite microparticles (MCM) respectively, to test their release behavior. Researchers knew that TGF-β1 release by GM was faster due to previous works. The control group consisted in cell aggregates cultured the first 2 weeks with chondrogenic medium with TGF-β1, and then 3 weeks with osteogenic medium with BMP-2, by exogenous and repeated supplementation. Comparing to the control, the system created was able to accelerate chondro- and osteogenesis, at week 2, proved by GAG quantification and ALP activity analysis. At the end of week 5, these aggregates showed higher levels of mineralization and bone markers (calcium, COL I, OPN, OCN). Without requiring the repeated supplementation of the culture media, this system represents a solution to achieve a faster implantation.[107] Whereas others took 7 to 8 weeks to induce ECO, this model successfully reduced cell culture time to 5 weeks. The angiogenic induction and evaluation in *in vitro* ECO approaches remains a poorly investigated topic. An interesting study uses mouse BMMSCs scaffold-free constructs system to recapitulate ECO, creating a vascular network, and explored the effect of the constructs on the maintenance of the vascular network. The constructs were built by seeding the cells in the holes of a thermo-responsive poly-N-isopropylacrylamide hydrogel, that is used as a mold. After 12h of culture, the constructs can be collected by decreasing the temperature from 37°C to RT. Then, 3D constructs were cultured in hypoxia conditions and using an osteogenic medium to stimulate both chondrogenesis and osteogenesis, respectively. Also, a constant stirring was necessary to avoid the adhesion of the constructs to the culture substrate. Chondrogenic, hypertrophic and osteogenic markers were evaluated up to 50 days. Alcian blue and Col *II* staining proved the cartilaginous nature of the constructs. These constructs presented an increase in Col *X* expression in inner layers over time, evidencing a maturation process of the cartilage tissue. Von Kossa staining allowed to evaluate the mineralization of the constructs, where the cartilaginous aggregates showed a mineralized core, resembling the beginning of ECO. OPN and OCN stainings revealed that no osteogenic differentiation occurred, because osteopontin, that is also produced by chondrocytes, was present but not OCN, which is exclusive of osteocytes. Despite not having accomplished the formation of a bone-like tissue, it was obtained a mature chondrogenic construct, with evidences of hypertrophic chondrocytes.[100] The most promising scaffold-free strategies are summarized in Table 2.

3.3.3 Cell-free approaches

Cell-free approaches only use the biomaterial architecture and composition to induce ECO. Without cell transplantation, they present less disadvantages regarding *ex vivo* cell manipulation, the risk of developing tumors and the ethical discussion.[108] On the other hand, they have to present the ability to recruit the host cells to the injury place and allow their differentiation *in situ*.[101,109] One strategy is to create a local delivery system of biomolecules to induce bone regeneration, as for example with parathyroid hormone (PTH). Several quantities of PTH (0, 1, 3, 10, or 30 μg) were loaded in a thiol-ene hydrogel and then polymerized with a poly (propylene fumarate) (PPF) scaffold. The biomaterial was able to release 80% of PTH in 3 days and what was left until day 14. Usually growth factors have a short half-life[110], but the bioactivity of the biomolecule was confirmed, and it lasted until 21 days. This biomaterial was tested in critical size femoral defects of Male Sprague–Dawley rats. There was no complete bone union, however all samples in the 10 μg PTH condition evidenced ECO because the two sides of the defect were connected by bone or a mixture of bone and hypertrophic chondrocytes. These are promising results when compared with the other conditions and with non-loaded biomaterial condition.[111] However, the majority of cell-free approaches do not use growth factors in its formulation because of their short half-life time, the increased costs, and their possible immunogenicity and toxicity.[110,112] So the next generation of approaches have provided other mechanical and structural cues to fulfill the lack of biochemical supplementation. Scaffold porosity became increasingly relevant in bone repair and has been subject of several studies. 3D printing β-tricalcium phosphate scaffolds with three different porous size, namely 100, 250 and 400 μm were implanted to improve bone repair.[113] Calcium phosphate materials are widely applied in bone TE strategies.[114–116] The scaffolds were placed in tibia bone defects, a long bone model inherently associated with ECO repair, of New Zealand rabbits. Animals were euthanized at weeks 1, 2 and weeks 4, 8 for vascularization and bone repair evaluation, respectively. During the two first time-points, cells were collected from the scaffold and their protein expression was analyzed by western blot (Sox9, Col II, Runx2, Col I and VEGF). The 400 μm scaffold showed an increased expression of Sox9 and Col-II at the first week, as well as higher vascularization at the second week, assessed by VEGF staining and immunochemistry assay, than the other two scaffolds. At week 4, histological sections of the scaffold were used for H&E and Masson's trichrome staining and the 400 μm scaffold presented more mineralized bone tissue, while the other conditions presented more connective tissue. In the end of experiment (week 8) the 400 μm scaffold achieved the greatest bone repair of the defects.[113] Beyond the importance of porosity of the scaffold, the pores alignment showed to be also relevant in the induction of ECO. Three different collagen scaffolds, with a pore network alignment perpendicular to bone marrow or with random alignment, were tested in vitro with seeded BMMSCs

and then, in vivo, with cell-free implantation in femoral bone defects of Sprague-Dawley rats.[117] In vitro, the expression of osteogenic (OCN and OPN), chondrogenic (aggrecan) and hypertrophic (GAGs) factors was evaluated. In vivo evaluation was made by second harmonic imaging and micro-computed tomography. The collagen scaffold with the same pore alignment as the bone marrow allowed to obtain ECO repair across the bone defect and higher host cells recruitment. Although, tissue vascularization proved to be easier in the other scaffolds, the present vascularization was enough to improve tissue repair.[117] The photofunctionalization of biomaterials is also used to enhance the potential of bone regeneration. A biomaterial with dome-like structure, composed by cobalt–chromium–molybdenum alloy, was tested with and without UVC irradiation when implanted in rabbit tibiae. The goal was to understand if the photofunctionalization enhances bone formation. The results were obtained by x-ray and computerized tomography analysis and, also, H&E histology. This approach shown bone formation by ECO, however, more conclusive results are needed.[118]

Hypoxia is described as a favorable condition to enhance ECO bone formation. Thus, a biomaterial able to generate hypoxia condition was used in vitro and in vivo to recapitulate ECO process. This biomaterial was an injectable hydrogel constituted by poly (glycerol sebacate)-co-poly (ethylene glycol)/polyacrylic acid (PEGS/PAA) that induces hypoxia by iron-chelation. The experiment in vitro used macrophages-like cells and HUVECs to understand if the hydrogels with BMMSCs can polarize the macrophages and induce angiogenesis, respectively. Furthermore, the expression of the hypoxia-inducible factor 1α by macrophages-like cells was evaluated, because induces early-stage chondrogenesis and late-stage angiogenesis in ECO process repair. The hypoxia condition proved to induce the HIF-1α expression, and consequently, bone repair. A stable HIF-1α expression was important to obtain higher efficiency ECO bone repair.[109] The most promising cell-free strategies are summarized in Table 3.

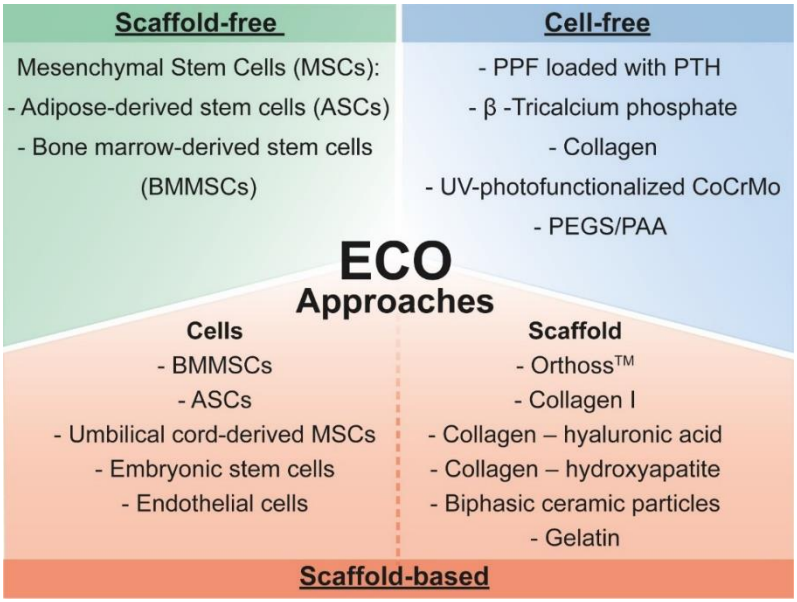

Figure 2. Representation of the most used cell types and biomaterials in the different ECO approaches; Division of the ECO approaches according to their use of only cells (scaffold-free approaches), only biomaterials (cell-free approaches) or a combination of both (scaffold-based approaches).
PPF- poly (propylene fumarate); PTH- parathyroid hormone; CoCrMo- cobalt–chromium–molybdenum alloy; PEGS/PAA- poly (glycerol sebacate)-co-poly (ethylene glycol)/polyacrylic acid;

Table 1– ECO scaffold-based approaches. (continued on the next page, 1/2)
Abbreviations: β-GP – β-glycerophosphate; AA – Ascorbic acid; ATB – antibiotic-antimycotic; DEX – dexamethasone; DMEM - Dulbecco's modified Eagle's medium; FBS – fetal bovine serum; ITS – insulin-transferrin-selenium; TGF – transforming growth factor.

Authors	Cell type	*In vitro* culture				*In vivo* study	Outcome
		Chondrogenic supplementation	Time	Hypertrophic supplementation	Time		
Marmotti *et al.* [59]	Umbilical cord MSCs	Chondrogenic differentiation Kit (EuroClone)	3 weeks	10mM Hepes Buffer, 1mM Na pyruvate, 1% ATB, 1% ITS-A, 4.7 μg/ml linoleic acid, 1.25mg/ml human serum albumin, 0.1 mM AA, 10^{-8} M DEX, 10 mM β-GP, 0.05 μM L-thyroxin	2 weeks	-	UCMSCs were seeded in Orthoss® granules and cultured in the described conditions. Two control groups were also tested using osteogenic or basal media. After 3 weeks, the deposition of the cartilaginous matrix and a slight upregulation of *SOX-9* expression was observed. *CBFA-1* was upregulated in both endochondral and osteogenic control groups. After 5 weeks, *SOX-9* was downregulated, while CBFA-1 upregulated.
Jukes *et al.* [96]	Embryionic stem cells	100 nM DEX, 50 µg/ml AA, 100 µg/ml sodium pyruvate, 40 µg/ml proline, and ITS-plus.	3 weeks	10^{-7} M retinoic acid (first 3 days), 0.2 mM AA, 2.5 µM compactin and 0.01 M β-GP	3 weeks	3 weeks	ESCs were seeded in biphasic calcium phosphate ceramic particles and were cultured in chondrogenic or osteogenic medium for 21 days. After implanted in nude mice it was possible to observe a gradual change of cartilage turning into bone. Bone tissue seemed to have a similar structure to bone marrow. Researchers observed that isolated chondrocytes do not produce the same results as derived chondrocytes, because no signs of ECO were found.
Thompson *et al.* [47]	Bone-marrow MSCs	20 ng/mL TGF-β3, 50 mg/mL AA, 40 mg/mL Proline, 100 nM DEX, 1xITS, 0.11 mg/mL sodium pyruvate	3 weeks	1 nM DEX, 1xITS 1nM l-thyroxine, 50 mg/mL AA, and 10mM β-GF	2 weeks	8 weeks	BMMSCs were seeded in collagen–hyaluronic acid (CHyA) and collagen–hydroxyapatite (CHA) scaffolds. Constructs were implanted Fischer F344 rats. Both ECO constructs enhanced *in vivo* vascularization. CHyA constructs presented the highest cartilage formation *in vitro* and the highest bone formation *in vivo* compared with CHA.

Table 1 - ECO scaffold-based approaches. (continuation 2/2)
Abbreviations: β-GP – β-glycerophosphate; AA – Ascorbic acid; ATB – antibiotic-antimycotic; DEX – dexamethasone; DMEM - Dulbecco's modified Eagle's medium; FBS – fetal bovine serum; ITS – insulin-transferrin-selenium; TGF – transforming growth factor.

Authors	Cell type	*In vitro* culture				*In vivo* study	Outcome
		Chondrogenic supplementation	Time	Hypertrophic supplementation	Time		
Daly *et al.* [97]	Bone marrow MSCs	100 U/ml penicillin, 100 µg/ml streptomycin, 100 µg/ml sodium pyruvate, 40 µg/ml L-proline, 50 µg/ml AA, 4.7 µg/ml linoleic acid, 1.5 mg/ml BSA, 1xITS, 100 nM DEX, 2.5 µg/ml amphotericin B, 500 ng/ml BMP-2 and 10 ng/ml TGF-β3	2 weeks	-	-	8 weeks	BMMSCs were seeded in GelMA hydrogel with 3D printed microchannels. These scaffolds were cultured in chondrogenic medium for 4 weeks. During the first 2 weeks of *in vitro* culture, scaffolds were exposed to 5% partial pressure of oxygen (pO_2), and then to 20% pO_2. Finally, the scaffolds were implanted in critical size defects of rats. Bone deposition was not as high as in the positive control, without microchannels, however the scaffolds with microchannels showed an improved interaction with the host cells, enhanced vascularization, and hydrogel degradation.
Leijten et *al.* [98]	Bone marrow MSCs	10 ng/mL TGF-β3	5 weeks	-	-	5 weeks	BMMSCs aggregates were cultured *in vitro* in chondrogenic medium and hypoxia (2.5%) or normoxia (21%) conditions. Aggregates were incorporated in sodium alginate hydrogels and implanted for 5 weeks in mice. Oxygen tension revealed to be an important factor to direct cell differentiation. In the end, only normoxia-preconditioned scaffolds showed matrix calcification, vascularization, and evidence of ECO.
Mikael *et al.* [101]	Bone marrow MSCs	10 nM TGF-β1, 1xITS, linoleic-BSA, 50 mg/mL ascorbate-2-phosphate, 100 mg/mL sodium pyruvate, 40 mg/mL proline and 100 nM DEX	2 weeks	50 nM Thyroxine, 7 mM β-GP, ITS+1, 50 µg/mL ascorbate-2-phosphate, 100 µg/mL sodium pyruvate, 40 µg/mL proline and 0.01 µM DEX.	2 weeks	8 weeks	BMMSCs were seeded in poly (85% lactide-co-15% glycolide) acid to attempt ECO. Scaffolds were cultured 4 weeks *in vitro*, to obtain the hypertrophic cartilaginous templates. Then, new BMMSCs were encapsulated with the scaffolds and implanted in mice. The hypertrophic cartilaginous templates were successfully obtained and after implanted, the new deposited matrix revealed to recruit host cells and enhance bone regeneration.

Table 2– ECO scaffold-free approaches.
Abbreviations: β-GP – β-glycerophosphate; AA – Ascorbic acid; ATB – antibiotic-antimycotic; DEX – dexamethasone; DMEM - Dulbecco's modified Eagle's medium; FBS – fetal bovine serum; ITS – insulin-transferrin-selenium; TGF – transforming growth factor.

Authors	Cell type	*In vitro* culture				*In vivo* study	Outcome
		Chondrogenic supplementation	Time	Hypertrophic supplementation	Time		
Wang *et al.* [106]	Bone marrow MSCs	Cyagen kit 100ml/L DEX, 3ml/L AA, 10ml/L ITS, 1ml/L sodium pyruvate, 1ml/L proline and 10 ml/L TGF- β3	3 weeks	10^{-8} M DEX, $2.5x10^{-4}$M AA, 50nM thyroxine, $7x10^{-3}$ M β-GP	1 week	-	BMMSCs aggregates were cultured in chondrogenic medium, exposed to 3 different pulsed electromagnetic (PEMF, 1, 2 and 5 mT), for 4 weeks. Only the 1 mT PEMF presented an improved degradation of the cartilaginous ECM and high levels of COL X expression. Then, a new condition was tested, namely 3 weeks of culture in chondrogenic medium and 1 week in hypertrophic medium, under a 1 mT PEMF stimulus. Results indicate that PEMF and hypertrophic supplementation may have caused the differentiation of hypertrophic chondrocytes into osteoblasts. This was reinforced by the high expression of osteogenic markers, namely BSP, COL I, and OSX. Even without the hypertrophic cues, 1 mT PEMF also presented high expression of these markers.
Sasaki *et al.* [100]	Bone marrow MSCs	-	-	10^{-2} M β-GP, 50 mg mL^{-1} AA and $1x10^{-6}$ M DEX	3 weeks	-	BMMSCs aggregates were cultured in hypoxia conditions and osteogenic supplementation simultaneously to induce to induce chondrogenic and osteogenic differentiation, respectively. Chondrogenic, hypertrophic and osteogenic markers were evaluated. Cartilaginous aggregates showed a mineralized core, resembling the beginning of ECO. OPN was present but not OCN. Despite not having accomplished the complete formation of a bone-like tissue, it was obtained a hypertrophic cartilaginous construct and osteogenic differentiation evidence.
Liu *et al.* [46]	Bone marrow MSCs	1% ATB, 1% ITS, 100 nM DEX, 50 μM AA, 23 μM L-proline, and 10 ng/mL TGF-β3	4 weeks	1% ATB, 10% FBS, 5mM β-GP, 10 nM DEX, and 50 μg/mL AA.	4 weeks	4 weeks	BMMSCs were cultured to promote the deposition of a denser ECM. The aggregates, created by this protocol, were sequentially cultured in chondrogenic medium and in osteogenic medium, for 4 weeks each, to reproduce the ECO process. Samples were also cultured for 8 weeks in osteogenic medium (IMO). Chondrogenic, hypertrophic and osteogenic markers were evaluated during the following 56 days. ECO constructs showed the highest expressions of chondrogenic, hypertrophic, and osteogenic markers.

Table 3. ECO cell-free approaches.

Authors	Biomaterial	Previous treatment/stimuli	*In vivo* study	Outcome
Wojda *et al.* [111]	Poly-propylene fumarate (PPF)	Parathyroid hormone loaded biomaterial	12 weeks	Several quantities of parathyroid hormone (PTH, 0, 1, 3, 10, or 30 µg) were loaded in a thiol-ene hydrogel and then polymerized with PPF biomaterial. This biomaterial was able to release 80% of PTH in 3 days and what was left until day 14. This biomaterial was tested in critical size femoral defects in rats. There was no complete bone union, however all samples in the 10 µg PTH condition evidenced ECO because the two sides of the defect were connected by bone or a mixture of bone and hypertrophic chondrocytes.
Diao *et al.* [113]	β-tricalcium phosphate	Three different porous size: 100, 250 and 400 µm	8 weeks	3D printed β-tricalcium phosphate biomaterials, with three different porous size, were implanted in tibia bone defects of New Zealand rabbits. Vascularization and bone repair evaluation was made up to 8 weeks. The 400 µm biomaterial showed an increased expression of chondrogenic markers, as well as higher vascularization at the second week, comparing to the other two biomaterials. At week 4, the 400 µm biomaterial presented more mineralized bone tissue, while the other conditions presented more connective tissue. In the end of experiment this biomaterial achieved the greatest bone repair of the defects.
Petersen *et al.* [117]	Collagen	Three different porous alignment: Equal to the bone marrow, perpendicular to bone marrow or random alignment,	6 weeks	Three different collagen scaffolds, with a pore network alignment as the bone marrow, perpendicular to bone marrow or with random alignment, were implanted in femoral bone defects of Sprague-Dawley rats to understand the influence of pore alignment in an ECO biomaterial. The collagen scaffold with the same pore alignment as the bone marrow allowed to obtain ECO repair across the bone defect and higher host cells recruitment. Although, tissue vascularization proved to be easier in the other scaffolds, the present vascularization was enough to improve tissue repair.
Zuchuat *et al.* [118]	cobalt–chromium–molybdenum alloy	Photofunctionalization with UVC irradiation	6 weeks	A cobalt–chromium–molybdenum alloy was tested with and without UVC irradiation when implanted in rabbit tibiae. The results obtained by x-ray and computerized tomography analysis and, also, H&E histology showed evidence of bone formation by ECO, however, more conclusive results are needed.

4. Conclusions

The majority of bone TE strategies rely on the mimicking of the IMO process. More recently, with the development of bone TERM, ECO is believed as the key to solve the main drawback of the preview strategy, namely the lack of vascularization of the mineralized microtissues. The existence of an intermediate hypertrophic cartilage template allows the production of not only osteogenic but also angiogenic factors, that induce bone formation/repair, while recruiting the host blood vessels. ECO approaches reported in the literature are very diversified, using different cell types, biomaterial, culture medium and stimuli timings. Regarding the cell types used, MSCs and ECs co-culture is the most promising setup due to the described crosstalk between these two cell types, and the hypertrophic cartilage template in the native environment of a bone fracture. Thus, the combination of these with hypertrophic chondrocytes can promote the osteogenic differentiation of the MSCs and the recruitment of ECs. However, optimal co-culture conditions are not yet well established. The biomaterials most important features are the diffusion of the nutrients, composition and stiffness, which should resemble the native ECM, and a porosity (~100-400 μm) that allows the scaffold invasion by blood vessels when implanted. Also, collagen is the most used polymer in biomaterials for ECO repair.

Cell culture is composed usually by two main steps, first the cells are cultured with chondrogenic supplementation factors to create the cartilage template and then, cultured with hypertrophic supplementation factors, which are quite similar to osteogenic factors. The hypertrophic medium is essentially an osteogenic medium but applied to cartilaginous tissue, which results in a different output.

Cells and biomaterials are not always used together mandatorily. Beyond the well-known scaffold-based approaches there are also scaffold-free and cell-free approaches, where are only used cells and biomaterials, respectively. Both approaches present examples where ECO repair is achieved. Highlight for the scaffold-free approach that enhanced the ECO process without hypertrophic supplementation, by using pulsed electromagnetic field stimuli in MSCs aggregates and, also for cell-free approaches, growth factors free, that enhance ECO repair through the optimization of the biomaterial porosity.

A lack of full *in vitro* ECO approaches exists when compared to all the *in vivo* studies executed. *In vitro* approaches can also be useful for a general understanding and improvement of the ECO process.

5. References

1. Ho-shui-ling, A. *et al.* Bone regeneration strategies: engineered scaffolds, bioactive molecules and stem cells Current stage and future perspectives. *Biomaterials* (2018). doi:10.1016/j.biomaterials.2018.07.017
2. Kiernan, C., Knuth, C. & Farrell, E. Endochondral Ossification: Recapitulating Bone Development for Bone Defect Repair. *Dev. Biol. Musculoskelet. Tissue Eng.* 125–148 (2018). doi:10.1016/B978-0-12-811467-4.00006-1
3. IOF - International Osteoporosis Foundation. Broken bones, broken lives. Available at: https://www.iofbonehealth.org/broken-bones-broken-lives. (Accessed: 21st February 2020)
4. WHO. *Assessment of osteoporosis at the primary health care level*. (2007).
5. Epple, C. *et al.* Prefabrication of a large pedicled bone graft by engineering the germ for de novo vascularization and osteoinduction. *Biomaterials* **192**, 118–127 (2019).
6. Giannoudis, P. V, Dinopoulos, H. & Tsiridis, E. Bone substitutes : An update. 20–27 (2005). doi:10.1016/j.injury.2005.07.029
7. Aghajanian, P. & Mohan, S. The art of building bone: Emerging role of chondrocyte-to-osteoblast transdifferentiation in endochondral ossification. *Bone Res.* **6**, (2018).
8. Wardlaw, D. *et al.* Efficacy and safety of balloon kyphoplasty compared with non-surgical care for vertebral compression fracture (FREE): a randomised controlled trial. *Lancet* **373**, 1016–1024 (2009).
9. Cited, R., Systems, T. T., Incorporated, T. S., The, A. & Company, B. Devices, kit and method for kyphoplasty. **2**, (2014).
10. Domb, B. G., El Bitar, Y. F., Sadik, A. Y., Stake, C. E. & Botser, I. B. Comparison of robotic-assisted and conventional acetabular cup placement in THA: A matched-pair controlled study hip. *Clin. Orthop. Relat. Res.* **472**, 329–336 (2014).
11. Thompson, E., Matsiko, A., Farrell, E., Kelly, D. & O'Brien, F. Recapitulating endochondral ossification: a promising route to in vivo bone regeneration. *J. Tissue Eng. Regen. Med.* 889–902 (2014). doi:10.1002/term
12. Sheehy, E. J., Kelly, D. J. & O'Brien, F. J. Biomaterial-based endochondral bone regeneration: a shift from traditional tissue engineering paradigms to developmentally inspired strategies. *Mater. Today Bio* **3**, 100009 (2019).
13. Wong, S. A. *et al.* Microenvironmental Regulation of Chondrocyte Plasticity in Endochondral Repair — A New Frontier for Developmental Engineering. **6**, 1–14 (2018).
14. Gorbet, M. B. & Sefton, M. V. Biomaterial-associated thrombosis: Roles of coagulation factors, complement, platelets and leukocytes. *Biomaterials* **25**, 5681–5703 (2004).
15. Gerstenfeld, L. C. *et al.* Impaired intramembranous bone formation during bone repair in the absence of tumor necrosis factor-alpha signaling. *Cells Tissues Organs* **169**, 285–294 (2001).
16. Rundle, C. H. *et al.* Microarray analysis of gene expression during the inflammation and endochondral bone formation stages of rat femur fracture repair. *Bone* **38**, 521–529 (2006).
17. Franz, S., Rammelt, S., Scharnweber, D. & Simon, J. C. Immune responses to implants - A review of the implications for the design of immunomodulatory biomaterials. *Biomaterials* **32**, 6692–6709 (2011).
18. Vervloet, M. G., Thijs, L. G. & Hack, C. E. Derangements of coagulation and fibrinolysis in critically ill patients with sepsis and septic shock. *Semin. Thromb. Hemost.* **24**, 33–44 (1998).
19. Baht, G. S., Vi, L. & Alman, B. A. The Role of the Immune Cells in Fracture Healing. *Curr. Osteoporos. Rep.* **16**, 138–145 (2018).
20. García-García, A. & Martin, I. Extracellular Matrices to Modulate the Innate Immune Response and Enhance Bone Healing. *Front. Immunol.* **10**, 1–8 (2019).
21. Batoon, L. *et al.* CD169 + macrophages are critical for osteoblast maintenance and promote intramembranous and endochondral ossification during bone repair. *Biomaterials* **196**, 51–66 (2019).
22. Cho, S. W. *et al.* Osteal macrophages support physiologic skeletal remodeling and anabolic actions of parathyroid hormone in bone. *Proc. Natl. Acad. Sci. U. S. A.* **111**, 1545–1550 (2014).
23. Jiang, W. & Xu, J. Immune modulation by mesenchymal stem cells. *Cell Prolif.* (2019). doi:10.1111/cpr.12712
24. Mansour, A. *et al.* Bone extracts immunomodulate and enhance the regenerative performance of dicalcium phosphates bioceramics. *Acta Biomater.* **89**, 343–358 (2019).

25. Rayahin, J. E., Buhrman, J. S., Zhang, Y., Koh, T. J. & Gemeinhart, R. A. High and Low Molecular Weight Hyaluronic Acid Di ff erentially In fl uence Macrophage Activation. (2015). doi:10.1021/acsbiomaterials.5b00181
26. Scotti, C. *et al.* Engineering of a functional bone organ through endochondral ossification. *Proc. Natl. Acad. Sci. U. S. A.* **110**, 3997–4002 (2013).
27. Nishimura, R., Hata, K., Nakamura, E., Murakami, T. & Takahata, Y. Transcriptional network systems in cartilage development and disease. *Histochem. Cell Biol.* **149**, 353–363 (2018).
28. Ikegami, D., Akiyama, H., Suzuki, A., Nakamura, T. & Nakano, T. Sox9 sustains chondrocyte survival and hypertrophy in part through Pik3ca-Akt pathways. **1519**, 1507–1519 (2011).
29. Berendsen, A. D. & Olsen, B. R. Bone development. *Bone* **80**, 14–18 (2015).
30. Scotti, C., Tonnarelli, B., Papadimitropoulos, A., Scherberich, A. & Schaeren, S. Recapitulation of endochondral bone formation using human adult mesenchymal stem cells as a paradigm for developmental engineering. **107**, (2010).
31. Samsa, W. E., Zhou, X. & Zhou, G. Signaling Pathways Regulating Cartilage Growth Plate Formation and Activity. *Semin. Cell Dev. Biol.* (2016). doi:10.1016/j.semcdb.2016.07.008
32. Studer, D., Millan, C., Maniura-weber, K. & Zenobi-wong, M. Molecular and biophysical mechanisms regulating hypertrophic differentiation in chondrocytes and mesenchimal stem cells. **24**, 118–135 (2012).
33. Houben, A. *et al.* B-Catenin Activity in Late Hypertrophic Chondrocytes Locally Orchestrates Osteoblastogenesis and Osteoclastogenesis. *Dev.* **143**, 3826–3838 (2016).
34. Chen, Y. *et al.* Beta-catenin signaling plays a disparate role in different phases of fracture repair: Implications for therapy to improve bone healing. *PLoS Med.* **4**, 1216–1229 (2007).
35. Huang, Y. *et al.* Inhibition of β-catenin signaling in chondrocytes induces delayed fracture healing in mice. *J. Orthop. Res.* **30**, 304–310 (2012).
36. Chen, S., Lee, B. H. & Bae, Y. Notch Signaling in Skeletal Stem Cells. 68–77 (2014).
37. Hosaka, Y. *et al.* Notch signaling in chondrocytes modulates endochondral ossi fi cation and osteoarthritis development. *Proc. Natl. Acad. Sci.* (2012). doi:10.1073/pnas.1207458110
38. Occhetta, P., Stüdle, C., Barbero, A. & Martin, I. Learn, simplify and implement: developmental re-engineering strategies for cartilage repai. *Swiss Med. Wkly.* **146**, w14346 (2016).
39. Almubarak, S. *et al.* Tissue engineering strategies for promoting vascularized bone regeneration. *Bone* (2015). doi:10.1016/j.bone.2015.11.011
40. Gao, F. *et al.* Mesenchymal stem cells and immunomodulation: Current status and future prospects. *Cell Death Dis.* **7**, (2016).
41. P. De Miguel, M. *et al.* Immunosuppressive Properties of Mesenchymal Stem Cells: Advances and Applications. *Curr. Mol. Med.* **12**, 574–591 (2012).
42. Beyth, S. *et al.* Human mesenchymal stem cells alter antigen-presenting cell maturation and induce T-cell unresponsiveness. *Blood* **105**, 2214–2219 (2005).
43. Hu, C., Wu, Z. & Li, L. Pre - treatments enhance the therapeutic effects of mesenchymal stem cells in liver diseases. 1–10 (2019). doi:10.1111/jcmm.14788
44. Yoo, J. U. *et al.* The Chondrogenic Potential of Human Bone-Marrow-Derived Mesenchymal Progenitor Cells*. *JBJS* **80**, (1998).
45. Ohgushi, H., Goldberg, V. M. & Caplan, A. I. Heterotopic Osteogenesis in Porous Ceramics Induced by Marrow Cells. *J. Orthop. Res.* (1989).
46. Liu, Y., Kuang, B., Rothrau, B. B., Tuan, R. S. & Lin, H. Robust bone regeneration through endochondral ossi fi cation of human mesenchymal stem cells within their own extracellular matrix. **218**, (2019).
47. Thompson, E. M., Matsiko, A. & Kelly, D. J. An Endochondral Ossification-Based Approach to Bone Cell-Laden Scaffolds Support Greater Repair of Critical-Sized Cranial Defects Than Osteogenically Stimulated Constructs In Vivo. **22**, 556–567 (2016).
48. Farrell, E. *et al.* In-vivo generation of bone via endochondral ossification by in-vitro chondrogenic priming of adult human and rat mesenchymal stem cells. *BMC Musculoskelet. Disord.* **12**, (2011).
49. Hellingman, C. A. *et al.* Fibroblast growth factor receptors in in vitro and in vivo chondrogenesis: Relating tissue engineering using adult mesenchymal stem cells to embryonic development. *Tissue Eng. - Part A* **16**, 545–556 (2010).
50. Wexler, S. A. *et al.* Adult bone marrow is a rich source of human mesenchymal 'stem' cells but umbilical cord and mobilized adult blood are not. *Br. J. Haematol.* **121**, 368–374 (2003).
51. Kern, S., Eichler, H., Stoeve, J., Klüter, H. & Bieback, K. Comparative Analysis of Mesenchymal Stem Cells from Bone Marrow, Umbilical Cord Blood, or Adipose Tissue. *Stem Cells* **24**, 1294–1301

(2006).
52. Marcacci, M. *et al.* Stem cells associated with macroporous bioceramics for long bone repair: 6- To 7-year outcome of a pilot clinical study. *Tissue Eng.* **13**, 947–955 (2007).
53. Perez, J. R. *et al.* Tissue Engineering and Cell-Based Therapies for Fractures and Bone Defects. **6**, 1–23 (2018).
54. Di Bella, C., Farlie, P. & Penington, A. J. Bone regeneration in a rabbit critical-sized skull defect using autologous adipose-derived cells. *Tissue Eng. - Part A.* **14**, 483–490 (2008).
55. Cui, L. *et al.* Repair of cranial bone defects with adipose derived stem cells and coral scaffold in a canine model. *Biomaterials* **28**, 5477–5486 (2007).
56. Mesimäki, K. *et al.* Novel maxillary reconstruction with ectopic bone formation by GMP adipose stem cells. *Int. J. Oral Maxillofac. Surg.* **38**, 201–209 (2009).
57. Lendeckel, S. *et al.* Autologous stem cells (adipose) and fibrin glue used to treat widespread traumatic calvarial defects: Case report. *J. Cranio-Maxillofacial Surg.* **32**, 370–373 (2004).
58. Huang, R. L. *et al.* Dispersion of ceramic granules within human fractionated adipose tissue to enhance endochondral bone formation. *Acta Biomater.* **102**, 458–467 (2020).
59. Marmotti, A. *et al.* Allogeneic Umbilical Cord-Derived Mesenchymal Stem Cells as a Potential Source for Cartilage and Bone Regeneration : An In Vitro Study. **2017**, (2017).
60. Silva-cote, I. *et al.* Strategy for the Generation of Engineered Bone Constructs Based on Umbilical Cord Mesenchymal Stromal Cells Expanded with Human Platelet Lysate. **2019**, (2019).
61. Weiss, M. L. *et al.* Immune Properties of Human Umbilical Cord Wharton's Jelly-Derived Cells. *Stem Cells* **26**, 2865–2874 (2008).
62. Van Pham, P., Bich, N. V. & Phan, N. K. Umbilical cord-derived stem cells (ModulatistTM) show strong immunomodulation capacity compared to adipose tissue-derived or bone marrow-derived mesenchymal stem cells. *Biomed. Res. Ther.* **3**, 687–696 (2016).
63. Selich, A. *et al.* Umbilical cord as a long-Term source of activatable mesenchymal stromal cells for immunomodulation. *Stem Cell Res. Ther.* **10**, 1–14 (2019).
64. Tipnis, S., Viswanathan, C. & Majumdar, A. S. Immunosuppressive properties of human umbilical cord-derived mesenchymal stem cells: Role of B7-H1 and IDO. *Immunol. Cell Biol.* **88**, 795–806 (2010).
65. Gorin, C., Rochefort, G. Y., Bascetin, R. & Al., E. Priming Dental Pulp Stem Cells With Fibroblast Growth Factor-2 Increases Angiogenesis of Implanted Tissue-Engineered Constructs Through Hepatocyte Growth Factor. *Stem Cells Transl. Med.* 392–404 (2016).
66. Laino, G. *et al.* A new population of human adult dental pulp stem cells: A useful source of living autologous fibrous bone tissue (LAB). *J. Bone Miner. Res.* **20**, 1394–1402 (2005).
67. Wang, L. *et al.* Injectable calcium phosphate with hydrogel fibers encapsulating induced pluripotent, dental pulp and bone marrow stem cells for bone repair. *Mater. Sci. Eng. C* **69**, 1125–1136 (2016).
68. Collignon, A. M. *et al.* Mouse Wnt1-CRE-Rosa Tomato Dental Pulp Stem Cells Directly Contribute to the Calvarial Bone Regeneration Process. *Stem Cells* **37**, 701–711 (2019).
69. Zhang, Y., Huang, K., Yuan, Q., Gu, Z. & Wu, G. Development of Arg-Based Biodegradable Poly(ester urea) Urethanes and Its Biomedical Application for Bone Repair. *J Biomed Nanotechnol.* 1909–1922 (2019). doi:10.1166/jbn.2019.2818.
70. Schlundt, C. *et al.* Macrophages in bone fracture healing: Their essential role in endochondral ossification. *Bone* (2015). doi:10.1016/j.bone.2015.10.019
71. Jeong, C. G., Zhang, H. & Hollister, S. J. Three-dimensional polycaprolactone scaffold-conjugated bone morphogenetic protein-2 promotes cartilage regeneration from primary chondrocytes in vitro and in vivo without accelerated endochondral ossification. *J. Biomed. Mater. Res.* 2088–2096 (2012). doi:10.1002/jbm.a.33249
72. Roberts, S. J. *et al.* A Semi-Autonomous Model of Endochondral Ossification. **18**, 1334–1343 (2012).
73. Boyce, M. K. *et al.* Non-terminal animal model of post-traumatic osteoarthritis induced by acute joint injury. *Osteoarthr. Cartil.* **21**, 746–755 (2013).
74. Chindler, O. S. S. Current concepts of articular cartilage repair. **77**, 709–726 (2011).
75. Ghanaati, S. *et al.* Rapid vascularization of starch-poly(caprolactone) in vivo by outgrowth endothelial cells in co-culture with primary osteoblasts. *J. Tissue Eng. Regen. Med.* **5**, e136-43 (2011).
76. Lin, Y. *et al.* Combination of polyetherketoneketone scaffold and human mesenchymal stem cells from temporomandibular joint synovial fluid enhances bone regeneration. *Sci. Rep.* **9**, 1–13 (2019).
77. Matsumoto, T. & Kawamoto, A. Therapeutic Potential of Vasculogenesis and Osteogenesis

Promoted by Peripheral Blood CD34- Positive Cells for Functional Bone Healing. *Am. J. Pathol.* **169**, 1440–1457 (2006).
78. Correia, C. R. *et al.* Semipermeable capsules wrapping a multifunctional and self-regulated co-culture microenvironment for osteogenic differentiation. *Sci. Rep.* **6**, 1–12 (2016).
79. Correia, C. R. *et al.* In vivo osteogenic differentiation of stem cells inside compartmentalized capsules loaded with co-cultured endothelial cells. *Acta Biomater.* **53**, 483–494 (2017).
80. Stegen, S., Gastel, N. Van & Carmeliet, G. Bringing new life to damaged bone : The importance of angiogenesis in bone repair and regeneration. *Bone* (2014). doi:10.1016/j.bone.2014.09.017
81. Kasten, P. *et al.* Comparison of Platelet-Rich Plasma and VEGF-Transfected Mesenchymal Stem Cells on Vascularization and Bone Formation in a Critical-Size Bone Defect. 523–533 (2012). doi:10.1159/000337490
82. Guo, P. *et al.* Platelet-derived growth factor-B enhances glioma angiogenesis by stimulating vascular endothelial growth factor expression in tumor endothelia and by promoting pericyte recruitment. *Am. J. Pathol.* **162**, 1083–1093 (2003).
83. Mitlak, B. H. *et al.* The effect of systemically administered PDGF-BB on the rodent skeleton. *J. Bone Miner. Res.* **11**, 238–247 (1996).
84. Farrell, E. *et al.* Chondrogenic Priming of Human Bone Marrow Stromal Cells : A Better Route to Bone Repair ? *Tissue Eng. - Part C* **15**, (2009).
85. Mueller, M. B. & Zellner, J. Hypertrophy in Mesenchymal Stem Cell Chondrogenesis : Effect of TGF-β Isoforms and Chondrogenic Conditioning. *Cells Tissues Organs* 158–166 (2010). doi:10.1159/000313399
86. Grimsrud, C. D. *et al.* BMP signaling stimulates chondrocyte maturation and the expression of Indian hedgehog. *J. Orthop. Res.* **19**, 18–25 (2001).
87. Bach, L. A. Endothelial cells and the IGF system. *J. Mol. Endocrinol.* 1–13 (2015). doi:10.1530/JME-14-0215
88. Sheng, M. H. C., Zhou, X. D., Bonewald, L. F., Baylink, D. J. & Lau, K. H. W. Disruption of the insulin-like growth factor-1 gene in osteocytes impairs developmental bone growth in mice. *Bone* **52**, 133–144 (2013).
89. Langenbach, F. & Handschel, J. Effects of dexamethasone , ascorbic acid and β -glycerophosphate on the osteogenic differentiation of stem cells in vitro. (2013).
90. Mano, J. F. Designing biomaterials for tissue engineering based on the deconstruction of the native cellular environment. *Mater. Lett.* 1–5 (2014). doi:10.1016/j.matlet.2014.11.061
91. Di Luca, A. *et al.* Gradients in pore size enhance the osteogenic differentiation of human mesenchymal stromal cells in three-dimensional scaffolds. *Sci. Rep.* **6**, 1–13 (2016).
92. The use of human umbilical vein endothelial cells (HUVECs) as an in vitro model to assess the toxicity of nanoparticles to endothelium: a review. *J. Appl. Toxicol.* **JAT 37**, 1359–1369 (2017).
93. Chen, L. *et al. 3D printing of a lithium-calcium-silicate crystal bioscaffold with dual bioactivities for osteochondral interface reconstruction*. *Biomaterials* **196**, (Elsevier Ltd, 2019).
94. Diao, J. *et al.* 3D-Plotted Beta-Tricalcium Phosphate Scaffolds with Smaller Pore Sizes Improve In Vivo Bone Regeneration and Biomechanical Properties in a Critical-Sized Calvarial Defect Rat Model. *Adv. Healthc. Mater.* **7**, 1–9 (2018).
95. Roberts, S. J. *et al.* The combined bone forming capacity of human periosteal derived cells and calcium phosphates. *Biomaterials* **32**, 4393–4405 (2011).
96. Jukes, J. M. *et al.* Endochondral bone tissue engineering using embryonic stem cells. (2008).
97. Daly, A. C., Pitacco, P., Nulty, J., Cunniffe, G. M. & Kelly, D. J. 3D printed microchannel networks to direct vascularisation during endochondral bone repair. *Biomaterials* (2018). doi:10.1016/j.biomaterials.2018.01.057
98. Leijten, J., Georgi, N., Moreira, L., Blitterswijk, C. A. Van & Post, J. N. Metabolic programming of mesenchymal stromal cells by oxygen tension directs chondrogenic cell fate. (2014). doi:10.1073/pnas.1410977111
99. Nishiguchi, A., Yoshida, H., Matsusaki, M. & Akashi, M. Rapid construction of three-dimensional multilayered tissues with endothelial tube networks by the cell-accumulation technique. *Adv. Mater.* **23**, 3506–3510 (2011).
100. Sasaki, J. I. *et al.* In vitro reproduction of endochondral ossification using a 3D mesenchymal stem cell construct. *Integr. Biol. (United Kingdom)* **4**, 1207–1214 (2012).
101. Mikael, P. E., Golebiowska, A. A., Xin, X., Rowe, D. W. & Nukavarapu, S. P. Evaluation of an Engineered Hybrid Matrix for Bone Regeneration via Endochondral Ossification. *Ann. Biomed. Eng.* **48**, 992–1005 (2020).

102. Athanasiou, K. A., Eswaramoorthy, R., Hadidi, P. & Hu, J. C. Self-organization and the self-assembling process in tissue engineering. *Annu. Rev. Biomed. Eng.* **15**, 115–136 (2013).
103. Alsowayan, B. Scaffold-Free 3-D Cell Sheet Technique Bridges the Gap between 2-D Cell Culture and Animal Models. *Int. J. Mol. Sci.* (2019).
104. Ovsianikov, A., Khademhosseini, A. & Mironov, V. The Synergy of Scaffold-Based and Scaffold-Free Tissue Engineering Strategies. *Trends Biotechnol.* **36**, 348–357 (2018).
105. Osinga, R., Di Maggio, N., Todorov, A., Allafi, N. & Barbero, A. Generation of a Bone Organ by Human Adipose-Derived Stromal Cells Through Endochondral Ossification. *STEMCELLS Transl. Med.* 1090–1097 (2016).
106. Wang, J., Xiao, Q., Zhang, L., Li, Y. & Li, J. Pulsed Electromagnetic Field May Accelerate in vitro Endochondral Ossification. **44**, 35–44 (2015).
107. Dang, P. N., Dwivedi, N. & Phillips, L. M. Controlled Dual Growth Factor Delivery From Microparticles Incorporated Within Human Bone Marrow-Derived Mesenchymal Stem Cell Aggregates for Enhanced Bone Tissue Engineering via Endochondral Ossification. *STEMCELLS Transl. Med.* 206–217 (2016).
108. Goldring, C. E. P. *et al.* Assessing the Safety of Stem Cell. *Stem Cell* **8**, 618–628 (2011).
109. Sun, L. *et al.* Recapitulation of In Situ Endochondral Ossification Using an Injectable Hypoxia-Mimetic Hydrogel. *Adv. Funct. Mater.* **2008515**, 1–19 (2020).
110. Han, Q. Q., Du, Y. & Yang, P. S. The role of small molecules in bone regeneration. *Future Med. Chem.* **5**, 1671–1684 (2013).
111. Wojda, S. J., Marozas, I. A., Anseth, K. S., Yaszemski, M. J. & Donahue, S. W. Thiol-ene Hydrogels for Local Delivery of PTH for Bone Regeneration in Critical Size defects. *J. Orthop. Res.* **38**, 536–544 (2020).
112. Tannoury, C. A. & An, H. S. Complications with the use of bone morphogenetic protein 2 (BMP-2) in spine surgery. *Spine J.* **14**, 552–559 (2014).
113. Diao, J. *et al.* Bone Defect Model Dependent Optimal Pore Sizes of 3D-Plotted Beta-Tricalcium Phosphate Scaffolds for Bone Regeneration. **1900237**, 1–11 (2019).
114. Habraken, W., Habibovic, P., Epple, M. & Bohner, M. Calcium phosphates in biomedical applications: Materials for the future? *Mater. Today* **19**, 69–87 (2016).
115. Boyan, B. D. & Schwartz, Z. Are calcium phosphate ceramics 'smart' biomaterials? *Nat. Rev. Rheumatol.* **7**, 8–9 (2011).
116. Lima, D. B. *et al.* Injectable bone substitute based on chitosan with polyethylene glycol polymeric solution and biphasic calcium phosphate microspheres. *Carbohydr. Polym.* **245**, (2020).
117. Petersen, A. *et al.* A biomaterial with a channel-like pore architecture induces endochondral healing of bone defects. *Nat. Commun.* doi:10.1038/s41467-018-06504-7
118. Zuchuat, J., Maldonado, Y., Botteri, J. & Decco, O. In vivo effect of UV-photofunctionalization of CoCrMo in processes of guided bone regeneration and tissue engineering. *J. Biomed. Mater. Res.* (2020). doi:10.1002/jbm.a.37004

II. Materials and Methods

1. Cell isolation and characterization

Human umbilical cords (UC) from two newborn babies were used to isolate both human umbilical cord mesenchymal stem cells (UCMSCs) and human umbilical vein endothelial cells (HUVECs). The tissues were used under the approval of the Competent Ethics Committee (CEC), COMPASS Research Group and Centro Hospitalar do Baixo Vouga, Aveiro and thanks to a cooperation agreement made by the two institutions. The consent declaration was obtained from all subjects and the human UC were transported and handled according to CEC guidelines. The tissues were collected to a container with phosphate-buffered saline solution (PBS, Sigma-Aldrich) supplemented with 1% v/v antibiotic/antimycotic (ATB, ThermoFisher Scientific) and kept at 4°C until the isolation procedure. UCs were transported and processed in the laboratory facilities within 24h.

1.1. Isolation of Human Umbilical Cord Mesenchymal Stem Cells

UCMSCs were isolated from the Wharton's jelly of the human UC of newborns. UC washing was performed with sterile PBS several times to remove blood and blood clots. During the isolation procedure, the UC was maintained in ice. WJ-MSCs were isolated using the explant method.[1] Briefly, the UC was cut into small pieces (3 cm), and the vein and two arteries were removed. Small pieces of the Wharton's jelly were sliced from the cord with a sterile scalpel and placed separated on adherent Ø60 mm petri-dishes (Starsted). The tissues explants were incubated at 37ºC and 5% of CO_2 for 2h. Minimum Essential Medium Alpha (α-MEM, Gibco) supplemented with 1% ATB and 10% heat-inactivated fetal bovine serum (v/v, FBS, Gibco) was added until immersion of all the tissues, following incubation at 37ºC and 5% of CO_2. The explant cultures were left undisturbed for 5 days at 37ºC and 5% of CO_2 in a humidified atmosphere to allow the migration of UCMSCs from the tissues to the petri-dishes. After cell migration, the tissue explants were removed. The culture medium was changed every 3-4 days. At 90% confluence, UCMSCs were detached using 1x trypsin-EDTA (ThermoFisher Scientific) and seeded in adherent cell culture T75-flasks and expanded until passage 5 in α-MEM supplemented with 1% ATB and 10% FBS. Culture medium was changed every 3-4 days.

1.2. Isolation of Human Umbilical Vein Endothelial Cells

HUVECs were isolated from human UC vein of two newborns. The umbilical vein was washed with PBS, placing a catheter extender with side shunt (Vygon) at one end of the UC. To detach the endothelial cells from the vein walls, the UC was immersed in a solution containing 0.1% w/v

collagenase type IA (MP Biomedicals) at 37°C for 25 min. The HUVECs suspension was obtained rising the vein walls with M199 medium (Sigma-Aldrich) supplemented with 1% v/v endothelial cell growth supplement (ECGS, 40 mg/mL, Merck), 10% v/v heparin (100 mg/mL, Sigma-Aldrich), 20% v/v FBS, and 1% v/v ATB. The resultant cell suspension was cultured in a cell culture T25-flask (InVitro Cell) previously coated with 0.7% w/v gelatin (porcine skin type A, Sigma-Aldrich) for 20 minutes, at 37ºC and 5% of CO_2 in a humidified atmosphere. HUVECs were expanded in M199 medium until passage 3. Culture medium was changed every 3-4 days.[2]

1.3. *In vitro* characterization

Cell phenotype characterization was performed by flow cytometry (Flow Cytometry BD Accuri C6 Plus). Both cell types, MSCs and HUVECs, were dissociated with triple express (TrypLE™ Express Enzyme, phenol red, ThermoFisher Scientific) and resuspend in a staining/washing solution containing 2% bovine serum albumin (BSA, Sigma-Aldrich) and 0.1% sodium azide (w/v, TCI) prepared in PBS. Triple express was used because does not change the expression of cells surface antigens, while trypsin-EDTA decreases their expression.[3] MSCs were incubated with the antibodies PE-conjugated CD73 (1:20), AlexaFluor 647-conjugated CD90 (1:20) and AlexaFluor 488-conjugated CD105 (1:11). Incubation with fluorescein isothiocyanate (FITC)-conjugated CD34 (1:20), and allophycocyanin (APC)-conjugated CD31 (1:20) was performed as negative markers.[4,5] HUVECs were incubated with the antibody APC-conjugated CD31 (1:20).[6] FITC-conjugated CD34 (1:20) and AlexaFluor 647-conjugated CD90 (1:20) were used as a negative marker. All the antibodies were purchased from BioLegend, except AlexaFluor 488-conjugated CD105, which was acquired to Miltenyi Biotec. For each cell type, a control sample without antibodies was also prepared. After 1 h at RT protected from light, samples were washed in the washing/staining solution, and subsequently resuspended in the acquisition buffer composed by 1% formaldehyde (Sigma-Aldrich) and 0.1% (w/v) sodium azide in PBS until analysis.

2. *In vitro* culture of isolated cells

2.1 *In vitro* culture of Human Umbilical Cord Mesenchymal Stem Cells

UCMSCs were cultured in adherent cell culture T175-flasks (InVitro Cell). Cells were maintained in expansion in α-MEM supplemented with 1% ATB and 10% FBS at 37ºC in a humidified 5% of CO_2 atmosphere until bioencapsulation. The culture medium was changed twice a week. Cells were harvested with trypsin-EDTA, following incubation at 37ºC and 5% of CO_2 for 5 min. The enzymatic

digestion was neutralized with culture medium, and the obtained cell suspension was centrifuged at 300g for 5 minutes at RT. The detachment of cell was performed at 80-90% confluence. UCMSCs were used for the encapsulation procedures at passage 6.

2.2 *In vitro* culture of Human Umbilical Vein Endothelial Cells

HUVECs were cultured in adherent cell culture T175-flasks previously coated with 0.7% w/v gelatin. Cells were maintained in M199 supplemented with 1% v/v ECGS, 10% v/v heparin, 20% FBS, and 1% v/v ATB, at 37ºC in a humidified 5% of CO_2 atmosphere. The culture medium was changed twice a week. Cells were harvested with 1x trypsin-EDTA, following incubation at 37ºC and 5% of CO_2 for 5 min. The enzymatic digestion was neutralized with culture medium, and the obtained cell suspension was centrifuged at 300g for 5min at RT. The detachment of cell was performed at 80-90% confluence. HUVECs were used for the encapsulation procedures at passage 5.

3. 3D micro-cartilaginous templates production and characterization

3.1. Production of 3D micro-cartilaginous templates

UCMSCs were expanded in cell culture T175-flasks ($5x10^3$ cells/cm^2) in α-MEM medium, supplemented with 1% v/v ATB and 10 % v/v FBS at pH 7.4 and incubated at 37 ºC in a humidified air atmosphere of 5 % CO_2. The medium was changed twice a week and cells were used at passage 5. At 90% confluency, cells were washed with Dulbecco's phosphate buffered saline (DPBS) and detached with a EDTA (Merck) solution, at 37 °C for 5 min. The cell suspension was centrifuged (RT, 300 g, 5 min) and the pellet was re-suspended ($6x10^4$ cells mL^{-1}) in Dulbecco's Modified Eagle's medium-high glucose (DMEM-HG) medium, with 2% FBS and 1% ATB, without (basal) or with chondrogenic differentiation factors (chondro), namely sodium pyruvate (1 mM, Thermo Fisher), insulin-transferrin-selenium (ITS, 1%, Thermo Fisher), ascorbic acid (AA, 50 μg mL^{-1}, Merck), transforming growth factor-beta 3 (TGF-β3, 10 ng mL^{-1}, Merck), and dexamethasone (DEX, 100 nM, Sigma Aldrich). The 3D micro-templates were created in Aggrewell plates (AggreWell™ 400, StemCell) according to the manufactures' specifications, represented in Figure 3 (*I*). These plates were treated with 500 μL of an anti-adherence solution (Anti-Adherence Rinsing Solution, StemCell), add to each well and then were centrifuged (RT, 1300g, 5 min). The solution was aspirated, and the wells were rinsed with DPBS. Afterwards, 2 mL of cell suspension ($1.2x10^5$ cells $well^{-1}$) were transferred to each well of the Aggrewell plate and centrifuged (RT, 100 g, 3 min). The

Aggrewell plate with the cell aggregates was incubated at 37ºC and 5% of CO_2 in a humidified atmosphere up to 21 days. Half of the culture medium was exchange every 3-4 days. Samples were collected after 1, 14 and 21 days and characterized.

3.2. Cell viability

Cell viability of 3D micro-templates, cultured in both basal and chondro conditions, was assessed by live-dead fluorescence assay, composed by acetomethoxy derivative of calcein (calcein-AM) and propidium iodide (PI). Samples were collected at 1, 7, 14, and 21 days post-aggregation. After DPBS washing, samples were incubated with calcein-AM (1:500, 4 mM, Thermo Fisher Scientific) and PI (1:1000, Thermo Fisher Scientific) in DPBS, protected from light at 37 °C for 20 min. Calcein-AM easily permeates live cells where it is converted in calcein (green staining), while PI permeates damaged cells and binds to the nucleic acids (red staining). Afterwards, samples were washed with DPBS and visualized by fluorescence microscopy (Axio Imager 2, Zeiss).

3.3. Diameter measurements

The size of the 3D micro-templates, both cultured in basal and chondro, was measured using ImageJ software (n= 50 for each formulation). The diameter values present correspond to the mean of the length and width for each measured microtemplates.

3.4. Glycosaminoglycans quantification

Glycosaminoglycans (GAGs) content in the 3D micro-templates, cultured in both basal and chondro conditions, was assessed using Blyscan sulfated GAGs assay (Biocolor), according to the manufactures' specifications. For each sample, the content of 2 wells (equivalent to 2400 3D micro-templates) of the Aggrewell plate was collected and analyzed. The collection of only one well per condition result in absorbance values under the quantification limit. A papain extraction reagent (1,6 U mL^{-1}, Sigma-Aldrich) was prepared using L-cysteine hydrochloride (0.8 g L^{-1}, Sigma-Aldrich), EDTA (4 g L^{-1}, TCI Chemicals), sodium acetate (8 g L^{-1}, Labkem) buffered with sodium phosphate (0.2 M, Sigma-Aldrich), at pH 6.4. Samples were centrifuged (400g, 5min) and the resultant pellet was digested with 1 mL of papain extraction reagent, at 65 ºC for 3 h to extract all the content of GAGs. The digested material was centrifuged (10000g, 10 min) and the supernatant was kept to proceed the protocol. To each tube, containing 100 µL of digested sample, 1 mL of blyscan dye reagent was added. Tubes were gently shacked with an orbital shaker for 30 min, then centrifuged (12000 rpm, 10 min) and carefully drained, remaining a blue pellet in the bottom. The pellet formed

is a precipitated complex formed by sulfated GAGs and the dye. Dissociation reagent (0.5 mL) was added to dissolve the bound dye, and tubes were shacked in a vortex mixer for 10 min. Afterwards, tubes were centrifuged (12000 rpm, 5 min) to remove foam that might be formed. A standard curve (2.5 – 30 µg mL^{-1}) was obtained with the provided GAGs reference standard. Aliquoted standards were analyzed as the digested samples. Samples, standards, and the blank were analyzed by absorbance measurement (656 nm, Gen 5 2.01, Synergy HTX, Bio-TEK). The GAG content was calculated per milliliter of culture medium.

3.5. Collagen II immunofluorescence

The presence of collagen II (Col II) was evaluated at day 21 post-aggregation, both in basal and chondro media. First, samples were washed with DPBS, fixed in paraformaldehyde (4 % v/v) for 30 min at RT and, once again, samples were washed with DPBS. Afterwards, 3D micro-templates were permeabilized for 5 min at RT with Triton-X (0,1 % v/v). To reduce unspecific binding, samples were blocked in FBS (5 % w/v in PBS) for 1 h at RT. Then, samples were incubated with the primary antibody rabbit anti-human Col II (1:100 in 5 % FBS/PBS, Biolegend) overnight at 4 ºC in an orbital shaker. Samples were incubated with the secondary antibody anti-rabbit AlexaFluor 647 (1:500 in 5% FBS/PBS, BioLegend) for 1 h at RT. Actin filaments were stained with Flash Phalloidin™ Green 488 (1:50 in DPBS, BioLegend) for 1 h at RT. Also, samples were counterstained with DAPI (1:1000, 1 $mg.mL^{-1}$, Thermo Fisher Scientific) for 5 min at RT. All staining incubation steps were done in the dark and before and after each of these steps, samples were washed with DPBS to remove non-specific binding. Samples were incubated in DPBS at 4 ºC in the dark until analyzed by fluorescence microscopy (AxioImager 2, Zeiss). Furthermore, using ImageJ image analysis software it was possible to calculate the Col II area in the fluorescence microscope images of 3D microtemplates, as well as count the number of cells per template. Thus, the area of Col II per cell was calculated and allows to compare the conditions.

3.6. Scanning electron microscopy (SEM)

The 3D micro-templates morphology, cultured in basal and chondro conditions, was analyzed by scanning electron microscopy (SEM, accelerating voltage 25 kV, S-4100 instrument, Hitachi). Prior to the analysis, the micro-templates were collected at day 21 post-aggregation. Then, samples were fixed in paraformaldehyde (4 % v/v) and dehydrated in a graded series of ethanol. Afterwards, micro-templates were placed in a carbon tape onto an aluminium stub (SEM Specimen Stub, Agar Scientific) and sputtered by a thin film of carbon (K950X Turbo-Pumped Carbon Evaporator).

4. Development of the endochondral ossification *in vitro* model and characterization

4.1. Co-encapsulation of micro-cartilaginous templates, mesenchymal stem cells and HUVECs within liquefied capsules

At 90% confluency, UCMSCs and HUVECS at passages 6 and 5, respectively, were washed with DPBS and detached with a trypsin-EDTA solution, at 37 °C for 5 min. The cell suspensions were centrifuged (300 g, 5 min), and then the obtained pellets were re-suspended ($2x10^6$ UCMSCs mL^{-1} and $3x10^6$ HUVECs mL^{-1}) in 2 % w/v sodium alginate (ALG, Merck) buffered with sodium chloride (0.15 M, NaCl, Labchem) and MES hydrate (25 mM, Alfa Aesar). The 3D micro-templates, basal and chondro, were collected by removing 1 mL of the culture medium from the well and then dispensing it firmly back onto the plate to remove the templates from the well surface, which were gently aspirated. Wells were carefully rinsed with culture medium to remove any remaining templates. Templates, in culture medium, were centrifuged (RT, 300g, 5 min) and the pellet was resuspended in the previous 2 % w/v sodium alginate ($6x10^5$ aggregates mL^{-1}), containing the MSCs and HUVECs. The 3D micro-templates cultured in basal and chondro media were studied separately. As schematized in Figure 3 (*II*), alginate microgels were obtained using EHDA technique with 10 kV of voltage, 50 mL h^{-1} of flow rate, 22 G needle and 8 cm from the tip to collector. The crosslinking was achieved in calcium chloride (0.1 M, $CaCl_2$, Merck) dissolved in NaCl (0.15 M)/MES (25 mM), under stirring for 10 min at 300 rpm. Microgels were collected and rinsed in a washing solution of NaCl (0.15 M) buffered with MES hydrate (25 mM) at pH 6.7. The external membrane was produced via layer-by-layer (LbL) technique with the subsequent adsorption of three oppositely charged polyelectrolytes Figure 3 (*III*)). Firstly, alginate microgels were immersed in a poly(L-lysine) solution (PLL, MW ~ 30000-70000, Merck), followed by ALG solution, water-soluble highly purified chitosan solution (CHT, NovaMatrix), and then ALG solution again. The CHT and PLL polyelectrolyte solutions (0.3 mg mL^{-1}) were dissolved in NaCl (0.15 M)/MES (25 mM)/$CaCl_2$ (0.1 M). The ALG polyelectrolyte solution (0.3 mg mL^{-1}) was dissolved in NaCl (0.15 M)/MES (25 mM), because in contact with Ca^{2+} ($CaCl_2$) it would crosslink. This procedure was repeated to obtain a 10-layered membrane. The polymer adsorption occurred for 10 min for each solution and the excess of macromolecules was removed by immersion in the washing solution of NaCl (0.15 M)/MES (25 mM) for 2 min after ALG layer deposition. After PLL and CHT layers deposition, the excess was removed by immersion in a NaCl (0.15 M)/MES (25 mM)/CaCl2 (0.1 M) solution for 1 min, followed by immersion in a NaCl (0.15 M)/MES (25 mM) solution for another minute. After the

construction of the membrane, the core-shell microgels were immersed in 0.02 M EDTA for 2-3 min to liquefy the core. The pH of all polyelectrolyte solutions was set to 6.7, except for CHT (pH 6.3).[7] Afterwards, liquefied and multilayered microcapsules were cultured in dynamic conditions using spinner flasks (Celstir, Wheaton) at 50 rpm, with good gas exchange, and incubated at 37 ºC, in a humidified air atmosphere of 5% CO_2. Four types of microcapsules were tested (Figure 3 (*IV*)), namely *(i)* microcapsules cultured in medium supplemented with osteogenic differentiation factors (osteo medium) and encapsulating chondrogenically primed MSCs-only 3D microtemplates, termed as the ECO microcapsules, *(ii)* microcapsules cultured in medium without osteogenic differentiation factors supplementation (basal medium) and encapsulating chondrogenically primed MSCs-only 3D microtemplates, termed as the ECO control microcapsules, *(iii)* microcapsules cultured in osteo medium and encapsulating non-chondrogenically primed MSCs-only 3D microtemplates, termed as the IMO microcapsules, and *(iv)* microcapsules cultured in basal medium and encapsulating non-chondrogenically primed MSCs-only 3D microtemplates, termed as the negative control. Basal medium consist in M199 medium supplemented with 20 % v/v FBS, 1 % v/v ATB, 1% v/v GlutaMAX, while osteo medium is the basal medium supplemented with 10 nM DEX, 50 μg mL^{-1}, AA and 5 mM β-GP. The experiments were executed under sterile conditions and using sterile solutions. Samples were collected after 1, 7, 14 and 21 days of culture.

4.2. Cell viability

Cell viability of encapsulated cells was assessed by live-dead fluorescence assay, composed by acetomethoxy derivative of calcein (calcein-AM) and propidium iodide (PI). Samples were collected at 1, 7, 14, and 21 days post-encapsulation. After DPBS washing, samples were incubated with calcein-AM (1:500, 4 mM, Thermo Fisher Scientific) and PI (1:1000, Thermo Fisher Scientific) in DPBS, protected from light at 37 °C for 20 min. Calcein-AM easily permeates live cells where it is converted in calcein (green fluorescent staining), while PI permeates damaged cells and binds to the nucleic acids (red staining). Afterwards, samples were washed with DPBS and visualized by fluorescence microscopy (Axio Imager 2, Zeiss).

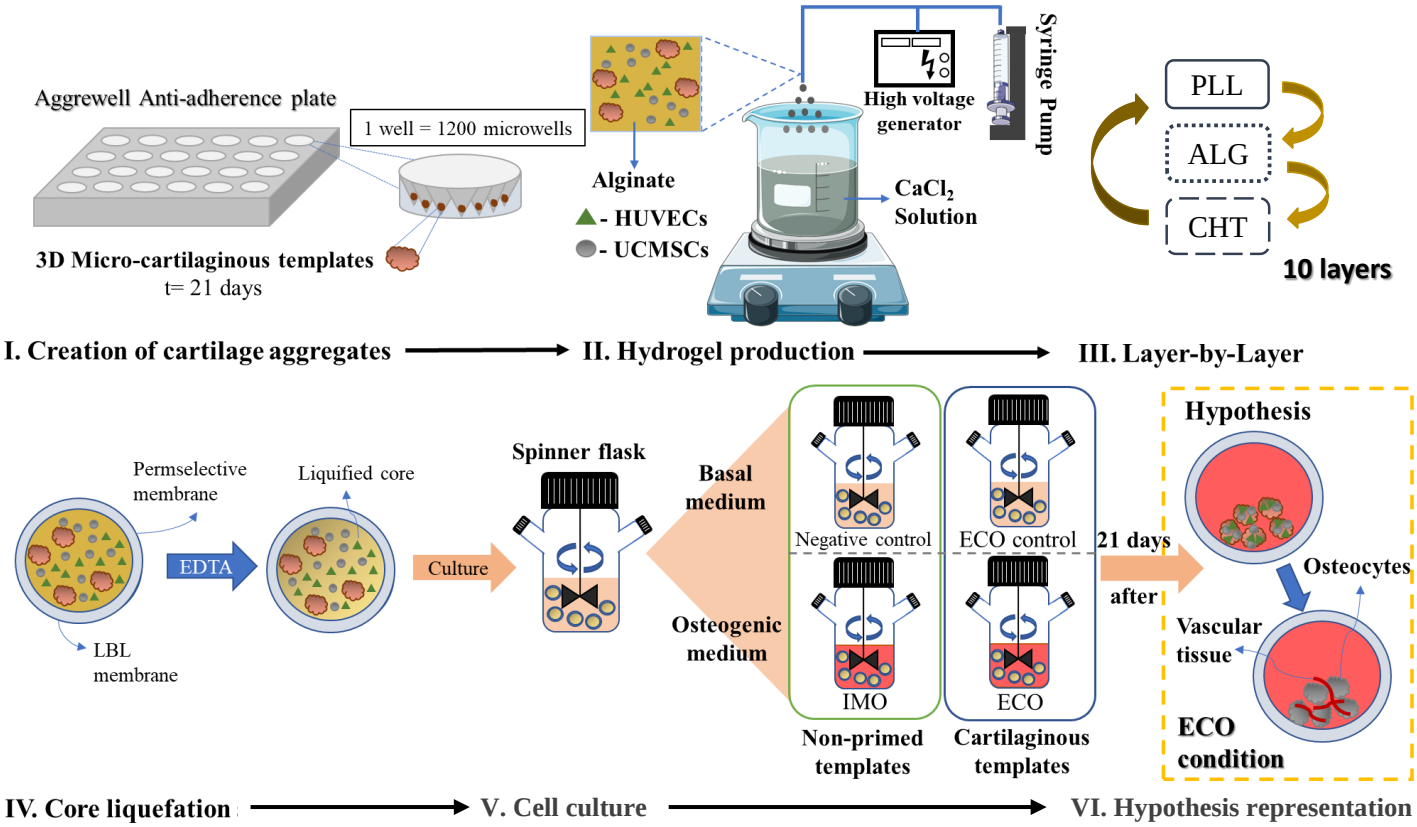

Figure 3. Schematic representation of the creation of the ECO *in vitro* model. ***I.*** High-efficiency production of chondrogenically-primed 3D micro templates, using Aggrewell anti-adherence plates in chondrogenic differentiation medium for 21 days. Similarly, non-chondrogenically primed 3D microtemplates were also produced in basal medium for 21 days. ***II.*** Co-culture of the 3D microtemplates with umbilical cord-derived mesenchymal stem/stromal cells (UCMSCs) and human umbilical vein endothelial cells (HUVECs) in an alginate solution, added dropwise to a calcium chloride ($CaCl_2$) solution to form spherical hydrogels by electrohydrodynamic atomization technique. ***III***. Layer-by-layer (LbL) deposition to produce the multilayered membrane. For that, the loaded alginate beads were first immersed in a poly(L-lysine) solution (PLL), followed by alginate (ALG), chitosan (CHT) and ALG solution again. This procedure was repeated until the production of a 10-layered membrane ***IV.*** Core liquefaction in ethylenediaminetetraacetic acid (EDTA). ***V.*** *In vitro* culture of the four types of microcapsules, namely *(i)* microcapsules cultured in medium supplemented with osteogenic differentiation factors (osteogenic medium) and encapsulating chondrogenically-primed UCMSCs-only 3D microtemplates, termed as the ECO microcapsules, *(ii)* microcapsules cultured in medium without osteogenic differentiation factors supplementation (basal medium) and encapsulating chondrogenically-primed UCMSCs-only 3D microtemplates, termed as the ECO control microcapsules, *(iii)* microcapsules cultured in osteogenic medium and encapsulating non-chondrogenically primed UCMSCs-only 3D microtemplates, termed as the IMO microcapsules, and *(iv)* microcapsules cultured in basal medium and encapsulating non-chondrogenically primed UCMSCs-only 3D microtemplates, termed as the negative control. ***VI.*** Hypothesis representation. The co-culture of chondrogenically-primed 3D microtemplates with UCMSCs and HUVECs, such privileged microenvironment will mimic the ECO process, leading to the *in vitro* production of vascularized bone-like microtissues.

4.3. Osteopontin and CD31 immunofluorescence

Microcapsules, collected at day 21, were placed in centrifuge tubes, washed with DPBS, and fixed in paraformaldehyde (4 % v/v) for 30 min at RT. Once again, samples were washed with DPBS. Afterwards, microcapsule membranes were destroyed to release their content, which was permeabilized with 0.1% v/v Triton (Triton X-100 BioXtra, Sigma-Aldrich) solution prepared with

distilled water for 5 min at RT. After washing with DPBS, unspecific binding was blocked using a solution of 5% FBS, prepared in PBS for 1 h at RT. Afterwards, samples were incubated with the primary antibody mouse anti-human CD31 (1:50 in 5% FBS/PBS, BioLegend) overnight at 4ºC in an orbital shaker. Then, were incubated with the secondary antibody anti-mouse AlexaFluor 488 (1:200 in 5% FBS/PBS, BioLegend) for 1 h at RT. The incubation process was repeated to osteopontin immune staining, using the primary antibody rabbit anti-human osteopontin (1:200 in 5% FBS/PBS, Biolegend) and then the secondary antibody anti-rabbit AlexaFluor 647 (1:500 in 5% FBS/PBS, BioLegend). Samples were counterstained with DAPI (1:1000, 1 mg.mL^{-1}, Thermo Fisher Scientific) for 5 min at RT. All staining steps occurred in the dark and were preceded and followed by a DPBS washing step. Samples were incubated in DPBS at 4 ºC in the dark until analyzed by fluorescence microscopy (Axio Imager 2, Zeiss). Furthermore, using ImageJ image analysis software it was possible to calculate the area occupied by osteopontin and CD31 in the fluorescence microscope images, as well as count the number of cells per aggregate. Thus, the area of osteopontin and CD31 per cell was calculated and allows to compare the conditions.

4.4. Hydroxyapatite immunofluorescence

The presence of hydroxyapatite in cell aggregates within the microcapsules was verified after 21 days of culture using the OsteoImageTM Mineralization Assay (Lonza), according to the manufactures' specifications. Samples were fixed in paraformaldehyde (4 % v/v) for 30 min at RT. After fixation, the microcapsule membranes were disrupted to release all their content and cells were rinsed with the diluted wash buffer. Then, samples were incubated with 1 mL of staining reagent for 30 min, in the dark. After incubation, samples were centrifuged (400 g, 5 min) to remove the staining reagent and were washed with the diluted wash buffer 3 times, leaving the solution 5 min per wash. Actin filaments were stained with Flash Phalloidin™ Red 594 (1:40 in DPBS, BioLegend) for 1 h at RT. After washing the samples, cell nuclei were stained with DAPI (1:1000 in DPBS, 1 mg.mL-1, Thermo Fisher Scientific) for 5 min at RT and were washed again. All staining steps occurred in the dark. Samples were incubated in DPBS at 4 ºC in the dark until analyzed by fluorescence microscopy (Axio Imager 2, Zeiss). Furthermore, using ImageJ image analysis software it was possible to calculate the area occupied by hydroxyapatite in the fluorescence microscope images, as well as count the number of cells per aggregate. Thus, the area of hydroxyapatite per cell was calculated and allows to compare the conditions.

4.5. Scanning electron microscopy and Energy-dispersive X-ray spectroscopy (SEM-EDS)

Cell aggregates morphology and elemental constitution were analyzed by scanning electron microscopy (accelerating voltage 15 kV, SEM Hitachi, SU-70 instrument) coupled with an energy dispersive x-ray detector (EDS Bruker, Quantax 400 detector). Prior to the analysis, the microcapsules were collected at day 21 post-encapsulation and disrupted to expose the core content. Then, samples were fixed in paraformaldehyde (4 % v/v) and dehydrated in a graded series of ethanol. Afterwards, microcapsules were placed in a carbon tape onto a graphite stub (Ted Pella) and sputtered by a thin film of carbon (K950X Turbo-Pumped Carbon Evaporator). Calcium (Ca) and phosphorous (P) composition was obtained by EDS spectra using Esprit software. The Ca/P ratio was calculated by deconvolution of Ca and P peaks removing the background effect.

5. Statistical analysis

All data were statistically analyzed using one-way analysis of variance (ANOVA) using the Tukey´s multiple comparison tests. The GAGs quantification data were analyzed using two-way ANOVA with Tukey´s multiple comparison tests. The analysis and the corresponding graphical representations were performed using GraphPad Prism 6.01. A p-value <0.05 was considered statistically significant.

6. References

1. Seshareddy, K., Troyer, D. & Weiss, M. L. Method to Isolate Mesenchymal-Like Cells from Wharton's Jelly of Umbilical Cord. *Methods Cell Biol.* **86**, 101–119 (2008).
2. Siufi, D. T. ;Covas J. L. C. . & Silva, M. D. O. A. R. L. Isolation and culture of umbilical vein mesenchymal stem cells. *Brazilian J. Med. Biol. Res.* **36**, (2003).
3. Tsuji, K. *et al.* Effects of different cell-detaching methods on the viability and cell surface antigen expression of synovial mesenchymal stem cells. *Cell Transplant.* **26**, 1089–1102 (2017).
4. Subramanian, A., Fong, C. Y., Biswas, A. & Bongso, A. Comparative characterization of cells from the various compartments of the human umbilical cord shows that the Wharton's jelly compartment provides the best source of clinically utilizable mesenchymal stem cells. *PLoS One* **10**, 1–25 (2015).
5. Mennan, C. *et al.* Isolation and characterisation of mesenchymal stem cells from different regions of the human umbilical cord. *Biomed Res. Int.* **2013**, 916136 (2013).
6. J. Medina-Leyte, D., Domínguez-Pérez, M. & Mercado, I. Use of Human Umbilical Vein Endothelial Cells (HUVEC) as a Model to Study Cardiovascular Disease: A review. *Appl. Sci.* (2020).
7. Nadine, S. Dynamic microfactories co-encapsulating osteoblastic and adipose-derived stromal cells for the biofabrication of bone units. *Biofabrication* **12**, 15005 (2020).

III. Bioencapsulation of stem and endothelial cells towards an *in vitro* model for endochondral ossification

Abstract

During the last decade, approaches based in endochondral ossification (ECO) have been increasingly explored, replacing the intramembranous ossification (IMO) approaches. The hypertrophic differentiation existent in the cartilage templates lead to the secretion of osteogenic and angiogenic factors, which simultaneously allow the development of bone tissue while stimulating vascularization. The main goal of this work is to develop an *in vitro* ECO model relying in the co-culture of 3D micro-cartilaginous templates with umbilical cord MSCs (UCMSCs) and human umbilical vein endothelial cells (HUVECs). Our hypothesis is that such engineered and privileged microenvironment would mimic the ECO process, leading to the *in vitro* production of vascularized bone-like microtissues. For that, MSCs-only 3D microtemplates were produced at high-rates and cultured *in vitro* for 21 days. Then, such microtemplates were co-cultured with UCMSCs and HUVECs within liquefied and multilayered microcapsules, in dynamic conditions, for another 21 days. Microcapsules with chondrogenically-primed 3D microtemplates were cultured with (ECO) and without (ECO control) osteogenic differentiation factors. Also, microcapsules with non-primed 3D microtemplates were cultured with (IMO) and without (negative control) osteogenic differentiation factors. Results show that cell viability was maintained during all the experiment, as shown by the live dead assay. The cartilaginous nature of the 3D templates cultured in chondrogenic medium was confirmed. After 21 days of encapsulation, the ECO microcapsules presented osteopontin (OPN) and hydroxyapatite (HA) staining, indicating bone extracellular matrix production. The elemental analysis by scanning electron microscopy and energy-dispersive X-ray spectroscopy showed a higher matrix mineralization in the ECO microcapsules, being the only condition to present a calcium/phosphorous (Ca/P) ratio (1.71) close to the native hydroxyapatite ratio (1.67). HA was widely dispersed and formed large nodule-like structures in the surface of the ECO cell aggregates. Furthermore, both ECO and ECO control conditions showed an increased endothelial cell recruitment compared to IMO. IMO microcapsules presented OPN and HA staining, however only nanocrystals of HA could be observed and presented a lower Ca/P ratio (1.11). These data show the relevance of using chondrogenically primed 3D microtemplates in bone repair,

highlighting the advantage of ECO over IMO approach. In conclusion, this ECO bioencapsulation approach revealed to be a promising bone regeneration strategy.

1. Introduction

Bone tissue presents an incredible intrinsic self-repair capability. However, large bone defects may result in cessation of the regenerative process. Aiming to solve challenges related to large bone non-unions, the first bone tissue engineering (TE) approaches focused in the recapitulation of the intramembranous ossification (IMO) process. IMO consists in a bone production mechanism where mesenchymal stem/stromal cells (MSCs) are directly stimulated to differentiate into osteoblasts. However, after implantation these tissues often lacked a functional vascular supply, resulting in necrotic cores. Recently, in order to develop close-to-native strategies, endochondral ossification (ECO) recapitulation is being increasingly explored in bone TE. ECO is the bone formation and repair process of most bones.

In bone tissue repair by ECO, firstly MSCs need to migrate and condensate *in situ* due to the expression of the transcription factor SOX9. At this stage, MSCs start the differentiation to become chondrocytes, and consequently lay down extracellular matrix (ECM) rich in collagen type II (Col II), aggrecan and sulfated glycosaminoglycans (GAGs), giving rise to a hyaline-like cartilaginous template.[1,2] Chondrocytes inside this template enter in a hypertrophic state, secreting different biomolecules, including collagen type X (Col X), vascular endothelial growth factor (VEGF), alkaline phosphatase, matrix metalloproteinase (MMP)-13, and bone morphogenic protein (BMP)-6.[1,3] The release of these key molecules causes a cascade of events, namely an increase in the volume of hypertrophic chondrocytes, the calcification of the template, and the modification in the composition of the newly deposited ECM from Col II to Col X. The secretion of osteogenic differentiation factors, induces the osteogenic differentiation of the MSCs present in the surroundings, beginning the deposition of bone tissue. MMP-13 facilitates the invasion of the template by blood vessels. Being established a vascular network, osteoprogenitor cells, such as osteoclasts and osteoblasts are brought to the repair site. More recently, it has been shown that osteoblasts in the repair site can also result of a particular chondrocyte-to-osteoblast transformation.[4] Bone deposition is enhanced by the increasing number of osteoblasts, while the osteoclasts aid at the degradation of the hyaline cartilage, which act as canals guiding and allowing the invasion of blood vessels. The bone defect is re-filled by bone tissue and a vascular network, responsible to bring essential molecules, such as nutrients and oxygen, aid to fulfill the normal functions of the tissue.

In bone TE, the majority of ECO approaches essentially try to recapitulate *in vitro* the hypertrophic cartilage template, and then the bone deposition is often achieved *in vivo*. MSCs are the most used source of cells for bone TE, including those focused in ECO approaches. Recapping, the formation of the cartilage template *in vivo* is accomplished by them, and, also, they differentiate into osteoblasts due to the osteogenic factors secreted by the hypertrophic cartilage template. MSCs have also a

number of appealing features, such as rapid proliferation, multipotency, self-renewal capacity, and ability to secrete a wide range of cytokines and growth factors.[3,5] In particular, these bioactive molecules have anti-inflammatory and immunosuppressive effects, which allow MSCs to play an immunomodulatory role, thus regulating inflammation and tissue regeneration.[5–9]

Umbilical cord stem cells (UCMSCs) are in a development level between adult MSCs and embryonic stem cells and are isolated from an otherwise discarded tissue, however, recently public and private companies have been storing them in cryobanks.[10–12] The isolation protocols have been significantly improved, and allow to obtain UCMSCs with high efficiency.[10,13] Their immune properties have been tested and it was found that they have immunosuppressive properties and low immunogenicity[14–17] Also, they were considered to have an increased immunomodulation ability comparing to others MSCs, as BMMSCs and ASCs.[15] UCMSCs combined with collagen microbeads were used to create constructs and then implant them to see their potential to create bone. Interestingly, UCMSCS were expanded in medium supplemented with human platelet lysate, instead of FBS. UCMSCs maintained their proangiogenic potential and the ability of osteogenic differentiation and the constructs prompted bone and vascular formation when implanted in mice. UCMSCs seemed to easily differentiate into chondrocytes, have more proangiogenic activity with no inflammatory response.[11] Endothelial progenitor cells (EPCs) can be also useful for ECO strategies. As referred before, bone vascularization is one of the challenges of bone TE strategies and is also the reason of using ECO approaches.[18] EPCs are found in the bone marrow and umbilical cord, and can be used to enhance vascularization during ECO due to their pro-angiogenic activity.[19] I*n vivo,* EPCs were shown to be able to identify damaged areas and consequently mobilize themselves. EPCs can be easily retrieved during surgery for fracture repair, and have potential to undergo chondrogenesis, hypertrophy, and calcification *in vitro*.[20]

ECO approaches supplementation is divided in two steps and two different supplementation culture media. A first step dedicated to the chondrogenic differentiation, which will allow the creation of the cartilaginous templates. The chondrogenic supplementation needed is already well studied and known. The second step consists in stimulate the hypertrophy of the template and the osteogenic differentiation. The hypertrophy is induced using the common osteogenic differentiation factors, dexamethasone (DEX), ascorbic acid (AA) and β-GP but in different concentrations. DEX induces and regulates *RUNX2* expression in hypertrophic chondrocytes. AA enhances collagen I (Col I) production by MSCs. β-GP provides phosphate for the mineralization stage, inducing the production of hydroxyapatite, and its inorganic phosphate also regulates osteogenic pathways.[21]

The approaches can consist in the utilization of materials and cells together, scaffold-based, or only cells or biomaterials, scaffold-free or cell-free, respectively. Scaffold-free approaches has becoming more used, because of the increasing interest in close-to-native strategies. The definition of the

scaffold-free approaches continues under discussion, however, usually is defined by using only cells, where they are the only responsible for the matrix and architecture creation. These approaches use spheroid cell aggregates, cells suspension or cell sheets and they can be used to create complex tissues.[22]

The aim of this study is to develop an *in vitro* ECO TE model relying in the co-culture of UCMSCs, HUVECs and also 3D micro-cartilaginous templates created only with UCMSCS. The 3D microtemplates were produced at high-rates and cultured *in vitro* for 21 days. Afterwards, such templates were co-cultured with dispersed UCMSCs and HUVECs within liquefied and multilayered microcapsules in dynamic conditions, for another 21 days. Four types of microcapsules were developed, namely *(i)* microcapsules cultured in medium supplemented with osteogenic differentiation factors (osteo medium) and encapsulating chondrogenically primed MSCs-only 3D microtemplates, termed as the ECO microcapsules, *(ii)* microcapsules cultured in medium without osteogenic differentiation factors supplementation (basal medium) and encapsulating chondrogenically primed MSCs-only 3D microtemplates, termed as the ECO control microcapsules, *(iii)* microcapsules cultured in osteo medium and encapsulating non-chondrogenically primed MSCs-only 3D microtemplates, termed as the IMO microcapsules, and *(iv)* microcapsules cultured in basal medium and encapsulating non-chondrogenically primed MSCs-only 3D microtemplates, termed as the negative control. The main novelty of this study is the development of a fully *in vitro* ECO model using the liquified and multilayered microcapsules technology in dynamic conditions. The utilization of dynamic conditions with the liquified microcapsules enhances the diffusion of nutrients within the microcapsules, as well as, allows an increased release of biomolecules produced by the cells that may help the crosstalk between UCMSCs and HUVECs.[23] Furthermore, this combination of conditions helps the physical interaction between cells, which is particularly important because of their anchorage-dependent nature. Also, these conditions resemble the native environment of bone tissue, which might induce higher osteogenic differentiation.[24] Our hypothesis is that such engineered and privileged microenvironment, of cartilaginous 3D microtemplates encapsulated with UCMSCs, HUVECs and osteogenic differentiation factors, would mimic the ECO process, leading to the *in vitro* production of vascularized bone-like microtissues.

2. Materials and Methods

2.1 Cell isolation and characterization

Human umbilical cords (UC) from two newborn babies were used to isolate both MSCs and HUVECs, with ethical approval of the Competent Ethics Committee (CEC), COMPASS Research Group and *Centro Hospitalar do Baixo Vouga*, the local hospital of Aveiro. MSCs were isolated from the Wharton's jelly of the umbilical cord by the explant method[25] and cultured at 37 ºC and 5% of CO_2 atmosphere in Minimum Essential Medium Alpha (α-MEM, Gibco) supplemented with 1% v/v antibiotic/antimycotic (ATB) and 10% v/v heat-inactivated fetal bovine serum (FBS, Gibco). HUVECs were dissociated from the umbilical cord vein wall by enzymatic digestion using 0.1% w/v collagenase type IA (MP Biomedicals, USA). Cells were maintained in culture flasks previously coated with 0.7% w/v gelatin at 37ºC and 5% of CO_2 atmosphere in M199 medium (Sigma-Aldrich) supplemented with 1% v/v of Endothelial Cell Growth Supplement (ECGS, 40 mg mL^{-1}, Merck, Germany), 10% v/v of heparin (100 mg mL^{-1}, Sigma-Aldrich), 20% FBS, 1% ATB. MSCs and HUVECs were cultured until passages 5 and 3, respectively. Both culture media were changed twice a week. Cell phenotype characterization was performed by flow cytometry (Flow Cytometry BD Accuri C6 Plus). Briefly, UCMSCs and HUVECs were washed with DPBS, dissociated with triple express (TrypLE™ Express Enzyme, phenol red, Thermo Fisher Scientific) and resuspend in a staining/washing solution containing 2% bovine serum albumin (BSA, Sigma-Aldrich) and 0.1% sodium azide (w/v, TCI) prepared in phosphate-buffered saline solution (PBS, Gibco) without calcium and magnesium ions (pH 7.4 – 7.6). MSCs were incubated with the antibodies PE-conjugated CD73 (1:20), AlexaFluor 647-conjugated CD90 (1:20) and AlexaFluor 488-conjugated CD105 (1:11). Incubation with FITC-conjugated CD34 (1:20), and APC-conjugated CD31 (1:20) was performed as negative markers.[26,27] HUVECs were incubated with the antibody APC-conjugated CD31 (1:20).[28] FITIC-conjugated CD34 (1:20) and AlexaFluor 647-conjugated CD90 (1:20) were used as a negative marker. All the antibodies were purchased from BioLegend, except AlexaFluor 488-conjugated CD105, which was acquired to Miltenyi Biotec. For each cell type, a control sample without antibodies was also prepared. After 1 h at room temperature (RT), protected from light, samples were washed in the washing/staining solution, and subsequently resuspended in the acquisition buffer composed by 1% formaldehyde (Sigma-Aldrich) and 0.1% (w/v) sodium azide in PBS until analysis. Samples were stored at 4ºC until analysis.

2.2 3D micro-cartilaginous templates production

UCMSCs were expanded in culture flasks ($5x10^3$ cells.cm^2) in α-MEM medium, supplemented with 1% v/v ATB and 10% v/v FBS at pH 7.4 and incubated at 37 ºC in a humidified air atmosphere of 5 % CO_2. The medium was changed twice a week and cells were used at passage 5. At 90% confluency, cells were washed with Dulbecco's phosphate buffered saline (DPBS) and detached with a trypsin-EDTA (Merck) solution, at 37 °C for 5 min. The cell suspension was centrifuged (RT, 300 g, 5 min) and the pellet was re-suspended ($6x10^4$ cells.mL^{-1}) in Dulbecco's Modified Eagle's medium-high glucose (DMEM-HG) medium, with 2% FBS and 1% ATB, without (basal) or with chondrogenic differentiation factors (chondro), namely sodium pyruvate (1 mM, Thermo Fisher), insulin-transferrin-selenium (ITS, 1%, Thermo Fisher), AA (50 μg.mL^{-1}, Merck), TGF-β3 (10 ng.mL^{-1}, Merck), and DEX (100 nM, Sigma Aldrich). The 3D micro-templates were created in Aggrewell plates (AggreWell™ 400, StemCell) according to the manufactures' specifications. These plates were treated with 500 μL of an anti-adherence solution (Anti-Adherence Rinsing Solution, StemCell), add to each well and then were centrifuged (RT, 1300g, 5 min). The solution was aspirated, and the wells were rinsed with DPBS. Afterwards, 2 mL of cell suspension ($1.2x10^5$ cells.well^{-1}) were transferred to each well of the Aggrewell plate and centrifuged (RT, 100 g, 3 min). The Aggrewell plate with the cell aggregates was incubated at 37ºC and 5% of CO_2 in a humidified atmosphere up to 21 days. Half of the culture medium was exchange every 3-4 days. Samples were collected after 1, 14 and 21 days, and characterized.

2.3 Bioencapsulation

UCMSCs were expanded in culture flasks ($5x10^3$ cells/cm^2) in α-MEM medium, supplemented with 1% v/v ATB and 10% v/v FBS at pH 7.4 and incubated at 37 ºC in a humidified air atmosphere of 5 % CO_2. HUVECs were expanded in culture flasks ($5x10^3$ cells cm^{-2}) in M199 medium, supplemented with 1% v/v ATB, 20% v/v FBS, 1% v/v ECGS and 10% v/v of heparin at pH 7.4 and incubated at the same conditions. Both media were changed twice a week. UCMSCs were used at passage 6 and HUVECs were used at passage 5. At 90% confluency, cells were washed with DPBS and detached with a trypsin-EDTA solution, at 37 °C for 5 min. The cell suspension was centrifuged (300 g, 5 min), and then the obtained pellet was re-suspended ($2x10^6$ UCMSCs mL^{-1} and $3x10^6$ HUVECs mL^{-1}) in 2 %w/v sodium alginate (ALG, Merck) buffered with sodium chloride (0.15 M, NaCl, Labchem) and MES hydrate (25 mM, Alfa Aesar). The 3D micro-templates, basal or chondro, were collected from the Aggrewell plate and were centrifuged (RT, 300g, 5 min). The pellet was resuspended in the previous 2 % w/v sodium alginate ($6x10^5$ aggregates mL^{-1}), containing the MSCs and HUVECs. The

3D micro-templates cultured in basal and chondro media were studied separately. Alginate microgels were obtained using EHDA technique with 10 kV of voltage, 50 mL h^{-1} of flow rate, 22 G needle and 8 cm from the tip to collector. The crosslinking was achieved in calcium chloride (0.1 M, $CaCl_2$, Merck) dissolved in NaCl (0.15 M)/MES (25 mM), under stirring for 10 min at 300 rpm. Microgels were collected and rinsed in a washing solution of NaCl (0.15 M) buffered with MES hydrate (25 mM) at pH 6.7. The external membrane was produced via layer-by-layer (LbL) technique with the subsequent adsorption of three oppositely charged polyelectrolytes. Firstly, alginate microgels were immersed in a poly(L-lysine) solution (PLL, M_W ~ 30000-70000, Merck), followed by ALG solution, water-soluble highly purified chitosan solution (CHT, NovaMatrix), and then ALG solution again. The CHT and PLL polyelectrolyte solutions (0.3 mg mL^{-1}) were dissolved in NaCl (0.15 M)/MES (25 mM)/CaCl2 (0.1 M). The ALG polyelectrolyte solution (0.3 mg mL^{-1}) was dissolved in NaCl (0.15 M)/MES (25 mM). This procedure was repeated to obtain a 10-layered membrane. The polymer adsorption occurred for 10 min for each solution and the excess of macromolecules was removed by immersion in the washing solution of NaCl (0.15 M)/MES (25 mM) for 2 min after ALG layer deposition. After PLL and CHT layers deposition, the excess was removed by immersion in a NaCl (0.15 M)/MES (25 mM)/$CaCl_2$ (0.1 M) solution for 1 min, followed by immersion in a NaCl (0.15 M)/MES (25 mM) solution for another minute. After LbL, the core-shell microgels were immersed in 0.02 M EDTA for 2-3 min to liquefy the core. The pH of all solutions was set to 6.7, excepting for CHT (pH 6.3).[24] Afterwards, liquefied and multilayered microcapsules were cultured in dynamic conditions using spinner flasks (Celstir, Wheaton) at 50 rpm, with good gas exchange, and incubated at 37 ºC, in a humidified air atmosphere of 5% CO_2. Four types of microcapsules were tested, namely *(i)* microcapsules cultured in medium supplemented with osteogenic differentiation factors (osteo medium) and encapsulating chondrogenically primed MSCs-only 3D microtemplates, termed as the ECO microcapsules, *(ii)* microcapsules cultured in medium without osteogenic differentiation factors supplementation (basal medium) and encapsulating chondrogenically primed MSCs-only 3D microtemplates, termed as the ECO control microcapsules, *(iii)* microcapsules cultured in osteo medium and encapsulating non-chondrogenically primed MSCs-only 3D microtemplates, termed as the IMO microcapsules, and *(iv)* microcapsules cultured in basal medium and encapsulating non-chondrogenically primed MSCs-only 3D microtemplates, termed as the negative control. Basal medium consists in M199 medium supplemented with 20 % v/v FBS, 1 % v/v ATB, 1% GlutaMAX, while osteo medium is the basal medium supplemented with 10 nM DEX, 50 μg.mL^{-1}, AA and 5 mM β-GP. The experiments were performed under sterile conditions and using sterile solutions. Samples were collected after 1, 7, 14 and 21 days of culture.

3.4. Cell viability

Cell viability of both 3D micro-cartilaginous templates and encapsulated cells was assessed by live-dead fluorescence assay, composed by calcein-AM and propidium iodide (PI). Samples were collected at 1, 14, 21 days post-aggregation and 1, 7, 14, or 21 days post-encapsulation. After DPBS washing, samples were incubated with calcein-AM (1:500, 4 mM, green staining, Thermo Fisher Scientific) and PI (1:1000, red staining, Thermo Fisher Scientific) in DPBS, protected from light at 37 °C for 20 min. Afterwards, samples were washed with DPBS and visualized by fluorescence microscopy (Axio Imager 2, Zeiss).

3.5. Diameter measurements

The size of the 3D micro-templates was measured using ImageJ software. The diameter values used correspond to the mean of the length and width for each measured micro-template. For each condition were made 20 diameter measurements.

3.6. 3D micro-cartilaginous aggregates evaluation

3.6.1. Collagen II immunoassay

The presence of Col II was evaluated at day 21 post-aggregation, both in basal and chondro media. First, samples were washed with DPBS, fixed in paraformaldehyde (4 % v/v) for 30 min at RT and, once again, were washed with DPBS. Afterwards, 3D micro-templates were permeabilized for 5 min at RT with Triton-X (0,1 % v/v). Samples were immersed in FBS (5 % w/v in PBS) for 1 h at RT. Then, samples were incubated with the primary antibody rabbit anti-human Col II (1:100 in 5 % FBS/PBS, Biolegend) overnight at 4 ºC in an orbital shaker. Samples were incubated with the secondary antibody anti-rabbit AlexaFluor 647 (1:500 in 5% FBS/PBS, BioLegend) for 1 h at RT. Actin filaments were stained with Flash Phalloidin™ Green 488 (1:50 in DPBS, BioLegend) for 1 h at RT. Also, samples were counterstained with DAPI (1:1000, 1 $mg.mL^{-1}$, Thermo Fisher Scientific) for 5 min at RT. All staining incubation steps were done in the dark and before and after each of these steps, samples were washed with DPBS to remove non-specific binding. Samples were analyzed by fluorescence microscopy (AxioImager 2, Zeiss). Using ImageJ image analysis software, it was possible to calculate the area occupied by Col II in the fluorescence microscope images, as

well as count the number of cells per template. Thus, such semiquantitative analysis allows the comparison of the different formulations of microcapsules tested.

3.6.2. Glycosaminoglycans quantification

GAGs content in the 3D micro-templates, cultured in both basal and chondro conditions, was assessed using Blyscan sulfated GAGs assay (Biocolor), according to the manufactures' specifications. For each sample, the content of 2 wells (equivalent to 2400 3D micro-templates) of the Aggrewell plate was collected and analyzed. A papain extraction reagent (1.6 $U.mL^{-1}$, Sigma-Aldrich) was prepared using L-cysteine hydrochloride (0,8 $g.L^{-1}$, Sigma-Aldrich), EDTA (4 $g.L^{-1}$, TCI Chemicals), sodium acetate (8 $g.L^{-1}$, Labkem) buffered with sodium phosphate (0,2 M, Sigma-Aldrich), at pH 6.4. Samples were centrifuged (400g, 5min) and the resultant pellet was digested with 1 mL of papain extraction reagent, at 65 ºC for 3 h to extract all the content of GAGs. The digested material was centrifuged (10000g, 10 min) and the supernatant was kept to proceed the protocol. To each tube, containing 100 µL of digested sample, 1 mL of blyscan dye reagent was added. Tubes were gently shacked with an orbital shaker for 30 min, then centrifuged (12000 rpm, 10 min) and carefully drained, remaining a blue pellet in the bottom. Dissociation reagent (0.5 mL) was added, and tubes were shacked in a vortex mixer for 10 min. Afterwards, tubes were centrifuged (12000 rpm, 5 min) to remove foam that might be formed. A standard curve (2,5 – 30 $\mu g.mL^{-1}$) was obtained with the provided GAG reference standard. Aliquoted standards were analyzed as the digested samples. Samples, standards, and the blank were analyzed by absorbance measurement (656 nm, Gen 5 2.01, Synergy HTX, Bio-TEK). The GAG content was calculated per milliliter of culture medium.

3.6.3. Scanning electron microscopy

The 3D micro-templates morphology, cultured in basal and chondro conditions, was analyzed by scanning electron microscopy (SEM, accelerating voltage 25 kV, S-4100 instrument, Hitachi). Prior to the analysis, the micro-templates were collected at day 21 post-aggregation. Then, samples were fixed in paraformaldehyde (4 % v/v) and dehydrated in a graded series of ethanol. Afterwards, micro-templates were placed in a carbon tape onto an aluminium stub (SEM Specimen Stub, Agar Scientific) and sputtered by a thin film of carbon (K950X Turbo-Pumped Carbon Evaporator).

3.7. Endochondral ossification evaluation

2.7.1 Osteopontin and CD31 immunofluorescence detection

Microcapsules, collected at day 21, were placed in centrifuge tubes, washed with DPBS, and fixed in paraformaldehyde (4 % v/v) for 30 min at RT. Once again, samples were washed with DPBS. Afterwards, microcapsule membranes were destroyed to release their content, which was permeabilized with 0.1% v/v Triton (Triton X-100 BioXtra, Sigma-Aldrich) solution prepared with distilled water for 5 min at RT. After washing with DPBS, non-specific binding was blocked using a solution of 5% FBS, prepared in PBS for 1 h at RT. Afterwards, samples were incubated with the primary antibodies mouse anti-human CD31 (1:50 in 5% FBS/PBS, BioLegend) and rabbit anti-human osteopontin (1:200 in 5% FBS/PBS, Biolegend) overnight at 4ºC in an orbital shaker. Then, were incubated with the secondary antibodies anti-mouse AlexaFluor 488 (1:200 in 5% FBS/PBS, BioLegend) and anti-rabbit AlexaFluor 647 (1:500 in 5% FBS/PBS, BioLegend) for 1 h at RT. Samples were counterstained with DAPI (1:1000 in PBS, 1 $mg.mL^{-1}$, Thermo Fisher Scientific) for 5 min at RT. All staining steps occurred in the dark and were preceded and proceeded with a DPBS washing step. Samples were incubated in DPBS at 4 ºC in the dark until analyzed by fluorescence microscopy (Axio Imager 2, Zeiss). Using ImageJ image analysis software, it was possible to calculate the area occupied by osteopontin and CD31 in the fluorescence microscope images, as well as count the number of cells per encapsulated aggregate. Thus, the area of osteopontin and CD31 per cell was calculated and allows to compare the conditions.

2.7.2 Hydroxyapatite fluorescence staining

The presence of hydroxyapatite in cell aggregates within the microcapsules was verified after 21 days of culture using the OsteoImage™ Mineralization Assay (Lonza), according to the manufactures' specifications. Samples were fixed in paraformaldehyde (4 % v/v) for 30 min at RT. After fixation, the microcapsule membranes were disrupted to release all their content and cells were rinsed with the diluted wash buffer. Then, samples were incubated with 1 mL of staining reagent for 30 min, in the dark. After incubation, samples were centrifuged (400 g, 5 min) to remove the staining reagent and were washed with the diluted wash buffer 3 times, leaving the solution 5 min per wash. Actin filaments were stained with Flash Phalloidin™ Red 594 (1:40 in DPBS, BioLegend) for 1 h at RT. After washing the samples, cell nuclei were stained with DAPI (1:1000 in DPBS, 1 $mg.mL^{-1}$, Thermo Fisher Scientific) for 5 min at RT and were washed again. All staining steps occurred in the dark. Samples were incubated in DPBS at 4 ºC in the dark until analyzed by fluorescence microscopy (Axio Imager 2, Zeiss). Using ImageJ image analysis software, it was possible to calculate the area

occupied by hydroxyapatite in the fluorescence microscope images, as well as count the number of cells per encapsulated aggregate. Thus, the area of hydroxyapatite per cell was calculated and allows to compare the conditions.

2.7.3 Scanning electron microscopy and energy-dispersive X-ray spectroscopy (SEM-EDS)

Encapsulated cell aggregates morphology and elemental constitution were analyzed by scanning electron microscopy (accelerating voltage 15 kV, SEM Hitachi, SU-70 instrument) coupled with an energy dispersive x-ray detector (EDS Bruker, Quantax 400 detector). Prior to the analysis, the microcapsules were collected at day 21 post-encapsulation and disrupted to expose the core content. Then, samples were fixed in paraformaldehyde (4 % v/v) and dehydrated in a graded series of ethanol. Afterwards, microcapsules were placed in a carbon tape onto a graphite stub (Ted Pella) and sputtered by a thin film of carbon (K950X Turbo-Pumped Carbon Evaporator). Calcium (Ca) and phosphorous (P) composition was obtained by EDS spectra using Esprit software. The Ca/P ratio was calculated by deconvolution of Ca and P peaks removing the background effect.

3.8. Statistical analysis

All data were statistically analyzed using one-way analysis of variance (ANOVA) using the Tukey´s multiple comparison tests. The GAGs quantification data were analyzed using two-way ANOVA with Tukey´s multiple comparison tests. Analysis and the corresponding graphical representations were performed using GraphPad Prism 6.01. A p-value <0.05 was considered statistically significant.

4. Results

4.1 Characterization of the isolated cells

In order to evaluate the success of the isolation of UCMSCs and HUVECs from the newborn umbilical cords, the presence of a specific set of antigens was assessed by flow cytometry, as represented in Figure 4. The UCMSCs phenotype was confirmed by the expression of CD73, CD90 and CD105 stemness markers, and the lack of the hematopoietic marker CD34 and the endothelial marker CD31. The endothelial marker CD31 was chosen as a negative marker to guarantee that UCMSCs were not contaminated with HUVECs, since both cell types were isolated from nearby components of the UC. HUVECs phenotype was also confirmed by the expression of CD31 antigen and the lack of CD90 and CD34 antigens. The absence of CD90 is a guarantee there is no contamination of the HUVECs with UCMSCs. The CD34 is an hematopoietic marker highly expressed in early endothelial cells, but poorly expressed in mature endothelial cells as HUVECs.[29]

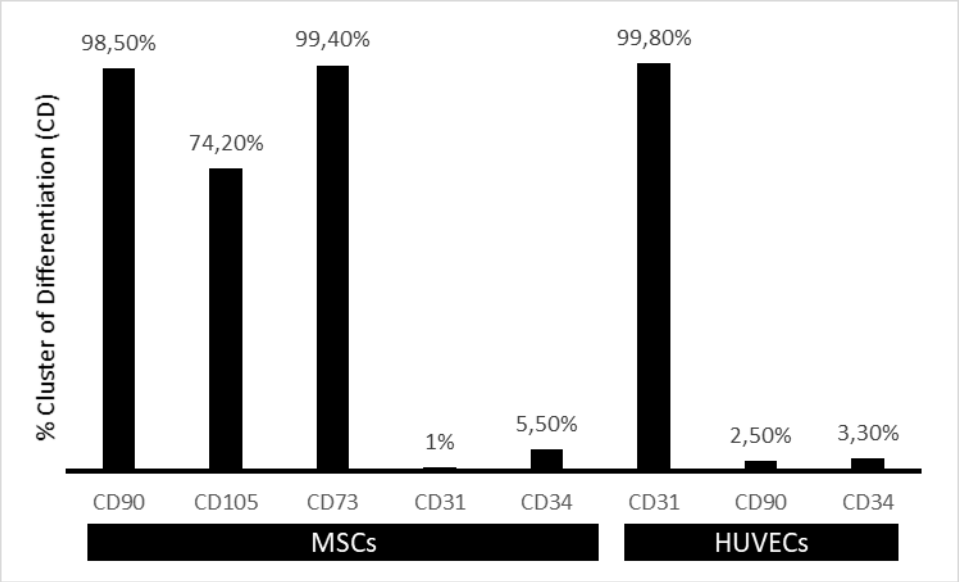

Figure 4. Flow cytometry analysis of the surface markers of MSCs and HUVECs after isolation. Cells were analysed at passage 5 and 3, respectively.

4.2 Chondrogenesis assessment of the 3D microtemplates

4.2.1 Cell viability and size of the 3D microtemplates

After being expanded until passage 5, UCMSCs were cultured in Aggrewell plates to induce their aggregation in 100-cell aggregates. These aggregates were named 3D microtemplates because they are intended to mimic the cartilaginous template formed after MSCs condensation and differentiation characteristic of the ECO process. The 3D microtemplates were cultured in basal (control) and chondro culture media, and their viability was evaluated up to 21 days of culture. The live/dead assay grant a qualitative assessment of cell viability, where living and dead cells are evidenced by green and red fluorescence, respectively. The results obtained are represented in Figure 5 (A). Both conditions present a slight presence of red fluorescence, however it was mostly negligible compared to the levels of green fluorescence. Importantly, no necrotic cores were observed at days 4 and 21. From these results we can conclude that the diffusion of essential molecules, such as nutrients and oxygen, occurred freely inside the templates. The size of the 3D microtemplates was measured using ImageJ software and their size distribution in both conditions at days 4 and 21 post-aggregation is represented in Figure 5 (B). The 3D microtemplates cultured in basal and chondro media display size differences in both days, namely at 4 and 21 days. At day 4, basal and chondro 3D microtemplates had an average diameter of 55,9 μm and 76,9 μm, respectively. At day 21, the average diameters were 75,3 μm and 90,6 μm, respectively. The size values between conditions in the same day were significantly different, as well as the size of 3D microtemplates from each condition is significantly different at the beginning and at the end of the aggregation period. Both 3D microtemplates of basal and chondro conditions increased their size along the 21 days but the chondro-cultured 3D microtemplates presented the highest diameter at both timepoints.

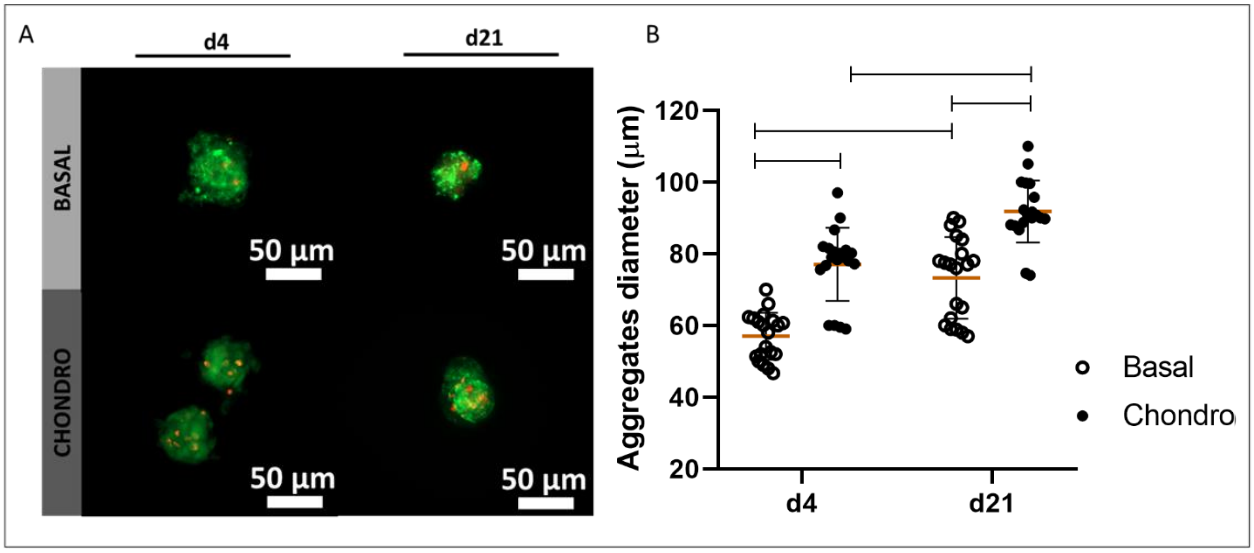

Figure 5. (A) Live/dead assay to evaluate the cell viability of the 3D microtemplates, cultured in basal and chondro conditions, at days 4 and 21 post-aggregation. (B) Size measurement of the 3D microtemplates in both conditions, using ImageJ image analysis software, at days 4 and 21 (n=20).

4.2.2. Chondrogenic differentiation evaluation

In order to visualize Col II, a main constituent of the cartilaginous ECM, presence and distribution in basal and chondro 3D microtemplates, an immunofluorescence staining (red) was performed at days 1, 14 and, 21 post-aggregation. Both basal and chondro 3D microtemplates presented Col II staining, as shown in Figure 6 (A). However, the chondro 3D microtemplates presented a wider Col II staining compared the basal microtemplates in all the timepoints tested. A more evidenced Col II staining in chondro 3D microtemplates might thus indicate that the chondrogenic media induced the chondrogenic differentiation of UCMSCs and, consequently, the production of a chondrogenic ECM. Of note, the presence of Col II is not exclusive of cartilaginous tissues, since it can be also present in other tissues and in undifferentiated MSCs aggregates.[30] Thus, explaining the detection of this protein in basal 3D microtemplates, although at lower levels. Using the Col II fluorescence microscopy images, Col II-stained area per cell was calculated using ImageJ software at day 21 post-aggregation. Despite being only a semi-quantitative evaluation of the 3D microtemplates, which cannot be used to present an absolute Col II expression value, it allows to understand that the expression of Col II seems to be significantly different between basal and chondro 3D microtemplates, as represented in Figure 6 (B). Such results corroborate the findings of the visual analysis of Col II in Figure 6 (A), since 3D microtemplates cultured in chondro medium present higher Col II values compared to 3D microtemplates cultured in basal medium. Additionally, the quantification of GAGs was performed, as presented in Figure 6 (C). At day 1 post-aggregation, basal (11.89 µg.mL^{-1}) and chondro (8.602

μg.mL^{-1}) 3D microtemplates do not present significant differences of GAG content, as expected. At day 14 post-aggregation, no significant differences were found in basal condition compared to day 1 (11.09 μg.mL^{-1}), while chondro 3D microtemplates significantly increased their GAGs content (17.21 μg.mL^{-1}). GAGs are also a main constituent of cartilaginous ECM[31,32], indicating that the chondrogenic supplements induced the differentiation of UCMSCs.

The morphology of both 3D microtemplates was analysed by SEM at day 1 and 21 post-aggregation. In Figure 7, the 3D microtemplates show evident differences of morphology between the two conditions. 3D microtemplates cultured in basal medium present a smooth ECM when compared with 3D microtemplates cultured in chondro medium, which present an irregular surface, characteristic of a denser ECM deposition.

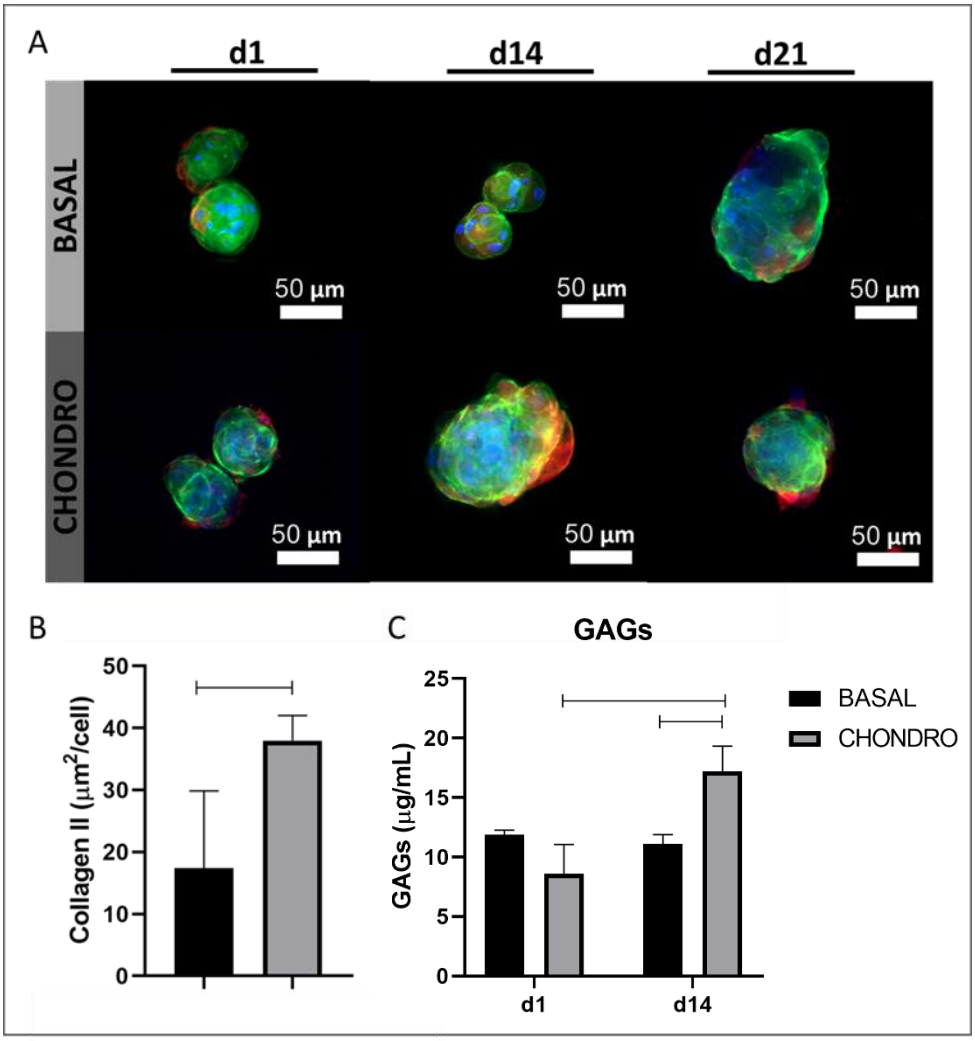

Figure 6. (A) Collagen II (red) and actin filaments (green) immunofluorescence staining of basal and chondro 3D microtemplates at day 21 post-aggregation. Cells were counterstained with DAPI (blue) for cell nuclei visualization. (B) Collagen II-stained area in the immunofluorescence staining per number of cells at day 21 post-aggregation, calculated using ImageJ image analysis software. (C) GAGs quantification in basal and chondro 3D microtemplates at days 1 and 14 post-aggregation.

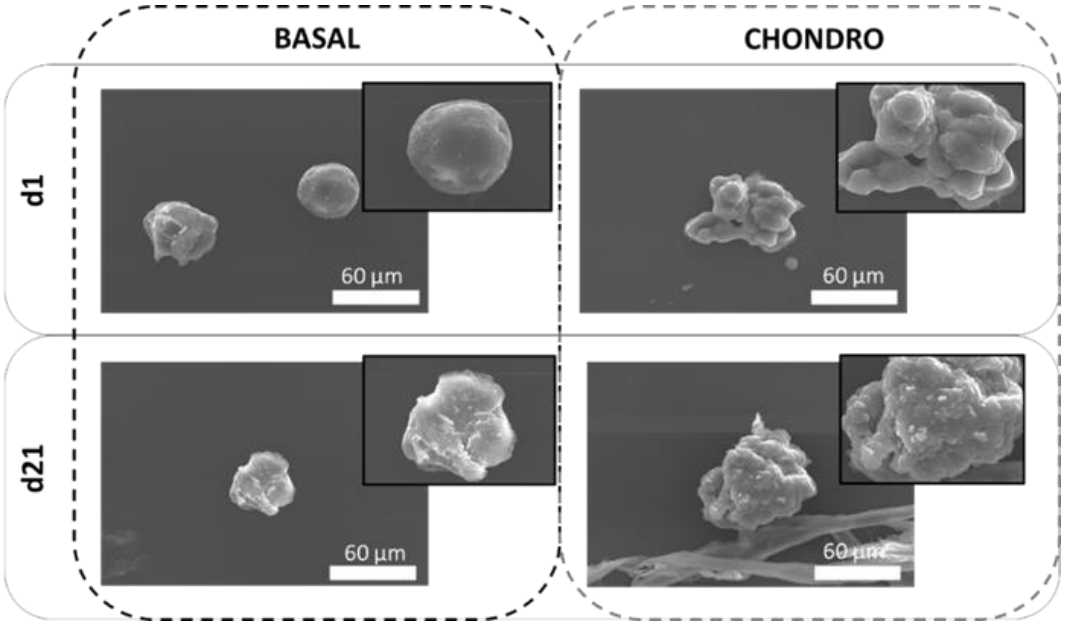

Figure 7. The morphology of basal and chondro 3D microtemplates was assessed by scanning electron microscopy (SEM) at days 1 and 21 of culture.

4.3 ECO assessment of the microtissues

4.3.1 Cell viability

The cartilaginous 3D microtemplates were created as an attempt to recapitulate the ECO process when encapsulated together with freely dispersed UCMSCs and HUVECs. Four types of microcapsules were tested, namely *(i)* microcapsules cultured with osteogenic medium and encapsulating chondrogenically primed 3D microtemplates (ECO microcapsules), (*ii*) microcapsules cultured in basal medium and encapsulating chondrogenically primed 3D microtemplates (ECO control microcapsules), (*iii*) microcapsules cultured with osteogenic medium and encapsulating non-chondrogenically primed 3D microtemplates, thus cultured in basal medium (IMO microcapsules), and (*iv*) microcapsules cultured in basal medium and encapsulating non-chondrogenically primed 3D microtemplates, thus cultured in basal medium (negative control). After the encapsulation, the co-culture is maintained up to 21 days in a dynamic environment, and the cell viability was evaluated along the 21 days by live/dead assay. The levels of red fluorescence, indicating the dead cells, are negligible comparing with green fluorescence, emitted by living cells, at days 1 and 21 post-encapsulation as represented in Figure 8. These results show that the different living components of the core, namely the 3D microtemplates, UCMSCs and HUVECs, were able to maintain their viability after the encapsulation process. The liquefied capsules system has already shown to support

higher viability of encapsulated cells compared to alginate hydrogels, the classical cell encapsulation system.[33] Of note, such results at day 21 post-encapsulation correspond to day 42 of *in vitro* culture for the case of the 3D microtemplates, and thus such system also successfully provided long-term cell survival, both in basal or osteo media. Therefore, it indicates that the diffusion of essential molecules, such as nutrients and oxygen, occurred freely throughout the entire volume of the microcapsules. Such outcome might be enhanced due to the dynamic culture environment used. Taking advantage of the liquefied environment of capsules, a dynamic culture system can be simply created by using a spinner flask. Such liquefied environment not only maximizes the diffusion of essential molecules for cell survival, as well as the interaction between the different core living components. Both UCMSCs and HUVECs are anchorage-dependent cells, and thus undergo anoikis in the absence of adhesion sites, which might be provided either by other cells or biomaterials. In the particular case of the system developed, in which only living components were encapsulated, the low quantity of dead cells detected evidences that the dispersed UCMSCs and HUVECs were able to adhere either to the 3D microtemplates or forming new aggregates. In fact, the cartilaginous 3D microtemplates intended to recapitulate the ECO process, by proving the cartilage template for the adhesion of MSCs and HUVECs, and thus to later induce the processes of osteogenic differentiation and angiogenesis, respectively.

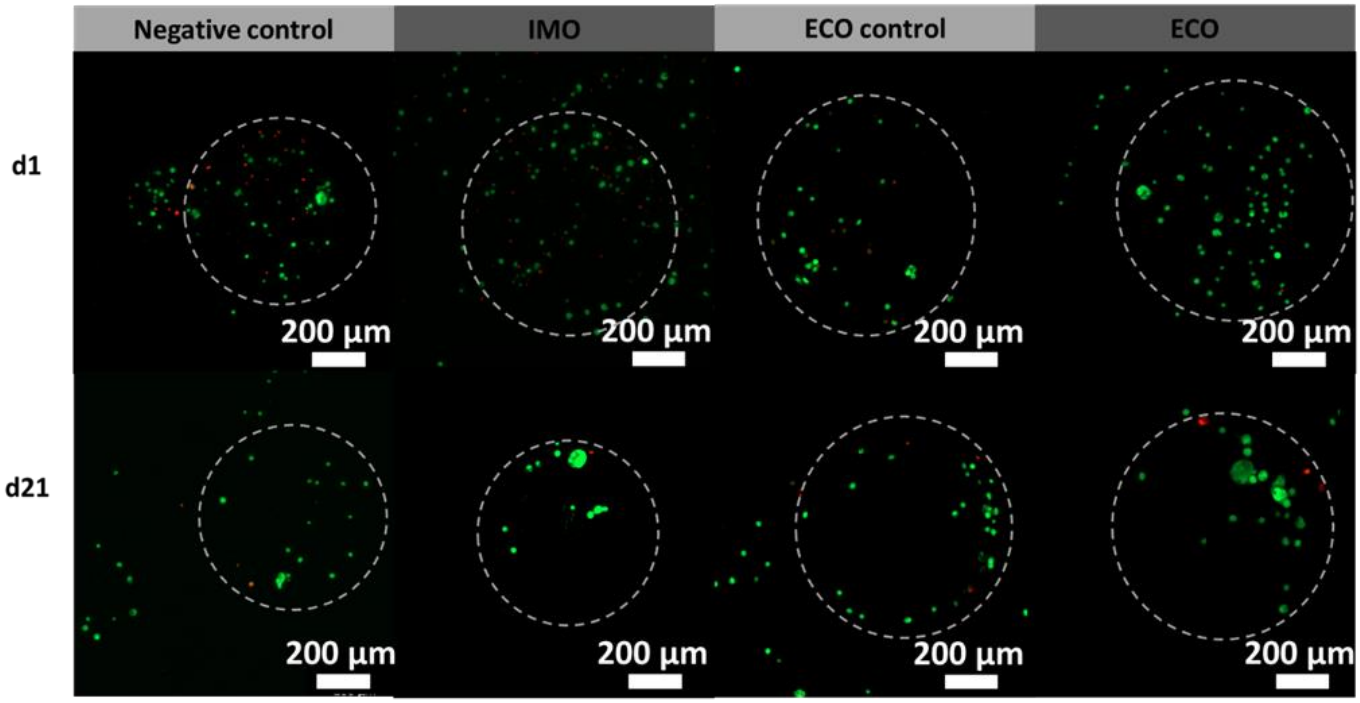

Figure 8. Live/Dead assay of the four different liquified microcapsules, namely *(i)* cultured in basal medium and encapsulating 3D microtemplates without chondrogenic stimulus (negative control), *(ii)* cultured in osteogenic medium and encapsulating 3D microtemplates without chondrogenic stimulus (IMO), *(iii)* cultured in basal medium and encapsulating chondrogenically primed 3D microtemplates (ECO control), and *(iv)* cultured in osteogenic medium and encapsulating chondrogenically primed 3D microtemplates (ECO) at days 1 and 21 post-encapsulation. Living cells are stained with calcein (green) and dead cells with propidium iodide (red). The dotted white lines represent the non-fluorescent membrane of capsules in order to facilitate the interpretation of the results.

4.3.2 ECO and angiogenesis evaluation

To evaluate if the cell aggregates formed within the liquefied core of microcapsules were induced towards the ECO process, key characteristic markers present in bone ECM were first evaluated. The secretion of osteopontin (OPN), a late osteogenic marker present in bone ECM, was assessed by an immunofluorescence assay (red staining), represented in Figure 9 (A). Additionally, the CD31 marker and cell nuclei are also stained by green and blue fluorescence, respectively. As showed, in the negative control, the expression of OPN could not be detected. On the other hand, in all the other conditions of microcapsules, the detection of OPN could be observed. IMO microcapsules, with osteogenic supplementation but non-chondrogenically primed 3D microtemplates, represent a well-known *in vitro* approach to create bone tissue, thus the presence of OPN was expected. Of note, ECO microcapsules presented the strongest staining of OPN. A more evidenced staining in ECO than in IMO microcapsules can indicate that the ECO approach is successfully inducing bone ECM production. It is also important to highlight the presence of OPN in ECO control microcapsules, which might indicate the deposition of a bone-like ECM even without osteogenic supplementation.

Therefore, the cartilaginous 3D microtemplates together with UCMSCs and HUVECs were able to stimuli the osteogenic differentiation of UCMSCs. The crosstalk between the cartilaginous template and the surrounding MSCs during ECO seems to be very important for the osteogenic differentiation of MSCs, but usually this effect is created when the cartilaginous template is in the hypertrophic state. Therefore, these results of the ECO control microcapsules might indicate that the cartilaginous 3D microtemplates achieved the hypertrophic state in basal medium, thus in the absence of osteogenic supplementation. Using the OPN fluorescence microscopy images, OPN-stained area normalized per cell was calculated using ImageJ software at day 21 post-aggregation. Such semi-quantitative evaluation of the microcapsules corroborates the findings of the observation of the OPN staining, showing that values of the IMO, ECO and ECO control microcapsules are not significantly different in terms of the OPN content and the negative control present the lowest values.

The secretion of the osteogenic marker hydroxyapatite (HA) was analysed after 21 days post-encapsulation for all the four conditions of microcapsules, as shown in Figure 9 (B). A visible difference in HA staining exists between the microcapsules cultured in osteogenic and basal media. Therefore, cell aggregates within microcapsules cultured with osteogenic supplementation, namely IMO and ECO microcapsules, present a stronger HA staining compared to the microcapsules cultured in basal supplementation, namely negative control and ECO control microcapsules. Those are the microcapsules with higher osteogenic potential and the results show that the osteo supplements were important to HA expression, regardless of the primed or not-primed 3D microtemplates. HA staining is almost negligible in the negative control. The HA-stained area per cell was calculated and represented in Figure 9 (C3). The results indicate that HA-stained area is significantly higher in ECO microcapsules, when compared to the other conditions of microcapsules.

The CD31 marker immunofluorescence assay was also performed to evaluate if the freely dispersed HUVECs were incorporated within the cell aggregates. The ECO control and ECO microcapsules presented a stronger CD31 staining than the other two conditions, which had the non-chondrogenically primed 3D microtemplates. Again, the crosstalk between hypertrophic cartilaginous templates, MSCs and HUVECs seems to be play a key role not only to induce osteogenic differentiation but also to recruit endothelial cells that will pre-vascularize the microtissues. The cartilaginous 3D microtemplates seem to induce a higher interaction with HUVECs, which might be enhanced due to the hypertrophic induction of MSC-derived chondrocytes from the 3D microtemplates. Another interesting detail is the diffusion of the HUVECs in the cell aggregates from ECO microcapsules, which seem to be more concentrated at the core region of the aggregates, whereas in ECO control microcapsules HUVECs are more dispersed through the cell aggregate. CD31-stained area per cell was calculated as showed in Figure 9 (C2). Results show that

CD31-stained area per cell is significantly higher in ECO microcapsules, when compared to the remaining conditions of microcapsules.

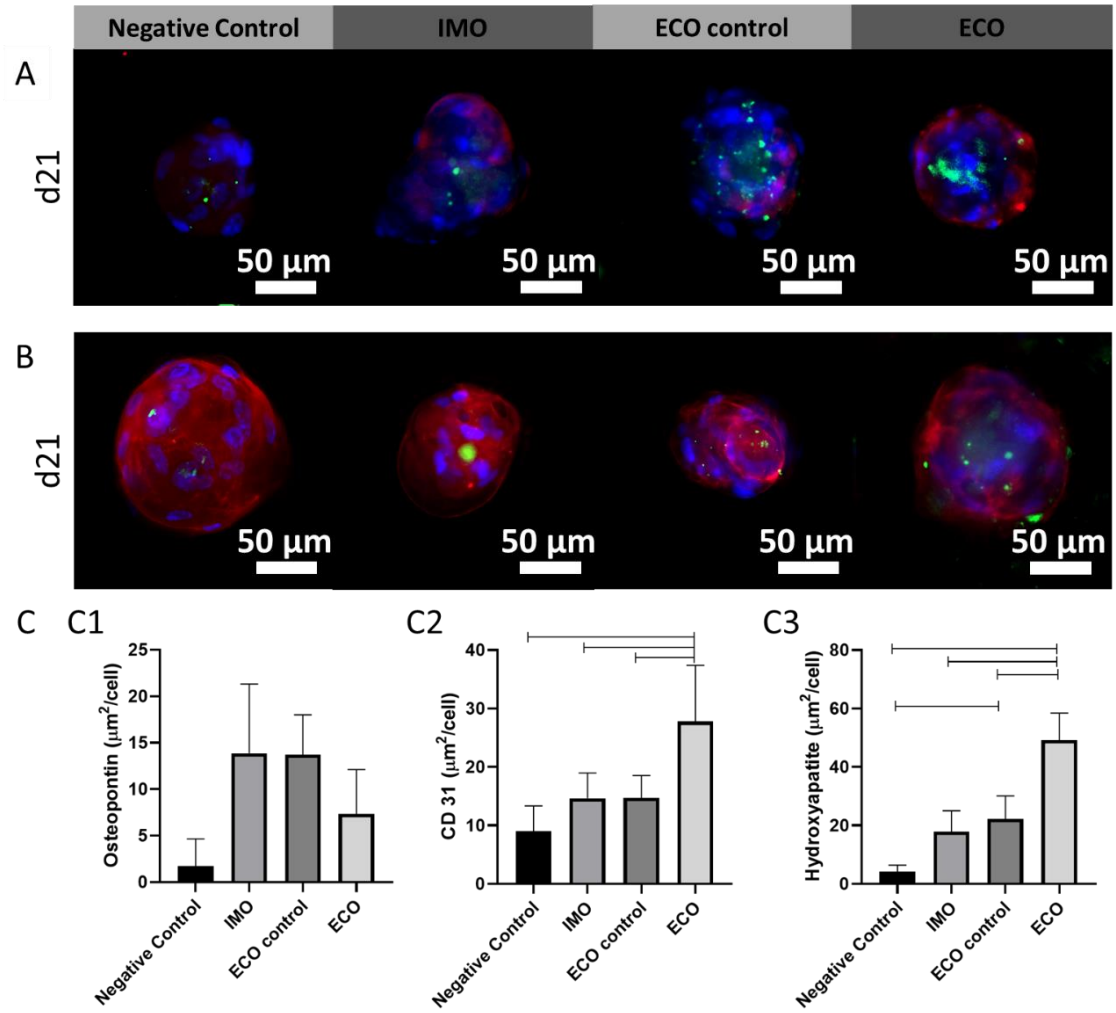

Figure 9. ECM analysis at day 21 post-encapsulation of the cell aggregates within the liquified core of four conditions of microcapsules namely *(i)* cultured in basal medium and encapsulating 3D microtemplates without chondrogenic stimulus (negative control), *(ii)* cultured in osteogenic medium and encapsulating 3D microtemplates without chondrogenic stimulus (IMO), *(iii)* cultured in basal medium and encapsulating chondrogenically primed 3D microtemplates (ECO control), and *(iv)* cultured in osteogenic medium and encapsulating chondrogenically primed 3D microtemplates (ECO) at days 1 and 21 post-encapsulation. (A) Immunofluorescence of osteopontin (OPN, red) and CD31 (green). Cells nuclei were counterstained with DAPI (blue). (B) Hydroxyapatite (HA, green) immunofluorescence assay counterstained with phalloidin (red) and DAPI (blue) for the visualization of actin filaments,and cells nuclei, respectively. (C) Semiquantitative analysis of (C1) osteopontin, (C2) CD31, and (C3) hydroxyapatite immunofluorescence assays normalized per number of cells at day 21 post-encapsulation, using the ImageJ software.

A deeper evaluation of HA deposition was analyzed by scanning electron microscopy (SEM) coupled with energy dispersive X-ray spectroscopy (EDS), 21 days post-encapsulation (Figure 10). As showed, microcapsules cultured in basal medium (Figure 10 (A)), namely negative control and ECO control microcapsules, do not present strong evidences of a mineralized ECM. On the other hand, microcapsules cultured in osteogenic medium (Figure 10 (B)), namely IMO and ECO microcapsules,

presented evidences of a mineralized ECM. Additionally, the chemical characterization of the cell aggregates formed inside the liquefied core of microcapsules was analyzed by EDS after 21 days of culture and expressed in Figure 10 (A-C). Results show that phosphorous (P) and calcium (Ca) contents are residual in the negative control and ECO control microcapsules when compared with IMO and ECO microcapsules, which presented higher levels of P and Ca deposition. Particularly, cell aggregates within ECO microcapsules presented significantly higher mineralization. Remarkably, only ECO microcapsules presented a Ca/P ratio (1.71) close to the native hydroxyapatite ratio of 1.67.[34] These results show that the ECO condition resulted in an increased mineralization compared to the IMO condition. Additionally, the SEM images highlight the differences between the ECM presented by ECO microcapsules and the other formulations of microcapsules (Figure 10 (D)). In particular, ECO microcapsules present large nodule-like structures, while the remaining microcapsules present a smooth surface.

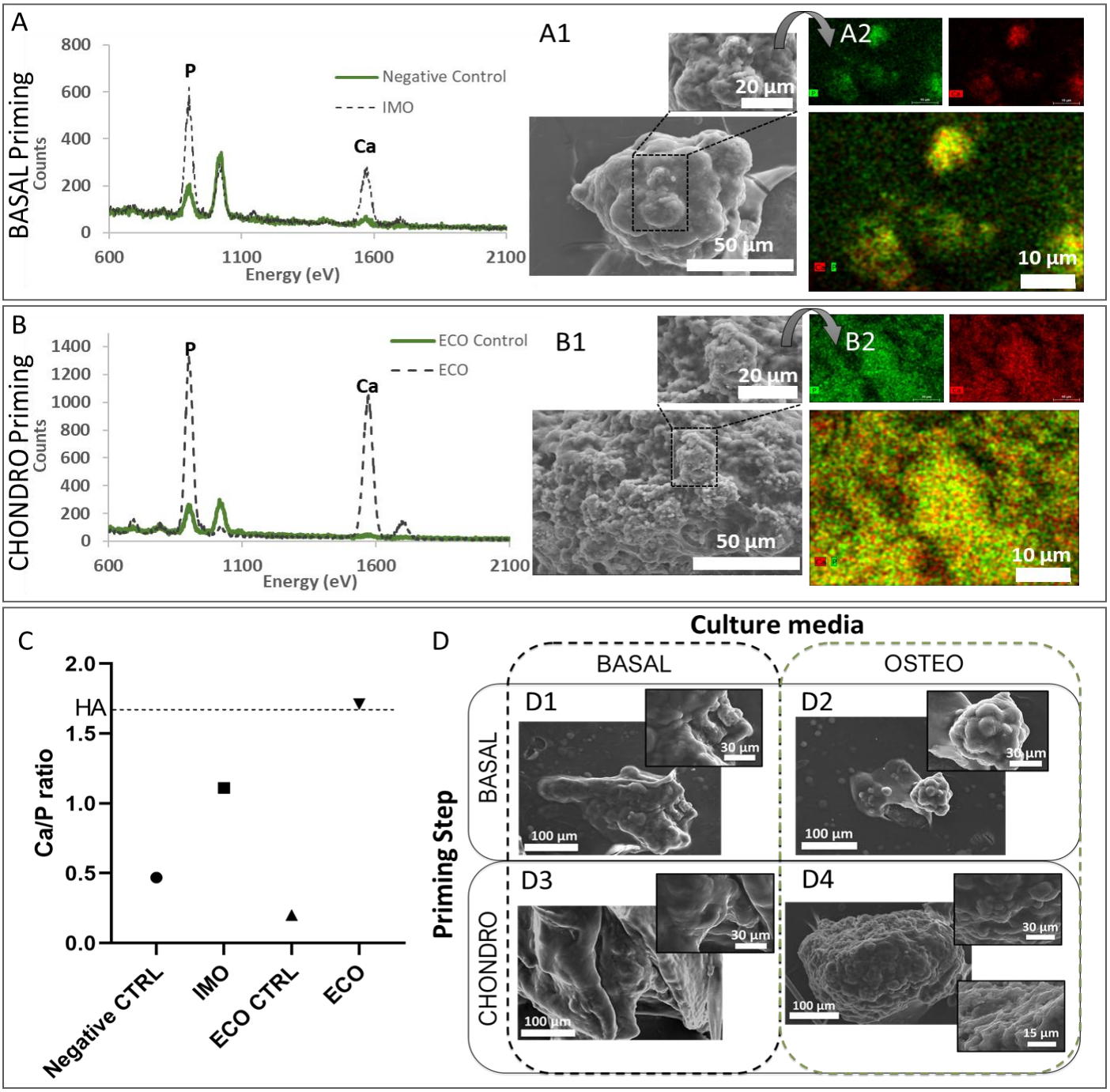

Figure 10. Bone ECM analysis of cell aggregates within the liquified core of four conditions of microcapsules namely *(i)* cultured in basal medium and encapsulating 3D microtemplates without chondrogenic stimulus (negative control), *(ii)* cultured in osteogenic medium and encapsulating 3D microtemplates without chondrogenic stimulus (IMO), *(iii)* cultured in basal medium and encapsulating chondrogenically primed 3D microtemplates (ECO control), and *(iv)* cultured in osteogenic medium and encapsulating chondrogenically primed 3D microtemplates (ECO) at days 1 and 21 post-encapsulation. Identification of phosphorous (P) and calcium (Ca) by EDS in capsules cultured in BASAL or OSTEO media, (A) without or (B) with previous chondrogenic priming of 3D microtemplates. (A1) Scanning electron microscopy (SEM) images of a cell aggregate within IMO microcapsules. (B1) SEM images of a cell aggregate within ECO microcapsules (A2) Elemental analysis of (A1) by EDS mapping of phosphorous (P, red) and calcium (Ca, green). (B2) Elemental analysis of (B1) by EDS mapping of phosphorous (P, red) and calcium (Ca, green). In the image below, Ca and P regions are overlapped, and the yellow colour represents the co-location of the two elements. (C) Ca/P ratio analysis of the cell aggregates within microcapsules in the four conditions. The dotted horizontal line of a Ca/P ratio of 1.67 corresponds to the value of native hydroxyapatite (HA). (D) Representative SEM images of the encapsulated aggregates and cells in all the four conditions of microcapsules, namely (D1) negative control, (D2) IMO microcapsules, (D3) ECO control microcapsules, and (D4) ECO microcapsules.

5. Discussion

The present work intends to create an *in vitro* ECO model relying on the bioencapsulation of MSCs and endothelial cells in liquified and multilayered microcapsules. Such proposed fully *in vitro* ECO model is composed by three essential components, namely (*I*) cartilaginous 3D microtemplates to mimic the hyaline cartilage templates existent in the *in vivo* ECO process, and potentially produce osteogenic and angiogenic factors for cells within the liquified environment, as well as provide anchorage points for co-encapsulated cells; (*II*) freely dispersed MSCs and HUVECs, which can self-organize within the liquified microcapsules in response to their specific needs; and (*III*) a permselective multilayered membrane, which allow an efficient diffusion of nutrients, oxygen, growth factors and cell metabolites, protects the cells from an immunological response and allows the microcapsules to be implanted by minimal invasive procedures using a syringe. Such bioencapsulation system was already successfully tested *in vitro* and *in vivo*[23,24,33,35,36] but herein it is the first time that it is used aiming towards the development of a fully *in vitro* ECO approach. Our hypothesis is that by co-culturing the cartilaginous 3D microtemplates with UCMSCs and HUVECs, this privileged microenvironment would mimic the ECO process, leading to the *in vitro* production of vascularized bone-like microtissues. The cartilaginous 3D microtemplates are the pivotal element in this ECO approach, because an adequate supplementation induces these templates to enter into a hypertrophic stage, and consequently produce osteogenic and angiogenic factors that will simultaneously induce UCMSCs to differentiate into osteoblasts and the creation of a pre-vascular network by HUVECs. The cell viability and chondrogenic evaluations of the 3D microtemplates were performed by live/dead assay, Col II immunofluorescence and GAGs quantification. The cell viability of non-primed and cartilaginous 3D microtemplates was confirmed up to 21 days after aggregation. The cartilaginous nature of the 3D templates cultured in chondrogenic medium was confirmed by the presence of COL II and the expression of GAGs at day 21, when compared with templates cultured in basal medium. The analysis of the 3D microtemplates dimensions and morphology from optical microscopy images and SEM images, respectively, indicates the deposition of a denser ECM by the 3D templates cultured in chondrogenic medium.

After the cartilaginous 3D microtemplates being validated, to evaluate the ECO hypothesis, four types of microcapsules were tested, namely *(i)* microcapsules cultured in medium supplemented with osteogenic differentiation factors and encapsulating chondrogenically primed MSCs-only 3D microtemplates (ECO microcapsules), *(ii)* microcapsules cultured in medium without osteogenic differentiation factors supplementation and encapsulating chondrogenically primed MSCs-only 3D microtemplates (ECO control microcapsules), *(iii)* microcapsules cultured in medium supplemented with osteogenic differentiation factors and encapsulating non-chondrogenically primed MSCs-only

3D microtemplates (IMO microcapsules), and *(iv)* microcapsules cultured in medium without osteogenic differentiation factors supplementation and encapsulating non-chondrogenically primed MSCs-only 3D microtemplates (negative control). The 3D microtemplates were thus co-encapsulated with freely dispersed UCMSCs and HUVECs to produce the four types of microcapsules. The live/dead assay at day 21 post-encapsulation proved the ability of microcapsules for long-term cell survival in all the four conditions of microcapsules. Both UCMSCs and HUVECs are anchorage-dependent cells, which means that if they do not adhere either to 3D microtemplates or between themselves they would undergo anoikis.[37] Therefore, the reduced number of apoptotic cells confirm the success of the co-culture. Both basal and osteo media used in the bioencapsulation were constituted by M199 medium, the endothelial cell culture medium, that was applied because of the higher sensibility of HUVECS culture compared to UCMSCs. The results of cell viability also reveal that UCMSCs have adapted to the endothelial cell culture medium.

The IMO microcapsules are an important control because the IMO approach is the standard bone TE approach to obtain bone microtissue *in vitro*. ECO approaches intend to surpass the lack of vascularization of the IMO approaches that often jeopardize cell viability due to the formation of necrotic cores. Also, ECO control microcapsules were important to understand if the co-culture *per se* was sufficient to induce the ECO process and produce vascularized bone-like microtissues, without osteogenic supplementation.

Bone formation via ECO is characterized by (a) cell proliferation, (b) ECM production, (c) mineralization and (d) endothelial cells recruitment. The osteogenic ECM production was evaluated by OPN immunofluorescence. At day 21 post-encapsulation, the negative control, with any osteo supplementation or primed microtemplates, was the only condition who did not presented OPN staining. The OPN staining area per cell in the other three conditions, namely IMO, ECO control and ECO microcapsules are not significantly different, and thus do not allow to select the condition with higher OPN expression. However, the results show that ECO microcapsules could express the late osteogenic marker as similar levels to those in the IMO microcapsules, the standard approach in bone TE. Of note, the presence of OPN in ECO control microcapsules may suggests that even without osteogenic supplementation, the cartilaginous 3D microtemplates in combination with UCMSCs and HUVECs were able to induce the osteogenic differentiation of UCMSCs, and consequently the expression of this osteogenic marker. I*n vivo*, during the native ECO process, the cartilaginous templates can induce the osteogenic differentiation of MSCs when a hypertrophic state is achieved. Therefore, the osteogenic supplementation in ECO microcapsules is used to stimulate the hypertrophy of the cartilaginous 3D microtemplates. However, the expression of OPN in the ECO control microcapsules might indicate that the cartilaginous 3D microtemplates achieved the hypertrophic state even in basal medium, thus without requiring osteogenic supplementation.

Mineralization was evaluated by HA immunofluorescence assay and by the elemental analysis of the aggregates by EDS mapping of phosphorous and calcium content. Cell aggregates within microcapsules cultured with osteo supplementation, namely the IMO and ECO, present a stronger HA staining than the microcapsules cultured in basal supplementation, namely the negative control and ECO control microcapsules. Both primed and not-primed 3D microtemplates cultured with osteogenic supplementation presented HA staining because of the β-GP supplement that induces the production of hydroxyapatite.[21] The comparison of HA-stained areas per cell between the four conditions indicates that HA expression is significantly higher in ECO microcapsules. The elemental analysis by SEM coupled with energy dispersive spectroscopy (EDS), 21 days post-encapsulation confirm that IMO and ECO microcapsules present evidence of mineralization. Remarkably, and despite both conditions have osteogenic supplementation, the chemical characterization by EDS shows that ECO microcapsules presented a Ca/P ratio (1.71) similar to the native hydroxyapatite ratio of 1.67.[34] These results show that ECO microcapsules presented an enhanced mineralized ECM compared to IMO microcapsules. SEM images also show evident differences between the ECM found in IMO and ECO microcapsules. The ECM of ECO microcapsules present large nodule-like structures that prove the high mineralization of such microtissues, while IMO microcapsules present a smoother surface of the ECM. The interaction of the 3D microtemplates with endothelial cells was assessed by CD31 immunofluorescence assay. Results show that ECO control and ECO microcapsules present an increased number of HUVECs surrounding the 3D microtemplates, compared with the negative control and IMO microcapsules. The results indicate that the co-culture of UCMSCs and HUVECs is promising in ECO repair. Those evidences indicate that the cartilaginous 3D microtemplates successfully fulfilled their role regarding the mimicking of the native recruitment of endothelial cells by cartilaginous templates.

6. Conclusions

ECO approaches gained increasingly interest by the scientific community dedicated to bone TE, because beyond the creation of mineralized bone microtissues, the tissue vascularization of such tissues is of utmost importance. Although the IMO approaches have been widely used in the tissue engineering and regenerative medicine field (TERM) to successfully obtain mineralized tissues, they lack vascularization, resulting in necrotic cores after implantation. Therefore, the number of ECO approaches has been increasing in the last decade. During ECO, a hyaline cartilage template is formed and when enters in hypertrophy secrete osteogenic and angiogenic factors, which induce MSCs osteogenic differentiation and endothelial cells recruitment. Inspired by the pivotal role of hypertrophic cartilage templates in ECO, cartilaginous 3D microtemplates were created and bioencapsulated with UCMSCs and HUVECs in liquified and multilayered microcapsules. Our hypothesis was that such co-culture system would recreate a privileged microenvironment that could recapitulate the ECO process, leading to the *in vitro* production of vascularized bone-like microtissues. This work represents the first attempt of the encapsulation of MSCs and endothelial cells in liquified and multilayered microcapsules towards a fully *in vitro* model aiming towards ECO. The cartilaginous nature of the 3D microtemplates cultured in chondrogenic medium was confirmed. The encapsulated cartilaginous 3D microtemplates shown to induce the production of bone ECM key molecules, such as osteopontin and hydroxyapatite, and presented a high mineralization level when supplemented with osteogenic factors. A lower level of mineralization was obtained in encapsulated cartilaginous 3D microtemplates without osteogenic supplementation, however this condition also presented osteopontin and hydroxyapatite expression. The appearance of ECO evidences in encapsulated cartilaginous 3D microtemplates cultured without osteogenic supplementation, indicates that the microtemplate can induce osteogenic MSCs differentiation without osteogenic supplementation. Furthermore, the ECO approach showed to favour the interaction with endothelial cells compared to IMO microcapsules, thus mimicking the *in vivo* recruitment of such key cells in the establishment of the vascular network of bone tissues. This work represents an important improvement towards the creation of a bone development model based in ECO and perhaps in the future, the creation of an injectable and non-invasive device for bone repair.

7. References

1. Kiernan, C., Knuth, C. & Farrell, E. Endochondral Ossification: Recapitulating Bone Development for Bone Defect Repair. *Dev. Biol. Musculoskelet. Tissue Eng.* 125–148 (2018). doi:10.1016/B978-0-12-811467-4.00006-1
2. Sheehy, E. J., Kelly, D. J. & O'Brien, F. J. Biomaterial-based endochondral bone regeneration: a shift from traditional tissue engineering paradigms to developmentally inspired strategies. *Mater. Today Bio* **3**, 100009 (2019).
3. Thompson, E., Matsiko, A., Farrell, E., Kelly, D. & O'Brien, F. Recapitulating endochondral ossification: a promising route to in vivo bone regeneration. *J. Tissue Eng. Regen. Med.* 889–902 (2014). doi:10.1002/term
4. Wong, S. A. *et al.* Microenvironmental Regulation of Chondrocyte Plasticity in Endochondral Repair — A New Frontier for Developmental Engineering. **6**, 1–14 (2018).
5. Occhetta, P., Stüdle, C., Barbero, A. & Martin, I. Learn, simplify and implement: developmental re-engineering strategies for cartilage repai. *Swiss Med. Wkly.* **146**, w14346 (2016).
6. Almubarak, S. *et al.* Tissue engineering strategies for promoting vascularized bone regeneration. *Bone* (2015). doi:10.1016/j.bone.2015.11.011
7. Gao, F. *et al.* Mesenchymal stem cells and immunomodulation: Current status and future prospects. *Cell Death Dis.* **7**, (2016).
8. P. De Miguel, M. *et al.* Immunosuppressive Properties of Mesenchymal Stem Cells: Advances and Applications. *Curr. Mol. Med.* **12**, 574–591 (2012).
9. Beyth, S. *et al.* Human mesenchymal stem cells alter antigen-presenting cell maturation and induce T-cell unresponsiveness. *Blood* **105**, 2214–2219 (2005).
10. Marmotti, A. *et al.* Allogeneic Umbilical Cord-Derived Mesenchymal Stem Cells as a Potential Source for Cartilage and Bone Regeneration : An In Vitro Study. **2017**, (2017).
11. Silva-cote, I. *et al.* Strategy for the Generation of Engineered Bone Constructs Based on Umbilical Cord Mesenchymal Stromal Cells Expanded with Human Platelet Lysate. **2019**, (2019).
12. Perez, J. R. *et al.* Tissue Engineering and Cell-Based Therapies for Fractures and Bone Defects. **6**, 1–23 (2018).
13. Wexler, S. A. *et al.* Adult bone marrow is a rich source of human mesenchymal 'stem' cells but umbilical cord and mobilized adult blood are not. *Br. J. Haematol.* **121**, 368–374 (2003).
14. Weiss, M. L. *et al.* Immune Properties of Human Umbilical Cord Wharton's Jelly-Derived Cells. *Stem Cells* **26**, 2865–2874 (2008).
15. Van Pham, P., Bich, N. V. & Phan, N. K. Umbilical cord-derived stem cells (ModulatistTM) show strong immunomodulation capacity compared to adipose tissue-derived or bone marrow-derived mesenchymal stem cells. *Biomed. Res. Ther.* **3**, 687–696 (2016).
16. Selich, A. *et al.* Umbilical cord as a long-Term source of activatable mesenchymal stromal cells for immunomodulation. *Stem Cell Res. Ther.* **10**, 1–14 (2019).
17. Tipnis, S., Viswanathan, C. & Majumdar, A. S. Immunosuppressive properties of human umbilical cord-derived mesenchymal stem cells: Role of B7-H1 and IDO. *Immunol. Cell Biol.* **88**, 795–806 (2010).
18. Stegen, S., Gastel, N. Van & Carmeliet, G. Bringing new life to damaged bone : The importance of angiogenesis in bone repair and regeneration. *Bone* (2014). doi:10.1016/j.bone.2014.09.017
19. Matsumoto, T. & Kawamoto, A. Therapeutic Potential of Vasculogenesis and Osteogenesis Promoted by Peripheral Blood CD34- Positive Cells for Functional Bone Healing. *Am. J. Pathol.* **169**, 1440–1457 (2006).
20. Lin, Y. *et al.* Combination of polyetherketoneketone scaffold and human mesenchymal stem cells from temporomandibular joint synovial fluid enhances bone regeneration. *Sci. Rep.* **9**, 1–13 (2019).
21. Langenbach, F. & Handschel, J. Effects of dexamethasone , ascorbic acid and β -glycerophosphate on the osteogenic differentiation of stem cells in vitro. (2013).
22. Ovsianikov, A., Khademhosseini, A. & Mironov, V. The Synergy of Scaffold-Based and Scaffold-Free Tissue Engineering Strategies. *Trends Biotechnol.* **36**, 348–357 (2018).
23. Correia, C. R. *et al.* Semipermeable capsules wrapping a multifunctional and self-regulated co-culture microenvironment for osteogenic differentiation. *Sci. Rep.* **6**, 1–12 (2016).
24. Nadine, S. Dynamic microfactories co-encapsulating osteoblastic and adipose-derived stromal cells

for the biofabrication of bone units. *Biofabrication* **12**, 15005 (2020).
25. Seshareddy, K., Troyer, D. & Weiss, M. L. Method to Isolate Mesenchymal-Like Cells from Wharton's Jelly of Umbilical Cord. *Methods Cell Biol.* **86**, 101–119 (2008).
26. Subramanian, A., Fong, C. Y., Biswas, A. & Bongso, A. Comparative characterization of cells from the various compartments of the human umbilical cord shows that the Wharton's jelly compartment provides the best source of clinically utilizable mesenchymal stem cells. *PLoS One* **10**, 1–25 (2015).
27. Mennan, C. *et al.* Isolation and characterisation of mesenchymal stem cells from different regions of the human umbilical cord. *Biomed Res. Int.* **2013**, 916136 (2013).
28. J. Medina-Leyte, D., Domínguez-Pérez, M. & Mercado, I. Use of Human Umbilical Vein Endothelial Cells (HUVEC) as a Model to Study Cardiovascular Disease: A review. *Appl. Sci.* (2020).
29. Hristov, M. & Weber, C. Endothelial progenitor cells: characterization, pathophysiology, and possible clinical relevance. *J. Cell. Mol. Med.* **8**, 498–508 (2004).
30. Liu, Y., Kuang, B., Rothrau, B. B., Tuan, R. S. & Lin, H. Robust bone regeneration through endochondral ossi fi cation of human mesenchymal stem cells within their own extracellular matrix. **218**, (2019).
31. Studer, D., Millan, C., Maniura-weber, K. & Zenobi-wong, M. Molecular and biophysical mechanisms regulating hypertrophic differentiation in chondrocytes and mesenchimal stem cells. **24**, 118–135 (2012).
32. Correia, C. R., Gil, S., Reis, R. L. & Mano, J. F. A Closed Chondromimetic Environment within Magnetic-Responsive Liquifi ed Capsules Encapsulating Stem Cells and Collagen II / TGF- β 3 Microparticles. 1346–1355 (2016). doi:10.1002/adhm.201600034
33. Correia, C. R., Reis, R. L. & Mano, J. F. Multilayered hierarchical capsules providing cell adhesion sites. *Biomacromolecules* **14**, 743–751 (2013).
34. Bett, J. A. S., Christner, L. G. & Keith Hail, W. Studies of the Hydrogen Held by Solids. XII. Hydroxyapatite Catalysts. *J. Am. Chem. Soc.* **89**, 5535–5541 (1967).
35. Correia, C. R. *et al.* In vivo osteogenic differentiation of stem cells inside compartmentalized capsules loaded with co-cultured endothelial cells. *Acta Biomater.* **53**, 483–494 (2017).
36. Correia, C. R., Sher, P., Reis, R. L. & Mano, J. F. Liquified chitosan-alginate multilayer capsules incorporating poly(l-lactic acid) microparticles as cell carriers. *Soft Matter* **9**, 2125–2130 (2013).
37. Lee, S., Choi, E., Cha, M. & Hwang, K. Cell Adhesion and Long-Term Survival of Transplanted Mesenchymal Stem Cells : A Prerequisite for Cell Therapy. **2015**, (2015).

IV. Conclusions and future perspectives

Initially, in Chapter *I*, was made an overview about the ECO process and the new strategies used to achieve this repair process. The advantage of ECO over IMO approaches became evident. While, in IMO approaches the tissues must be pre-vascularized to prevent the formation of necrotic cores, in ECO a hyaline cartilage template is formed and when enters in hypertrophy secrete osteogenic and angiogenic factors, which induce MSCs osteogenic differentiation and endothelial cells recruitment. Therefore, the number of developed ECO approaches has been increasing in the last decade. The strategies were divided in scaffold-based, scaffold-free, and cell-free approaches. The cell-free approaches prove the importance of biomaterials porosity and pore alignment. However, scaffold-based continues the most used strategy because of the support that scaffolds give to cells and the "catalytic" effect of the cells in ECO repair. The scaffold-free approaches allow more freedom to cells and comparing the research work made using the three strategies, need shorter cell culture times to obtain bone tissue. In a nutshell, all three strategies have interesting features but in the future is necessary to shorten their experimental time to make it possible to transpose into real medical applications.

Inspired by the pivotal role of hypertrophic cartilage templates in ECO, cartilaginous 3D microtemplates were created and bioencapsulated with UCMSCs and HUVECs in liquified and multilayered microcapsules. Our hypothesis was that the co-culture would create a privileged microenvironment that could recapitulate the ECO process, leading to the *in vitro* production of vascularized bone-like microtissues. Chapter *II* consists in a detailed compilation of the methods and materials needed to create this *in* vitro ECO model. The evaluation of osteogenic differentiation and tissue vascularization is presented during Chapter *III*. This work represents the first attempt of stem and endothelial cells bioencapsulation in liquified and multilayered microcapsules towards an *in vitro* model for ECO. The cartilaginous nature of the 3D microtemplates cultured in chondrogenic medium was confirmed. The encapsulated cartilaginous 3D microtemplates shown to induce the production of bone ECM molecules as osteopontin and hydroxyapatite and presented a high mineralization level when supplemented with osteogenic factors. A lower level of mineralization was obtained in encapsulated cartilaginous 3D microtemplates without osteogenic supplementation, however this condition also presented osteopontin and hydroxyapatite expression. The appearance of ECO evidences in encapsulated cartilaginous 3D microtemplates cultured without osteogenic supplementation, indicates that the microtemplate can induce osteogenic MSCs differentiation without specific supplementation. Furthermore, the ECO approach shown to induce endothelial cells

recruitment with and without the use of osteogenic supplementation, while IMO almost did not recruit any endothelial cell.

It is the first time that this bioencapsulation system is used aiming towards the development of a fully *in vitro* ECO approach, but revealed to be a promising bone repair strategy. The utilization of UCMSCs in this approach was important because this type of MSCs were poorly explored in ECO. Also, both UCMSCs and HUVECs are isolated from a perinatal tissue that otherwise would be discarded. However, more quantitative data is required to support the evaluation of the hypertrophic state of the chondrogenically primed 3D microtemplates, as well as the quantification of relevant bone ECM markers. Also, the reduction of cell culture time would make easier to transpose this approach for real bone repair applications. Nevertheless, the relevance of using chondrogenically primed 3D microtemplates in bone repair is herein demonstrated, highlighting the advantage of ECO over the classical IMO approach in the production of vascularized and mineralized bone microtissues.